University of Basel

Hazard and Risk Assessment of Wind Erosion and Dust Emissions in Denmark - A Simulation and Modelling Approach

Inauguraldissertation

zur

Erlangung der Würde eines Doktors der Philosophie

vorgelegt der

Philosophisch-Naturwissenschaftlichen Fakultät

der Universität Basel

von

Ali Mohammadian Behbahani

aus Behbahan, Iran

Basel, 2015

Genehmigt von der Philosophisch-Naturwissenschaftlichen Fakultät
auf Antrag von

Prof. Dr. Nikolaus J. Kuhn
(Universität Basel)
Fakultätsverantwortlicher

Dr. Wolfgang Fister
(Universität Basel)
Dissertationsleiter

Dr. Goswin Heckrath
(Universität Aarhus)
Korreferent

Basel, den 23.06.2015

Prof. Dr. Jörg Schibler
Dekan

DEDICATIONS

I would like to dedicate this dissertation to my country and my countrymen

Reference: Night Earth. Persian Gulf. Elements of this image furnished by NASA

SUMMARY

Wind erosion is considered to be one of the major global environmental problems. For example dust storms can cause serious damages and the protection of civil, industrial and agricultural areas represents a major environmental and economic challenge. Global 'anthropogenic' dust emissions have been estimated up to 50% of the total atmospheric dust (IPCC 2001), but recent studies indicated that less than 10-25% of global dust emissions originate from agricultural soils.

Wind erosion is an important land surface process in Europe, which has caused the emission of the finest and most valuable soil particles and nutrients. More than 70% of the soil types in Denmark have a sandy texture. Denmark is also subject to strong offshore and onshore winds, therefore, Danish soils are considered especially vulnerable to wind erosion.

On such poorly aggregated soils, which are treated with conventional farming, tillage ridges are the only roughness element that are able to protect soils against wind erosion in the absence of plant cover. Historical evidence demonstrates that wind erosion has had significant effects on Danish agricultural lands. Various actions have been implemented to control wind erosion in Denmark such as wind break establishment and implementation of protective cultivation techniques. However, there are still some concerns among farmers and researchers regarding local wind erosion, particularly during early spring, when highest wind erosivity coincides with mostly bare fields.

The primary motivation for this study was the occurrence of wind erosion in one of the four study sites (field C) in central Jutland, North of Viborg in Denmark, although this field was managed and maintained similarly to the other test sites. The urge to find the main reason for this event propelled us to accomplish this investigation. The main aim of this study was to assess the effect of tillage direction on hazard and risk of soil, dust, and nutrient losses by wind erosion from agricultural land in Denmark. The study was based on scenario analysis of erosive winds, ridge height, soil moisture, and field orientation. Indeed, the principal originality of this dissertation is the use of erosive wind probability distributions during dry periods and two main tillage direction scenarios (parallel and perpendicular to the wind) to calculate the hazard and risk assessment of soil, dust and nutrient loss for a single wind erosion event. Furthermore, due to the lack of quantitative information in the study area about wind erosion rate and dust emissions, testing the effects of wind break establishment around agricultural fields on wind erosion rates was another aim of the present PhD-project.

In this study, the amounts of soil and nutrients losses were examined using a wind tunnel under different surface conditions: flat surface, parallel tillage, and perpendicular tillage direction in relation to the dominant wind direction. Four different types of soils from four different study sites were chosen for the simulations and modelling: three soils with loamy sand texture (D50 of 178µm, 194µm, and 214µm) and about 1.5% of carbon content. The fourth soil was an organic soil rich in organic matter (SOC) (12%) with slightly less sand (D50 of 69µm). The results of the wind tunnel tests were

also used to correlate the nutrient and dust ($PM_{2.5}$ and PM_{10}) enrichment in wind erosion sediments for different tillage directions.

Since some of the erosive winds occur simultaneously with precipitation or when the lands are wet after a rainfall event, this research employed a practical approach to use erosive winds during dry periods to improve the quality of predictions. In order to determine the hazard and risk of wind erosion on total soil, dust, and nutrient losses by erosive winds during dry periods, a single-event wind erosion evaluation program (SWEEP) was applied. 32 different scenario simulations on theoretical ploughed agricultural fields were performed. These included: wind speed, ridge height, ridge orientation, and soil moisture content. In addition, all of these scenarios were calculated for unsheltered and sheltered conditions by a single row wind break network.

In order to test the model performance, the results of the predicted total soil loss were evaluated against the observed results from wind tunnel experiments using three common criteria coefficient: Root Mean Square Error (RMSE), coefficient of determination (R^2), and index of agreement (d). Finally, a relative sensitivity analysis was performed to find the most important input parameters for the scenarios, in order to evaluate which parameter controls or accelerates the wind erosion process on poorly aggregated sandy soils. All of these scenarios were assumed in the absence of crop cover or residue or stone cover.

Results showed that the parallel tillage operation experienced the greatest erosion rates for all soil types. However, due to a greater enrichment ratio of dust size particles from perpendicularly tilled surfaces, the scenarios with perpendicular tillage experienced the most significant nutrient enrichment. The main reason for this phenomenon is most probably the trapping of larger particles by the perpendicular furrows. This indicates that the highest rate of soil protection does not necessarily coincide with lowest soil nutrient loss and dust emissions. Therefore, for the evaluation of protection measures on these soil types in Denmark, it is important to differentiate between their effectivity to reduce total soil erosion, dust emission, and nutrient loss.

Results from wind data analysis regarding the general trend of wind direction demonstrated that the prevailing wind direction is predominantly from westerly direction. Temporal analysis of erosive wind velocities indicate that the most sensitive time for the occurrence of an erosive wind erosion event is March in the time between 12:00 to 15:00.

The results from the model performance evaluation for loamy sands class 2 and 3 proved a remarkable similarity between the SWEEP model results and observed values from wind tunnel simulations, but for loamy sand class 1, the SWEEP model under-estimated total soil loss. Regardless of the different scales of a wind tunnel simulation and the field scale model, it seems that SWEEP was not able to predict accurately soil loss for very fine sandy soils. The relative sensitivity analysis confirmed that ridge orientation and wind direction were the most sensitive factors which accounted together for 51 percent of total sensitivity (equally 25.5% for each parameter). This implies that ridge orientation in

relation to the wind direction in ploughed lands, without vegetation cover, can accelerate the total soil loss by wind erosion.

Results showed that all of the scenario numbers, which were performed for the average amount of soil surface water content (0.15 Mg/Mg), have not shown any hazard and risk values for soil loss regardless of soil type. Except of one scenario with a 10 cm ridge height perpendicular to the wind (SN12), there were no predicted hazard and risk values for the perpendicular ploughed soil surface with a 10 cm ridge height under all conditions of soil moisture and wind speed. Therefore, there were only 9 scenarios among all 32 possible scenarios with a minimum amount of total soil loss and PM_{10}.

Since in the current condition of the four study sites, fields A and B are ploughed perpendicularly to the wind and parallel tillage to the wind direction was done for fields C and D, the scenario analysis for current conditions showed that field C with loamy sand class 3 observed the highest potential risk to wind erosion with 6 active scenarios in contrast to 3 active scenarios for farms A and B. Results demonstrated that a 5 cm increase of ridge height in unsheltered area during highest erosive winds led to a minimum of seven times reduction of total soil loss hazard (55.80 versus 7.70 t/ha) and risk values (10.04 versus 1.39).The results also showed that the highest risk of nutrient losses were related to TOC and $CaCO_3$ with 137.09 (761.89 kg/ha of hazard) and 29.99 (166.66 kg/ha of hazard) values respectively in scenario number 31 as the worst case scenario. Using a single row wind break could reduce these risk values by up to 4 times. On field D with organic soil, like in field C, the land is currently ploughed parallel to the erosive wind direction. However, because of this soil type inherent resistance to wind erosion, there was only one scenario with the minimum amount of hazard and risk value (SN32). Other potential scenarios for this field did not show any values for the total soil, PM10, and nutrient losses. In addition, the establishment of a wind break could decrease the risk of total soil loss, dust emission (PM_{10}), and all nutrient loss risks in the worst case scenario to more than 70 %. Results illustrated that unlike in hazard assessments, which represented SN32 as the worst case scenario to total soil loss, dust emission, and nutrient mobilization, among all potential risk scenarios, the highest risks have occurred in SN31 due to a higher probability of accordance for erosive winds in dry periods compared to SN32 (18% versus 2.5%).

By using appropriate land management techniques to control the destructive effect of wind erosion in the study sites, especially by establishing a wide network of shelterbelts around the farms, the effect of wind erosion could be considerably reduced. However, the results of this study show that wind erosion is still a potential hazard and risk in sandy soils, if parallel tillage is performed.

Keywords: *Wind erosion, Dust, Simulation, Modeling, Hazard, Risk, Tillage, Nutrient, Denmark*

Acknowledgements

"Knowledge is in the end based on acknowledgement"
Ludwig Wittgenstein (1889-1951)

I would like to take this opportunity to acknowledge various contributions and supports that enabled the completion of the research reported herein.

First and foremost I would like to express my sincere gratitude to my supervisors Professor Dr. Nikolaus Kuhn and Dr. Wolfgang Fister who gave me opportunity to join their research group at the University of Basel and providing an excellent atmosphere for my studies and research. I never forget their helpful advices and patience during field work, laboratory analysis and for their constructive remarks on thesis, without whom would not have been possible.

I am deeply grateful to my co-referee Dr. Goswin Heckrath, for his valuable guidance, comments and encouragement on thesis. I wish to thank Professor Dr. Peter Nagel for serving as the chair for my doctoral dissertation defense.

I would like to express my deepest gratitude to my internal advisor in Iran, Professor Dr. Majid Ownegh for his excellent guidance, from the time of my undergraduate to now and for his physical geography course.

I would like to thank the Ministry of Science, Research and Technology of Iran for financial support of this research and the scientific representative of the Iranian students in the Schengen area for his help during my studies in Switzerland.

Many people have contributed in some way to the completion of the thesis, and I am grateful to all of them for their cooperation and support. A special word of thanks goes to the following persons:

I would like to thank Eahsan Shahriyari, who as a good friend was always willing to help and give his best suggestions in statistical analysis.

I gratefully acknowledge the invaluable technical support for the experiments and laboratory analysis carried out for the completion of this thesis that provided by Ruth Strunk and Hans-Rudolf Rüegg. I would like to remember dearly departed Marianne Caroni, a member of laboratory staff who is still sorely missed in the department.

Many other individuals provided much valuable advices and scientific guidance. In no particular order, thank you to Mohammadali Saremi Naeini, Rosmarie Gisin, Florence Bottin, Dr. Philip Greenwood, Matthias Hunziker, Liangang Xiao, Dr. Harald Hikel, Lukas Zimmermann and Matthias Würsch.

I would however like to express my gratitude to Dr. Ali Najafinejad, Dr. Amir Sadoddin, Dr. Vahedberdi Sheikh, Dr. Hamidreza Asgari and Dr. Mohsen Hosseinalizadeh, my colleagues at the Department of Watershed and Arid Zone Management, Gorgan University of Agricultural Sciences and Natural Resources, Iran.

Finally, My special thanks to my parents for everything that they have given me, my wife, Somayeh, for her patience and understanding, and my daughter (Pooneh) and my son (Taha) for their lovely smiles which sweep away my stress.

List of Contents **Page**

List of Figures **Page**

Chapter 1

Chapter 2

Chapter 3

Chapter 4

List of Tables **Page**

Chapter 1

Chapter 2

Chapter 3

University of Basel

Hazard and Risk Assessment of Wind Erosion and Dust Emissions in Denmark - A Simulation and Modelling Approach

Introduction

"If you cannot calculate something accurately, you probably don' t understand it very well"

Lord Kelvin (1824-1907)

CHAPTER 1

1. Introduction and state of the art

One of the major environmental challenges for present-day humans is to live and grow food sustainably for a growing population on rather fragile soils. Among others, wind erosion, including detachment, transport, and deposition of fine particles in the landscape, has been identified as one of the most important processes leading to soil degradation (Wang and Shao, 2013). Roughly 28% of land, equaling over 500 million hectares, is affected worldwide. These areas are emitting between 500 and 5000 Tg of dust into the atmosphere annually (Oldeman, 1994; Callot et al., 2000; Prospero et al., 2002; Grini et al., 2003). Global 'anthropogenic' dust emissions have been estimated to be up to 50% of the total modern dust (IPCC 2001). Tegen and Fung (1995) proposed that about 50% of the total atmospheric dust originates from disturbed soils as a consequence of cultivation, deforestation, and lack of vegetation caused by droughts and reduced rainfall. However, recent investigations indicate that probably less than 10-25% of the global dust emissions originate from agricultural soils (IPCC, 2005). Nevertheless, wind erosion on agricultural land can be a serious problem for soil quality and could create strong negative effects on air quality and visibility, even in humid areas. Although wind erosion dominantly occurs in arid and semi-arid areas and water erosion is dominant in more humid areas, both are a global phenomenon (Yang et al., 2006). An example for the presence of wind erosion in humid regions are the agricultural areas of north and central Europe, where the land surface mainly consists of poorly aggregated sandy substrates, which are readily eroded by strong wind events after the protective vegetation cover has been removed for agricultural purposes (Riksen and de Graaff, 2001). Because of this reason, relatively large areas, for example in northern Germany (about 2 million ha), the Netherlands (97,000 ha), western Denmark (about 1 million ha), southern Sweden (170,000 ha) and southeastern and eastern England (260,000 ha), are affected by wind erosion (Riksen et al., 2003).

The first part of this introductory chapter presents an overview on wind erosion processes, its spatial distribution in Europe, and more specifically, its occurrence in Denmark, then the problem and aims of this study have been addressed.

1.1 Wind erosion

1.1.1 Overview on processes and effects

Wind erosion, a worldwide problem, is the erosion, transport, and deposition of soil particles by wind. This process is of special importance, because this phenomenon can have considerable effects on the air and water quality, human health, quantity and quality of crop production, and other on-site as well as off-site effects (Chappell and Thomas, 2002). The release of organic matter and nutrients from the soil by wind erosion can lead to a loss of these valuable materials into the atmosphere, and by that reduce the amount of available nutrients on the ground (Raupach et al., 1994; Leys et al., 2008). Wind erosion is, therefore, recognized as an important process for removing and redistributing topsoil and its nutrients (Sterk et al., 1996; Larney et al., 1998; Wang et al., 2006). The dust emissions contain a considerable amount of soil organic carbon and nutrients which are attached to the fine particles or are suspended freely in the atmosphere (Zobeck and Fryrear, 1986; Van pelt and Zobeck, 2007). Because of its negative effects on the environment and health of human beings and animals, the EPA (Environmental Protection Agency) has set the allowable limit for dust particulate matter less than 10 micrometers (PM_{10}), as an air quality standard index, at 150 $\mu g/m^3$ per 24 hours. From the physical point of view, wind erosion also has a strong effect on particle size distribution and water holding capacity of soils (Zhao et al., 2006), which in return, severely affect the likelihood of occurrence of wind erosion.

Generally, a wind erosion event and the associated soil particle movement are induced when one of the following atmospheric and soil surface conditions occur (Riksen et al., 2003; Shao, 2008 and Borrelli et al., 2014a):

1) The wind is strong enough to mobilize soil particles (a factor that depends on threshold wind velocity, wind intensity, wind frequency, duration, and wind direction)
2) The soil surface characteristics are susceptible to the initiation of particle movement (a factor that depends on soil texture, organic matter, and soil surface moisture)
3) The soil surface is mostly bare of vegetation, stone, snow, and any other natural and artificial obstacles.

There are three distinct transport modes by a wind erosion event (Figure 1.1), which depend on particle size (Shao, 2008): creep or reptation for material coarser than 500 microns, saltation for material of sizes between 70 to 500 microns, and suspension of particles smaller than 70 microns.

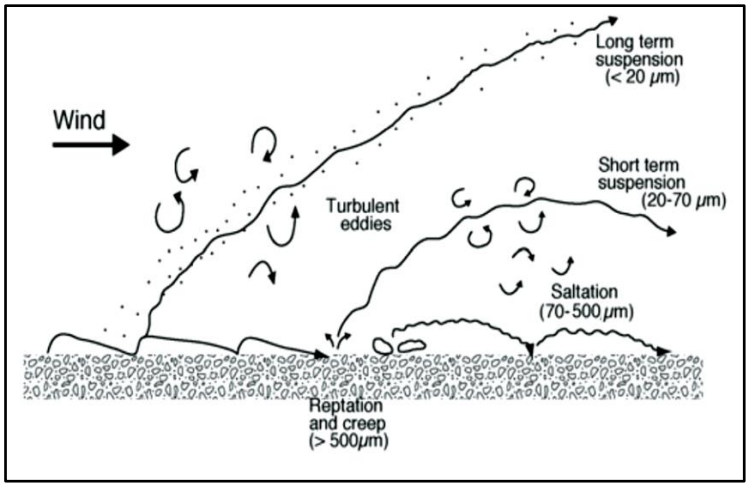

Figure 1.1. The different wind transport processes and the size of the particles (after Pye, 1987).

The negative effects of wind erosion on the soil surface itself, the so-called on-site effects, can be differentiated as follows (Leys, 1999; Riksen and de Graaff, 2001):

1) Loss of organic material and rich nutrients in topsoil;
2) Selective removal of fine particles;
3) Loss of seeds and plants;
4) Loss of fertilizers and pesticides;
5) Damage to stems and leaves of plants;
6) Damage to machinery;
7) Damage to roads and construction works;
8) Postponement of agricultural operations.

The off-site effects of wind erosion are mainly the result of dust emission into residential areas as follows (Lal, 2001; Riksen and de Graaff, 2001; Webb, 2008)

1) Eutrophication due to dust deposition/damage to nature reserves and ground water;
2) Dust in residential areas and damage to the human and animal health;
3) Penetration of dust in machinery, road and decrease of atmospheric visibility;
4) Spread of herbicides and pesticides off-farm;
5) Sedimentation in ditches, hedges.

1.1.2 Parametrization of wind erosivity and soil erodibility

Basically, the wind erosivity and the soil erodibility are considered as the most influential wind erosion factors (Webb and Strong, 2011), accordingly the sediment transport rate depend on both the wind erosivity and the soil erodibility. Nordstrom and Hotta, (2004) state

that the factors affecting the susceptibility of the surface to aeolian transport include climate, sediment supply (controlled by soil properties and surface characteristics), effectiveness of ground cover (controlled by vegetation characteristics), and active farming operations. Therefore, simulations and predictions of wind erosion and dust emission require a better representation of both land characteristics (soil and land surface) and the driving meteorological parameters, such as wind patterns and velocities (McTainsh et al., 1999).

Wind erosivity is defined as the capacity of a wind to induce sufficient erosion to remove the top soil layer. It depends on the interactions between different climatic parameters which control an erosive wind event such as intensity, frequency and duration of wind velocity and wind direction (Funk and Reuter, 2006). Table 1.1 shows the various wind and soil parameters that are controlling the wind erosivity and soil erodibility in a wind erosion event:

Table 1.1. General parameters that influence wind erosivity and soil erodibility in a wind erosion process

Wind erosivity	Soil erodibility	
	Soil and aggregate parameters	Surface parameters
• Velocity	• Grain size and erodibility fraction	• Vegetation and crop residue (Height,
• Frequency and probability	• Height of aggregates	Orientation, Density)
• Duration	• Dry aggregate stability	• Soil moisture
• Area	• Aggregate orientation	• Soil roughness (ridges, clods)
• Shear stress	• Power of particles to abrasion	• Surface length
• Turbulence	• Organic matter	• Topography
	• Clay content	• Field size
	• Bulk density	• Surface crust

Soil erodibility is defined as the soil sensitivity to be eroded by wind erosion and has been known as inherent resistance of soils to the erosive factors (Webb and McGowan, 2009). The erodibility of a soil can be determined by two main indexes:

1) Assessment of the wind-erodible fraction (EF):

The wind-erodible fraction (EF) was introduced as one of the key parameters for estimating the susceptibility of soil to wind erosion (Borrelli et al., 2014b). Chepil (1950) determined relative erodibilities of soils based on measurements of dry soil aggregates of various sizes. The results showed that aggregates larger than 0.84 mm in diameter were non-erodible, so EF was presented as the percentage of soil aggregates smaller than 0.84 mm in diameter. Fryrear et al., (1994) proposed an empirical formula to calculate EF based on contents of organic matter, sand, silt, clay and calcium carbonate as predictive variables (equation 1.1):

$$EF = (29.09 + 0.31\ sand + 0.17\ silt + 0.33\ sand/clay - 2.59\ organic\ matter - 0.95\ CaCO3)/100 \quad (1.1)$$

where all of the parameters are in percentages.

2) Threshold wind velocities (U_t^*) index that have been extrapolated for different soil types are widely used for the soil erodibility, especially in the regional scales. Threshold wind velocities depend on spatio-temporally of soil conditions for blowing the particles by the erosive winds. For example, soil moisture is one of the main factors which are directly affected wind erosion and dust emission rates. The threshold wind speed for a bare, dry surface is a function of particle size and can be parameterized by considering the positive and negative forces that act upon the soil particles which is control wind erosion transport rate (Lu and Shao, 2001). Also, soil moisture by increasing inter-particle cohesive forces exceeds the threshold wind velocity (Webb and McGowan. 2009). Therefore, wind erosion transport (q) conditions could be formulized as equation 1.2 and 1.3 (Stout and Zobeck, 1996):

$$U \leq U_t^* \qquad q = 0 \quad (1.2)$$

$$U > U_t^* \qquad q = 1 \quad (1.3)$$

1.1.3 Parametrization of soil surface roughness

The soil surface roughness effects on both the soil erodibility and the wind erosivity (Zobeck, 1991). Soil surface aggregates (random roughness) and ridges (oriented roughness) can reduce soil loss by wind erosion (Fryrear et al., 1994; Colazo and Buschiazzo, 2010). Therefore, using tillage operations to create a rough surface is often recommended to control wind erosion in source areas (Hevia et al., 2007). By increasing the surface roughness, the threshold wind velocity increases and the wind erosion potential is theoretically reduced. One of the main direct impacts of rough surface created by tillage, especially in uncovered soils, is trapping efficiency. The parallel tillage to the prevailing wind has low efficiency to particles and aggregates trapping whereas perpendicular tillage to the wind can decrease particle movement considerably via trapping of particles (Zobeck and Van Pelt, 2014). Figure 1.2 shows a schematic diagram of trapping efficiency for the perpendicular (Figure 1.2a) and parallel (Figure 1.2b) ploughed surface to the prevailing wind direction.

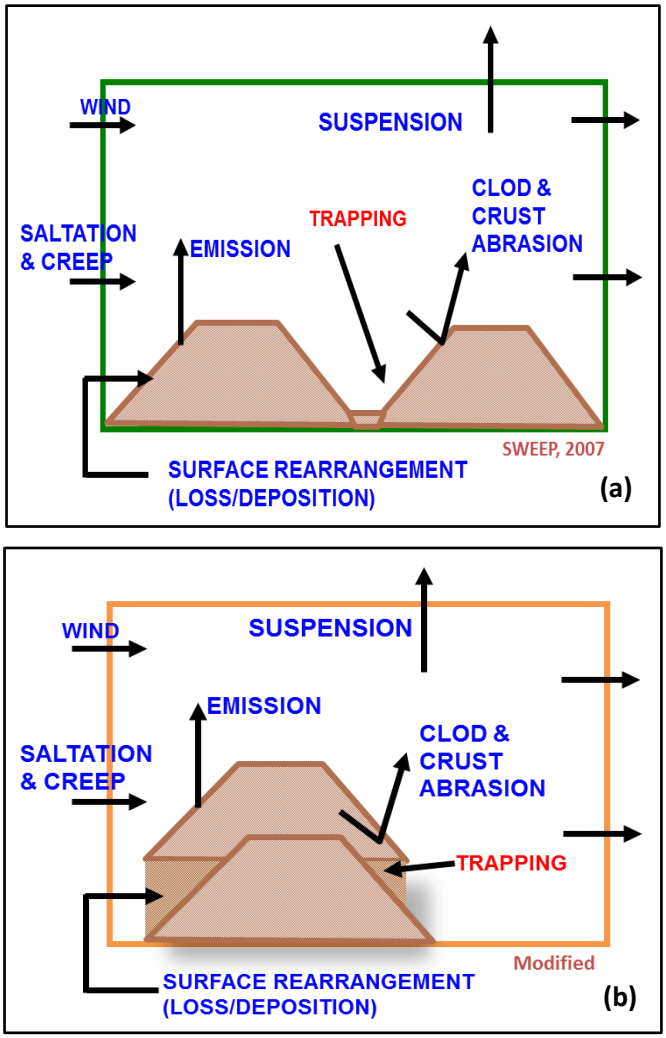

Figure 1.2. Diagram of trapping efficiency with a ridged bare soil illustrating the sources and sinks used in the SWEEP model under different ridge orientation to the prevailing wind; (a): perpendicular to the wind and (b): parallel to the wind (Hagen and Armbrust, 1992)

However, in poorly aggregated soils, this increase of parallel-oriented roughness to the wind direction can, in contrast, lead to an increase of soil loss compared to flat surfaces (Lopez et al., 2000; Hevia et al., 2003; Gomes et al., 2003; Liu et al., 2006; Buschiazzo and Zobeck 2008; Zobeck and Van Pelt, 2011). Wang et al., 2006 demonstrate that soil loss by wind can be reduced by up to 79% on arable land, when the conventional tillage system changes to no-till. Therefore using reduced tillage or no-tillage has a significant effect on sand mobilisation and dust emission compared to the conventional tillage (Gomes et al., 2003; Kardous et al., 2005; Liu et al., 2006). However, Goossens et al., (2001) state that agricultural practice by machinery itself could be one of the main factors responsible for dust emission into the atmosphere.

1.2 Wind tunnel simulations

Since 1940s, wind tunnels have been used in many wind erosion researches. The first efforts to simulate wind erosion using wind tunnel-based investigations were carried out by Bagnold (1943) and Chepil (1950) and mainly focused on erodibility of soils with sandy textures. Therefore, the main purpose for using wind tunnel experiments in wind erosion studies is to investigate the physics of particles movement. The results from different researches over the last three decades have demonstrated that almost all data were obtained from wind tunnel experiments used to simulate the mechanism of wind erosion, determination of soil erodibility, movement of fugitive dust emissions and sediment particles, measuring the nutrient losses from soil surfaces, simulation of reshaping sand dunes and development and validation of numerical models (Hagen, 2001; Feng et al., 2009; Han et al., 2009; McKenna Neuman et al., 2009; Hagen et al., 2010; Roney and White, 2010; Van Pelt and Zobeck, 2013).

Using a wind tunnel and the classification of its results for the various soil types and in the range of wind speeds, is able to determine of soil erodibility. Therefore, a major advantage of wind tunnel studies is that they make it possible to conduct experiments under scientifically controlled conditions. It is easier to control the number of variables operating at any one time, compared with typical field situations, and conditions can be held constant long enough for experiments to be completed and repeated (Liu et al., 2006; Shao, 2008; Van Pelt and Zobeck, 2013). The main drawbacks relate to problems of scaling, but these need not undermine the value of modelling work if appropriate precautions are taken. Despite the problem that the conditions in a wind tunnel are just a simplified model of the natural situation, they have always been an essential tool for simulating quasi-natural wind-erosion processes under controlled conditions (Maurer et al., 2006; Van Pelt et al., 2010).

1.3 Wind erosion modelling and efficiency criteria

Transformation of environmental complexity to simple equations for assessment of natural processes is called a model. In a phrase expressed by Wainwright and Mulligan, (2013), a model is "*finding simplicity in complexity*". In other words, models are simple or multiple resultants of statistical proportions between dependent and independent variables which are reached from distinctive practical and laboratory analysis results. Over time and according to researchers' requirements, many wind erosion models as a part of environmental models have been developed to calculate important indices affecting aeolian processes. A major problem for scientists is the scale of models. The area of investigation and therefore the model scale ranges from point to global scale up to multi-scale models. As shown in Figure 1.3, these

different scales are often referred to as field or farm, regional, continental, and global dimension (Webb, 2008). In addition, the structure of models (empirical, physically or process-based) and the quality of input and expected output data are concerns of model developers. Obviously, model performance, calibration, verification, validation, and sensitivity analysis of the model parameters play key roles in the model selection process (Webb et al., 2006).

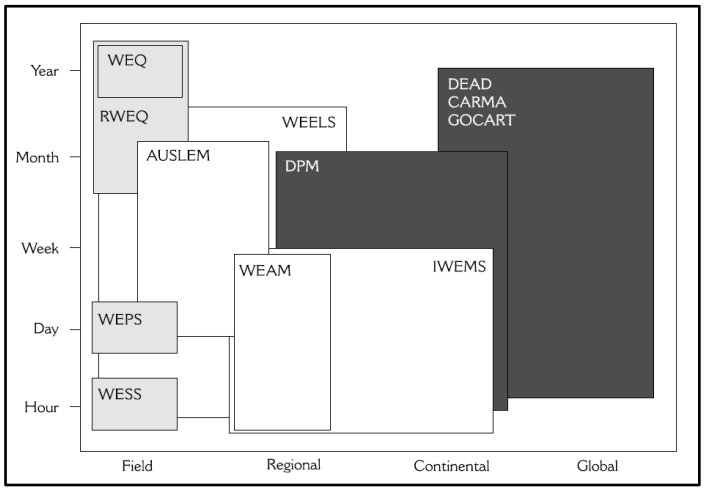

Figure 1.3. Spatial and temporal scales of wind erosion models reviewed by Webb and McGowan, (2009). Light gray boxes represent field scale models, white boxes represent regional scale models and dark gray boxes represent global scale models.

In general, wind erosion models are developed based on two transport processes, which occur simultaneously during a wind erosion event and can be expressed with two indices (Okin, 2005): 1) Horizontal soil flux and Vertical dust flux

Vertical flux (dust emission) is a result of horizontal soil flux (saltation flux), because saltating particles sandblast the soil surface and eject fine particles (Okin, 2005). Vertical dust flux affects atmospheric composition, air quality and climate change. $PM_{2.5}$ (Particulate matter of diameter less than 2.5 micrometers) and PM_{10} are the most common dustiness indices which are commonly used for the air pollution monitoring. Based on the research focus and background of the scientists, a large number of aeolian models have been developed to estimate wind erosion and dust emission fluxes. Table 1.2 gives an overview of different models according to the scale of the model, the input data and main outcomes. Models have several capabilities to predict and simulate different stages of aeolian processes such as: the threshold friction velocity representing main index of detachment, the rate of sand transport to measure horizontal soil flux and the rate of dust emission representing soil surfaces capabilities to produce dust storms.

Table 1.2. Summary of wind erosion and dust emission models reviewed, indicating spatial scale, time step, main input and output for each model (modified Webb, et al., 2006)

	Model	Spatial scale: Plot Field Region National	Time step: Event Daily Monthly Annual	Main input data	Basis of erosion component	Output	References
1	EPIC- Wind Erosion sub-model	F	D	Climatic conditions, landscape characteristics, soil properties and management	Process based	Wind erosion	Williams et al, 1989
2	Et, Ew, Em indices	N+R	M+A	Wind, precipitation, evaporation	Climatic records	Dust storm frequency/intensity	Burgess et al., 1989; McTainsh et al., 1998, 1990
3	WEAM	P+F+R	A	Climate, soil types, vegetation cover	Physically based	Dust flux	Shao et al., 1994
4	DPM	R+N	E	Wind profiles, Soil characteristics, Particle fluxes	Physically based	Dust flux	Marticorena and Bergametti, 1995
5	DUSTRAN	P+F+R+N	E	Sediment load, source areas, soil loss rates	Source based	Dust flux	Butler et al., 1996
6	Dust Storm Index (DSI)	R+N	D	Dust event observation	Climatic records	Dust storm frequency/intensity	McTainsh and Tews, 1998
7	LEI	P+F+R	M+A	Dust flux	Indices	Land erodibility index	McTainsh et al., 1999
8	WEELS	R	M+A	Wind, land use and soil conditions	Physically based	sand and dust fluxes	European union, WEELS Report, 2000
9	DREAM	R+N	D+M+A	Surface conditions, vegetation Soil moisture, atmospheric turbulence	Physically based	Dust flux	Nickovic et al., 2001
10	IWEMS	F+R	E+M	Climate, soil state, surface roughness	Physically based	Dust flux	Lu and Shao, 2001
11	DEAD	R+N	D+M+A	Wind speeds, Soil erodibility, Soil moisture, Satellite data	Physically based	Dust flux	Zender et al., 2003
12	TEAM	P+F	E	Wind, Soil moisture, humidity, Wind breaks, cover	Process based	Deflation, dust flux	Gregory et al., 2004
13	(R)WEQ	F	E+M+A	Soil surface condition, Climate, Field length, Vegetation cover	Process based spreadsheet	Deflation, dust flux	Van Pelt et al., 2004; Visser et al., 2005
14	WEPS	F	D	Climate, crop, soil, management	Process based	Deflation, dust flux	Hagen, 2004
15	WESS	F	E	Wind, soil surface, ridge height	Process based	Deflation, dust flux	Van Pelt and Zobeck, 2004
16	AUSLEM	F+R+N	M	Rainfall, Soil surface condition, Vegetation,	Physically based	Landscape erodibility	Webb, N.P., et al., 2006
17	BoDEx	R	D	Wind velocity, vegetation, Snow, particles of size fraction, air density	Physically based	Dust flux	Washington et al., 2006
18	WRAP	R	A	Soil surface condition, Vegetation, climate Factor	Physically based	Dust emission	Tonnesen et al., 2006
19	CEMSYS	R+N	E+M+A	Atmospheric conditions, land surface, GIS database	Physically based	sand and dust fluxes	Shao et al., 2007
20	SWEEP	F	E	Soil layer, Soil surface, Biomass, Weather	Process based	Deflation, dust flux	USDA-ARS Wind Erosion Research Unit, 2008
21	WACM	R	A	Water use, Vegetation, Soil, Meteorological conditions	Physically based	Wind erosion	Yong and Yuan-sheng, 2010

In order to determine the accuracy or goodness of fit of models, the evaluation techniques are needed. There are many efficiency criteria for the evaluation of environmental models (Table 1.3): root mean square error (RMSE), coefficient of determination (R^2), coefficient of residual mass (CRM), Nash-Sutcliffe efficiency (NSE) and modified NSE method (MNSE) (Krause et al., 2005; White and Chaubey, 2005; Jakeman et al., 2006; Zar 2010). However, there are three efficiency criteria that are recommended to be used to test the reliability and accuracy of model prediction against data from wind tunnel simulations, being coefficient of determination, root mean square error and index of agreement (Legates 1999; Feng and Sharratt 2007, Youssef et al., 2012).

Table 1.3. Statistical measures for the model evaluation

Coefficient	Equation	Range of variability	Publication
Root mean square error	$\mathrm{RMSE} = \left[\sqrt{\frac{\sum_{i=1}^{n}\left(Q_i^{pre} - Q_i^{obs}\right)^2}{n}}\right]$	0 to $-\infty$	Legates and McCabe (1999), Feng and Sharratt (2007)
Nash-Sutcliffe efficiency	$\mathrm{NSE} = 1 - \left[\frac{\sum_{i=1}^{n}\left(Q_i^{obs} - Q_i^{pre}\right)^2}{\sum_{i=1}^{n}(Q_i^{obs} - Q_{mean}^{obs})^2}\right]$	$-\infty - 1$	Nash and Sutcliffe (1970)
Modified Nash-Sutcliffe efficiency	$\mathrm{MNSE} = 1 - \left[\frac{\sum_{i=1}^{n}\left\|Q_i^{obs} - Q_i^{pre}\right\|}{\sum_{i=1}^{n}\left\|Q_i^{obs} - Q_{mean}^{obs}\right\|}\right]$	$-\infty - 1$	Willmott (1981)
Percent bias	$\mathrm{PBIAS} = \left[\frac{\sum_{i=1}^{n}\left(Q_i^{obs} - Q_i^{pre}\right) * 100}{\sum_{i=1}^{n}(Q_i^{obs})}\right]$	(%)	Moriasi et al., (2007)
Ratio of the root mean square error to the standard deviation of measured data	$\mathrm{PSR} = \frac{\mathrm{RMSE}}{STDEV_{obs}} - \left[\frac{\sqrt{\sum_{i=1}^{n}\left(Q_i^{obs} - Q_i^{pre}\right)^2}}{\sqrt{\sum_{i=1}^{n}(Q_i^{obs} - Q_{mean})^2}}\right]$	-	Legates and McCabe (1999), Moriasi et al., (2007)
Coefficient of determination	$r^2 = \left[\frac{\sum_{i=1}^{n}(Q_i^{obs} - Q_{mean}^{obs})(Q_i^{pre} - Q_{mean}^{pre})}{\sqrt{\sum_{i=1}^{n}(Q_i^{obs} - Q_{mean}^{obs})^2}\sqrt{\sum_{i=1}^{n}\left(Q_i^{pre} - Q_{mean}^{pre}\right)^2}}\right]^2$	$0 - 1$	Dodge (2008)
Coefficient of residual mass	$\mathrm{CRM} = \frac{\sum_{i=1}^{n} Q_i^{obs} - \sum_{i=1}^{n} Q_i^{pre}}{\sum_{i=1}^{n} Q_i^{obs}}$	$-\infty - \infty$	Loague and Green (1991), Feng and Sharratt (2007)
Index of agreement	$\mathrm{d} = 1 - \left[\frac{\sum_{i=1}^{n}\left(Q_i^{pre} - Q_i^{obs}\right)^2}{\sum_{i=1}^{n}\left(\left\|Q_i^{pre} - Q_{mean}^{obs}\right\| + \left\|Q_i^{obs} - Q_{mean}^{obs}\right\|\right)^2}\right]$	$0 - 1$	Youssef et al., (2012)
Modeling efficiency	$\mathrm{EF} = \left[\frac{\sum_{i=1}^{n}\left(Q_i^{obs} - Q_{mean}^{obs}\right)^2 - \sum_{i=1}^{n}\left(Q_i^{pre} - Q_i^{obs}\right)^2}{\sum_{i=1}^{n}(Q_i^{obs} - Q_{mean}^{obs})^2}\right]$	-	Loague and Green (1991),
Maximum errors	$\mathrm{ME} = \mathrm{Max}\left\|Q_i^{pre} - Q_i^{obs}\right\|_{i=1}^{n}$	-	Feng and Sharratt (2007), Youssef et al., (2012)

1.4 Nutrient loss and enrichment ratio

Nutrient loss from soils is recognized as an on-site effect of wind erosion (Riksen and Graaff, 2001). Depending on the dominating processes, the amount of nutrients transported by horizontal sand flux or vertical dust flux vary significantly (Saxton et al., 1999; Wang et al., 2006; Li et al., 2007; Yan et al., 2011) and effects the soil nutrient balance (Visser et al., 2005; Warren 2007; Yan et al., 2011; Munodawafa, 2011). Therefore, wind erosion is known as one of the key variables to estimate nutrient levels of natural ecosystems (McCoy et al., 2007).

The nutrient enrichment ratio represents the relation between the amount of nutrients in eroded sediment versus the amount of nutrients in the original soil and has been documented in many wind erosion studies (Sterk et al., 1996; Larney et al., 1998; Leys and McTainsh, 1999; Bielders et al., 2002; Visser et al., 2005; Buschiazzo et al., 2007; Sankey et al., 2012; Webb et al., 2013). The redistribution and enrichment of nutrients play a key role in the nutrient cycles (Webb et al., 2013; Buschiazzo and Funk, 2015). Most of the soil nutrients are transported via saltation and suspension (Sterk et al., 1996). This demonstrates that the enrichment of suspended particles with nutrients is higher than in creep material. Because of the selectivity of the aeolian process, the fine particles with highest nutrient contents are the most prone to detachment and transport (Zobeck and Fryrear, 1986; Sterk et al., 1996; Chappell and Thomas, 2002; Visser et al., 2005; Buschiazzo et al., 2007).

Soil organic carbon (SOC) is recognized as a sensitive index for soil nutrient loss and shows a good relationship with wind erosion intensity (Yan et al., 2005; Aimar et al., 2012). Sandy soils, because of having poor or non-aggregated conditions, have a low threshold friction velocity and are, therefore, classified as highly susceptible to wind erosion, especially in agricultural lands (Warren, 2007). Sterk et al. (1997) showed a total nutrient loss during two erosion events including 79.6 kg/ha Carbon, 57.1 kg/ha Potassium, 18.3 kg/ha Nitrogen, and 6.1 kg/ha Phosphorus in the Sahelian zone of Niger. The enrichment ratio of the nutrients in the eroded sediment in a height up to 50 cm were 2.25 for C, 1.72 for K, 1.44 for N and 1.07 for P, respectively. This revealed that soil loss by wind erosion may cause to decline crop productivity and soil aggregate properties over times.

1.5 Wind erosion hazard and risk

Risk and hazard assessment have become a key part of management plans for environmental threats. Unlike hazard that has a deterministic concept, basically a risk has a probabilistic concept. The terms risk and hazard can be defined as follows:

Hazard: Something that has the potential to cause wind erosion increase in comparison to natural erosion.

Risk: A 'risk' is the probability of the occurrence of a hazard that could accelerate wind erosion in a land or ecosystem system.

The risk assessment process provides a method to control, monitor, and review of a risk factor, whether this risk occurs right now or could happen or accelerate in the future. Therefore, risk is an event, which is (UN, 2002):

1) uncertain, and

2) has a negative impact due to wind erosion.

The general concept of risk can be presented in the equation 1.4 (UN, 2002):

$$Risk = Hazard * Probability \quad (1.4)$$

In order to mitigate an erosion risk condition, it is necessary to develop a risk management strategy. Commonly, there are two main distinguished concepts for the soil erosion risk: Firstly, the potential soil erosion risk, which is defined as the inherent risk of an erosion event, regardless of the current land use or any conservation practices. This represents the worst case scenario. Secondly, the actual soil erosion risk that involves the protective aspects provided by current land management scenarios and also the intrinsic threat of applied land use change practices (CORINE, 1992). Therefore, determination of wind erosion hazard and risk are considered to be main components of a risk management plan (Figure 1.4).

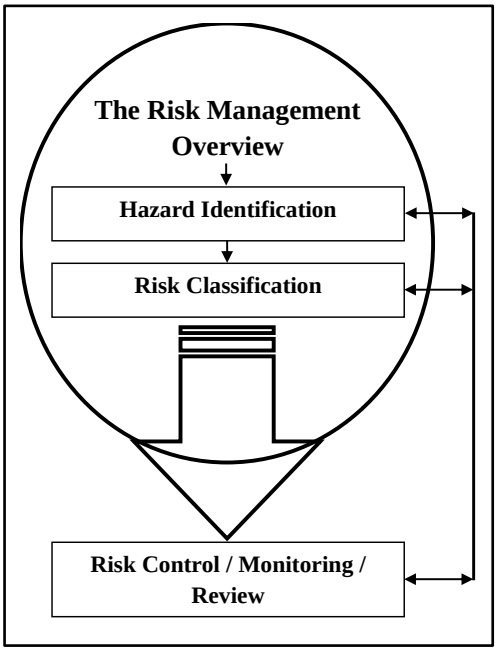

Figure 1.4. Risk management overview

A risk **control** is a mechanism or process that minimizes the risk of the hazard. Therefore, it protects the land from destructive effects of wind erosion. A risk assessment considers not only the incidence of a wind erosion hazard but also it calculates the vulnerability of a hazard under different probability scenarios.

Several erosion indices and models are used to predict wind erosion rates and to assess soil erosion risk. Assessing the vulnerability of different soil types to wind erosion is done by using different qualitative and quantitative approaches. In order to classify the risk of wind erosion, the qualitative methods are mostly restricted to regional or larger scales (Vrieling et al., 2002). They are dominantly based on: (1) qualitative mapping of soil using soil texture and land use management (Conrad et al., 2006; Li et al., 2010; Reiche et al., 2012), (2) site comparison methods (Deumlich et al., 2004) and (3) using a combination of climatic factors together with land cover and soil moisture (Mezösi and Szatmàri, 1998). For example, soils with low vegetation cover or well developed drainage systems (Deumlich et al., 2006) have more risk to experience wind erosion. Another example is the inherent soil characteristics that directly affect the soil susceptibility to wind erosion. For instance, sandy soils are, in comparison to well-aggregated soils, much more susceptible to wind erosion. Another approach for risk assessments is the use of meteorological data-based indices. They are mainly based on threshold wind velocities for specific regions. This method is used as a common approach for mapping and classifying the susceptibility of specific areas to wind erosion from a local to regional scale. Furthermore, Podhrazska and Novotny (2007) used a GIS- based technique that used the tolerable field length as parameter to predict the risk of wind erosion. They introduced 850 meter as a threshold field length, above which the wind erosion risk increases.

The quantitative methods to calculate the risk of wind erosion can be divided into index- and model-based indices:

1) Index-based methods

The most frequent method employed to classify the wind erosion risk is, mapping different soil types based on soil erodibility. This index was proposed by Woodruff and Siddoway (1965) for the first time and then utilized in the wind erosion equation (WEQ) as ‘I’ factor. The others indices that have been modeled afterwards are somehow derived from WEQ and RWEQ (revised wind erosion equation) models. For example, FAO (1980) presented a wind erosion risk (WER) method according to the WEQ model, by multiplying soil erodibility (I) by climatic factor (C) as equation 1.5.

$$WER = I * C \tag{1.5}$$

Beinhauer and Kruse (1994) introduced the wind force integral index (WFI). The WFI defines the potential transport capacity of the wind at the soil surface as a function of the wind force and the threshold wind velocity, which depend on the surface moisture. This WFI index is for example used in the RWEQ model with following formula (equation 1.6):

$$WFI = \sum_{i=1}^{n} (U - U_t) * U^2 \tag{1.6}$$

U: wind speed at 2 meter height

U_t: threshold wind velocity at 2 meter height

n: number of wind speed observations (i) in a time step of 1-15 days

Yang et al., (2011) presented a wind erosion risk index (WERI) which is a normalized estimation of wind erosion risk. This model can be applied for modelling and mapping between different amounts of wind erosion and dust concentration risk in Australia from time-series of ground cover (V), soil moisture (S) and wind speed (C) as following (equation 1.7):

$$WERI = \frac{Wind\ speed\ (C) * bare\ soil(V)}{soil\ moisture\ (S)} \tag{1.7}$$

where soil moisture and bare soil ranged between 0 and 1 (0– 100%), while wind speed ranged from 0 to 13.89 m/s.

2) Model- based methods

Varying model-based approaches have been used to assess the wind erosion risk in different countries. Following is a short overview on the most common models.

The integrated wind erosion modeling system (IWEMS) developed by Lu and Shao (2001), combines atmospheric and land surface data from local to global scale for the assessment of wind erosion. Recently, this model has renamed to computational environmental management system (CEMSYS) and was used to predict the risk of dust generation by wind erosion in Australia. Using soil properties, surface characteristics, and different climate data to determine the pattern and intensity of wind erosion in a high-resolution atmospheric environment, provides appropriate applicability for tracking and predicting dust emission by the IWEMS model.

The Wind erosion on European light soils (WEELS) model is also a process-based model. It was developed to predict soil loss by wind under various climate and land use conditions in North European quaternary plains (Böhner et al., 2003). This model has combined six main modules, which have key roles in wind erosion prediction, including wind (speed), wind erosivity (barriers), soil moisture, soil erodibility (grain size), soil roughness and land use.

The wind erosion prediction system (WEPS) is a process-based, continuous daily time step model. It uses hourly wind speeds and changing management practices to calculate an event based wind erosion risk in Germany (Funk et al., 2004).

Shi et al., (2007) proposed a combination between a neural network and GIS technique in order to calculate wind erosion risk, which they called the radial basis function network (RBFN) model. They used the factors average relief degree of land surface, percentage of sandy soil, the contents of fine sand, percentage of vegetation, degree of soil dryness and intensity of wind energy (from RWEQ model) as main input data to assess the wind erosion risk in Inner Mongolia.

1.6 Wind erosion in Europe and Denmark

Wind erosion is not as significant a problem in Europe as it is in the arid and semi-arid parts of the world, but it nevertheless constitutes one of the major threats to European soils, distinguished by differences in frequency and severity (Borrelli et al., 2014a). During the 18th century and the beginning of the 19th century, concomitant with big land use changes, intense land degradation occurred on European agricultural lands (Table 1.4).

Table 1.4. Temporal classifications of increased wind erosion in Europe since the last glaciation (Deumlich et al., 2006)

Stage	Time	Event
Phase I	late glacial-early Holocene	Most of the recent surfaces were formed. Surface is covered with highly erodible glacial deposits without protective vegetation cover on the ground.
Phase II	18th-19th century	Increasing wind erosion due to deforestation and overgrazing. Severe wind erosion on sand dunes.
Phase III	20th century	Period I: (1947–1960): increase of root crops and decrease of perennial crops and cereals.
		Period II: (1965–1975): rapid increase of areas planted with maize, increasing field sizes and improvement measures.
		Period III: (since 1980): further decrease of areas with grassland and increase of arable land

This land degradation can be attributed to the development of agricultural systems regardless of the land's susceptibility to wind erosion and lack of knowledge on how to prevent or combat wind erosion (Deumlich et al., 2006).

Also amalgamating small fields into larger ones lead to an increase of the fetch length and thus, enhanced the wind's power to erode the soil particles. This land-use change led to more wind erosion and dust emission, with all of its negative outcomes, such as reduced visibility, loss of nutrients, and etc. (Riksen and de Graaff, 2001). The European Union (EU) estimates that about 42 million hectares, or 4% of European lands, are affected by wind erosion at present. Most of the affected areas are used for agricultural purposes (EEA, 2003; European Commission, 2006).

Another key factor that can influence soil erosion in Europe is climate, which acts via the creation of changes in temperature and precipitation that can cause an acceleration of wind erosion. For example, based on a report by the UK Climate Impacts Program, a 50% reduction in the summer precipitation by 2080 may cause up to a 40% decline in soil moisture content (Tye, 2007). This reduction would quite significantly increase the wind erosion risk during this time of the year. Cihacek et al. (1992), Weinan et al., 1996, Warren (2003), and Deumlich et al. (2006) showed that most of the wind erosion of agricultural lands in central Europe takes place during springtime, especially when the land is freshly cultivated, lacks plant cover, has a low soil moisture content, and is not protected by other conservation practices (e.g., wind breaks).

The situation in Denmark roughly follows this general development in Europe. Since more than 70% of the soils in Denmark have a light sandy texture, and the area is subject to strong offshore and onshore winds, Denmark is considered especially prone to wind erosion. Besides the coastal dune fields, which are geomorphological evidence that strong winds occurred throughout the Holocene (Clemmensen et al., 1996), the areas that are most susceptible to wind erosion in Denmark are agricultural sandy soils (Kuhlman 1986). Historical evidence indicates that wind erosion had been a significant problem in Denmark for a long time (Jönsson, 1994; Schjønning et al., 2009; Odgaard and Rømer 2009). Schjønning et al., (2009) show that wind erosion as an environmental challenge in Denmark goes back more than a century (see also Table 1.5). Because of the huge wind erosion events during that period, Denmark started to protect its agricultural lands from wind erosion via systematically establishing an extensive windbreak networks (Jönsson, 1994). About 1000 kilometers of shelterbelts were established per year (in total 75000-100000 km of windbreak around farmlands) and Denmark is, therefore, considered a pioneer country in Europe in terms of

wind erosion protection (Riksen et al., 2003). However, Kristensen (2001) showed that 9% of the length of shelterbelts network has been declined between 1972 and 1995 in central Jutland. The development of an optimal windbreak design is crucial to ensure its effectiveness to reduce wind erosion. The main parameters that have to be considered are: height, width, length, orientation to dominant wind direction, porosity (density), and distance between barrier rows. There are two types of windbreaks: living (natural) and non-living (artificial). In the case of tree shelterbelts (living wind break), some of these parameters are related to inherent characteristics of the plants. For example, the height of a windbreak depends on the type of the plant, the growing conditions, and the age (Zhang et al., 2010).

After implementation of this extensive windbreak system, erosion rates decreased so far that the threat of wind erosion was almost forgotten in Denmark (Schjønning et al., 2009). This lack of sufficient attention could maybe explain that several changes in agricultural practice have led to a period with strong wind erosion events again (1950s to 1970s). The negative changes included for example intensification of root crops instead of perennial crops, increases in field sizes, intense use of heavy machinery, and the removal of hedges surrounding the fields (Riksen and de Graaff, 2001). Kuhlman (1986) showed that the most heavily affected areas during that time period were the sandy soils characterized by low soil fertility, which are located predominantly in the western part of Denmark (Figure 1.5).

Figure 1.5. Major agricultural areas affected by wind erosion during the period of 1960–70 (Kuhlman, 1986).

With the establishment of a set of laws (Law no. 812 of 21 December 1988; Notification no. 17 of 18 January 1996; Notification no. 812 of 21 September 2001) and the re-development of different protective methods such as wind breaks (since 1988), preparation of rough surfaces by harrowing, and using residue plants in order to control wind erosion and its implications in Denmark, a considerable reduction in the volume of land degradation could be observed (Veihe et al., 2003). Nowadays, wind erosion occurs mostly on a local scale on very specific fields and farms, it is still considered to be a threat to Danish agriculture and concerns, especially about soil and nutrient loss. Despite all improvements in land management and in understanding the wind erosion process, the human land-use is still the main reason, why wind erosion occurs on agricultural land in Denmark. It seems that various factors influence on this issue, such as: intensive cultivation and to some part burning of plant residues together with a further shift to maize and root crops are the driving forces (Leys, 1999). In future, due to an increasing demand for energy crops, this negative development could perhaps lead to a situation where wind erosion becomes a major hazard again. A second process, besides the generally disadvantageous soil conditions, that could have the potential to worsen the situation, is the present climate change. Assumed warmer temperatures and longer dry spells during spring and summer might increase the risk of wind erosion, despite the expected higher annual average rainfall amounts (Funk et al., 2004 and Borrelli et al, 2014a; Hoffmann and Funk, 2015).

1.7 Problem Statement

Tilled surfaces due to lack of plant cover and crop residue are considered as prone area to wind erosion. In cultivated fields without any plant and residue cover, wind erosion risk depends mostly on the soil and aggregate characteristics, soil surface moisture, severity and time of erosive winds and field or rough orientation. Therefore, improving wind erosion and dust emission simulations requires a better representation of the land surface conditions (soil layer, soil surface, crop and biomass) and the driving meteorological parameters, such as wind patterns and velocities.

The prime motivation for doing this study was related to occurrence of local wind erosion in one of the study sites, while this farm was managed and maintained similar to the other farm lands. Finding the main reason of this event propelled us to investigate the effect of tillage orientation on soil, dust and nutrient loss variations by wind erosion. Awareness of the frequency of this hazard and rate of soil loss, dust and nutrient losses due to wind erosion could be an appropriate help for future environmental planning. As described above, far more

protection measures against wind erosion than in any other neighboring country have been implemented in Denmark. However, the general wind erosion problem on these light sandy soils still exist. Therefore, the general wind erosion risk and its development with regards to climate and land use change in the future are very important issues that need to be investigated. In addition, the main questions for research include the following:

1) What are the soil loss potentials under different tillage directions in comparison to flat surfaces (seedbed) in different soil types?
2) What are the nutrients and dust enrichment ratios under different tillage directions and soil types?
3) What is the reliability of wind erosion model results in comparison to results of wind tunnel simulations?
4) What are the main factors leading to an acceleration of wind erosion, based on a sensitivity analysis of the model?
5) What are the effects of erosive winds, soil moisture and tillage direction on the hazard and risk assessment of total soil, dust and nutrient losses?
6) What is the effect of a wind break network on controlling hazard and risk of total soil, dust and nutrient losses?

1.8 Aims

Based on the above mentioned research questions, the aim of this study was to determine the hazard and risk of total soil, dust and nutrient losses by wind erosion. In order to provide a quantification of wind erosion rates on different agricultural soils in Denmark, wind tunnel simulations and a modelling approach have been compared to each other. The fourfold objectives of study were:

1) Introducing an analytical approach to the wind data analysis for modelling wind erosion risk based on extrapolation erosive wind data during dry periods.

2) Assessment of the role of different tillage directions (parallel and perpendicular) on soil and nutrient loss, and dust emissions (PM_{10} and $PM_{2.5}$), by wind erosion from different soils. This approach aimed on finding a relationship between the enrichment ratio of different particle sizes and the amount of eroded nutrients.

3) Assessment of performance and reliability of modelling results (predicted values) versus observed values which are achieved by wind tunnel simulations.

4) Investigation of hazard and risk variations of wind erosion and PM_{10} under different scenario combinations based on probability occurrence of erosive winds:

a) Determination of field and tillage orientation effect on soil, dust and nutrient losses hazard and risk by wind erosion.
b) Investigation of windbreak effect on hazard/risk of soil, dust and nutrient losses.
c) Finding the best management scenario to combat wind erosion based on risk assessment.

Figure 1.6 shows the conceptual model which is used in this thesis. The influence of erosive wind velocity, farm management (field orientation or ridge height), and soil erodibility (soil texture and soil moisture) are investigated. The different scenario combinations are changed by including a windbreak network surrounding the field or by removing it.

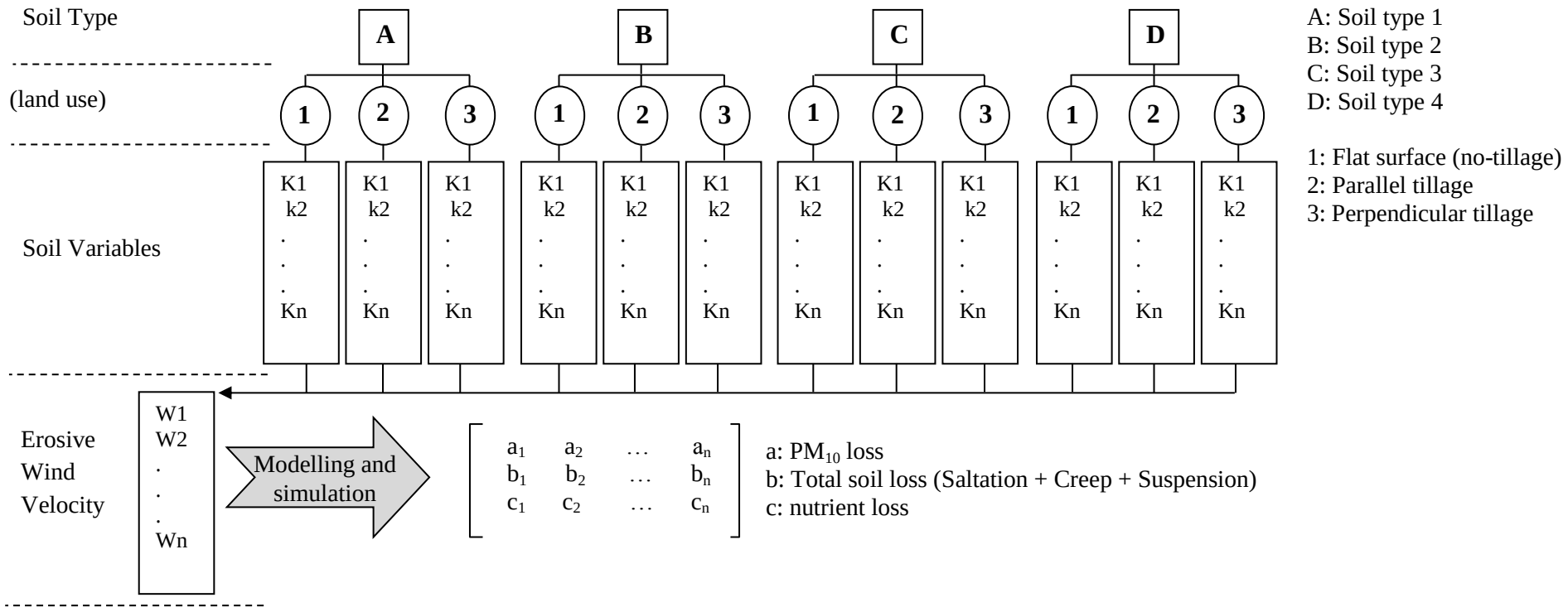

Figure 1.6. General conceptual model of thesis: The figure shows components and relationships includes between different soil, climatic and management scenarios, which have an effect on wind erosion rate, dust emission (PM_{10}) and nutrient loss.

University of Basel

Hazard and Risk Assessment of Wind Erosion and Dust Emissions in Denmark - A Simulation and Modelling Approach

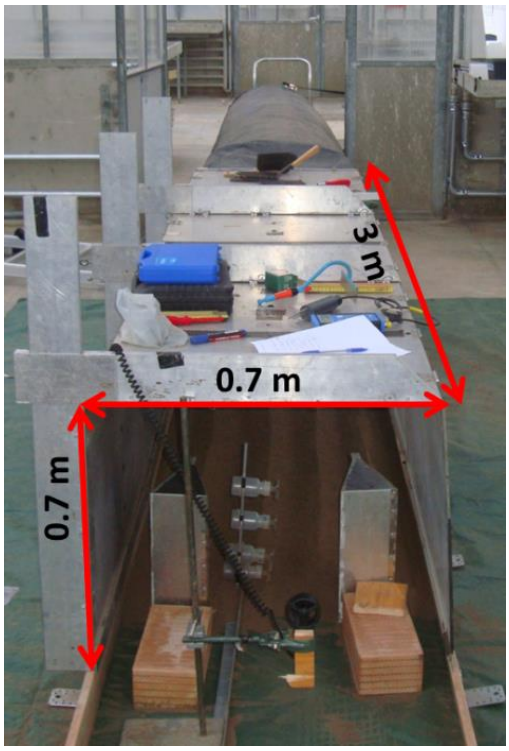

Materials and Methods

"An expert is a person who has made all the mistakes that can be made in a very narrow field."

Niels Bohr (1885-1962)

CHAPTER 2

2. Materials and Methods

This chapter will describe various methods employed in the field and laboratory components of the study for wind erosion simulating and modelling, and more specifically, the analysis of the physical and chemical properties of soil and sediment samples. Following the introduction and description of the study site is a chapter that describes the methodology of field sampling and the data, which were collected with the climate station. The third sub-chapter introduces the setup and procedure of the wind tunnel experiments and the laboratory analysis of the soil samples is described as the fourth sub-chapter. In the fifth chapter the statistical analysis, including the calculation of indices and parameters, necessary to accomplish the final risk assessment are shown. Sub-chapters six and seven deal with the description of the wind erosion model and the method how to evaluate the results of the model based on a sensitivity analysis. The final sub-chapter defines the methodological procedure that was used to accomplish the hazard and risk assessment.

2.1 Study area

2.1.1 Soil distribution in Denmark

The Danish soil classification from 1974 was based on the texture analysis of 36000 samples from ploughed and subsoil layers. Overall, the western soils of Denmark contain a high sand percentage, whereas the eastern parts are dominated by the more heavy soils with clay and silt. In addition, the soil types have been divided into eight main soil classes. As shown in Figure 2.1, the different types of sandy soils represent more than 70 percent of the area of Denmark. Because of their particle size distribution, these soils have the high intrinsic potential to be transported by wind erosion events (Kuhlman, 1986).

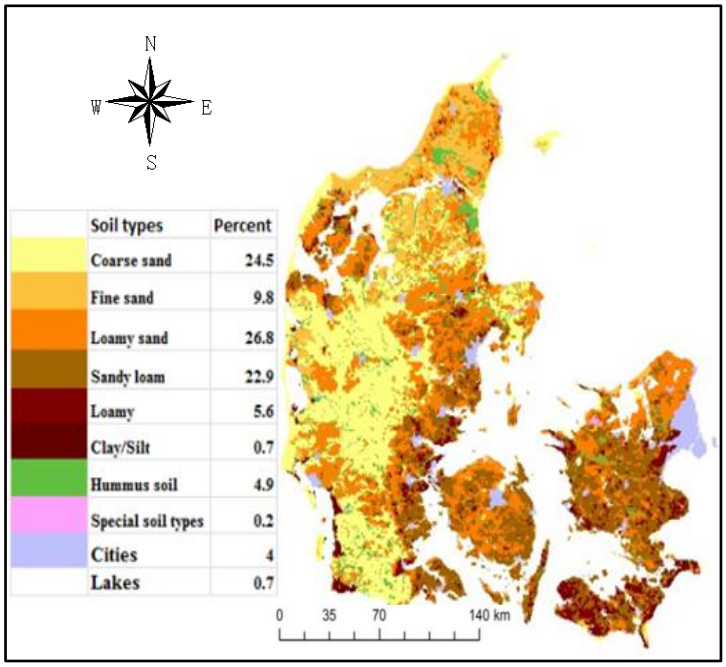

Figure 2.1. Soil types distribution in Denmark

Reference: http://www.jggj.dk/torpjord.htm

2.1.2 Study sites

The study area is located in the western part of central Jutland, north of Viborg, Denmark. It is located between latitude 56° 30' 10" and 56° 32' 16" East, and longitude 9° 20' 10" and 9° 23' 36" North (Figure 2.2). Four fields with four different soil types were selected. Based on Danish soil classification system, the soils for each field are categorized as fine sand (field A), loamy sand (field B), coarse sand (field C) and organic soil (field D). However, according to the USDA soil taxonomy, these soils were classified into three loamy sand classes (1, 2 and 3) with different amounts of sands and the texture of organic soil was classified into sandy loam with more than 10 % organic matter. Field C (loamy sand class 3) and field D, are oriented northwest to southeast whilst field A and B are elongated from north to south. This difference in orientation will become crucial when analysing the actual wind erosion risk for this fields.

2.1.3 Agricultural and crop management

In comparison to conventional farming and due to the application of technical recommendations by Danish land protection organizations, the present farming land management in the study area can be considered as conservation agriculture to control wind erosion. Farmers established shelterbelt networks, leave crop residues on the field after harvesting of crops, and use appropriate mechanization.

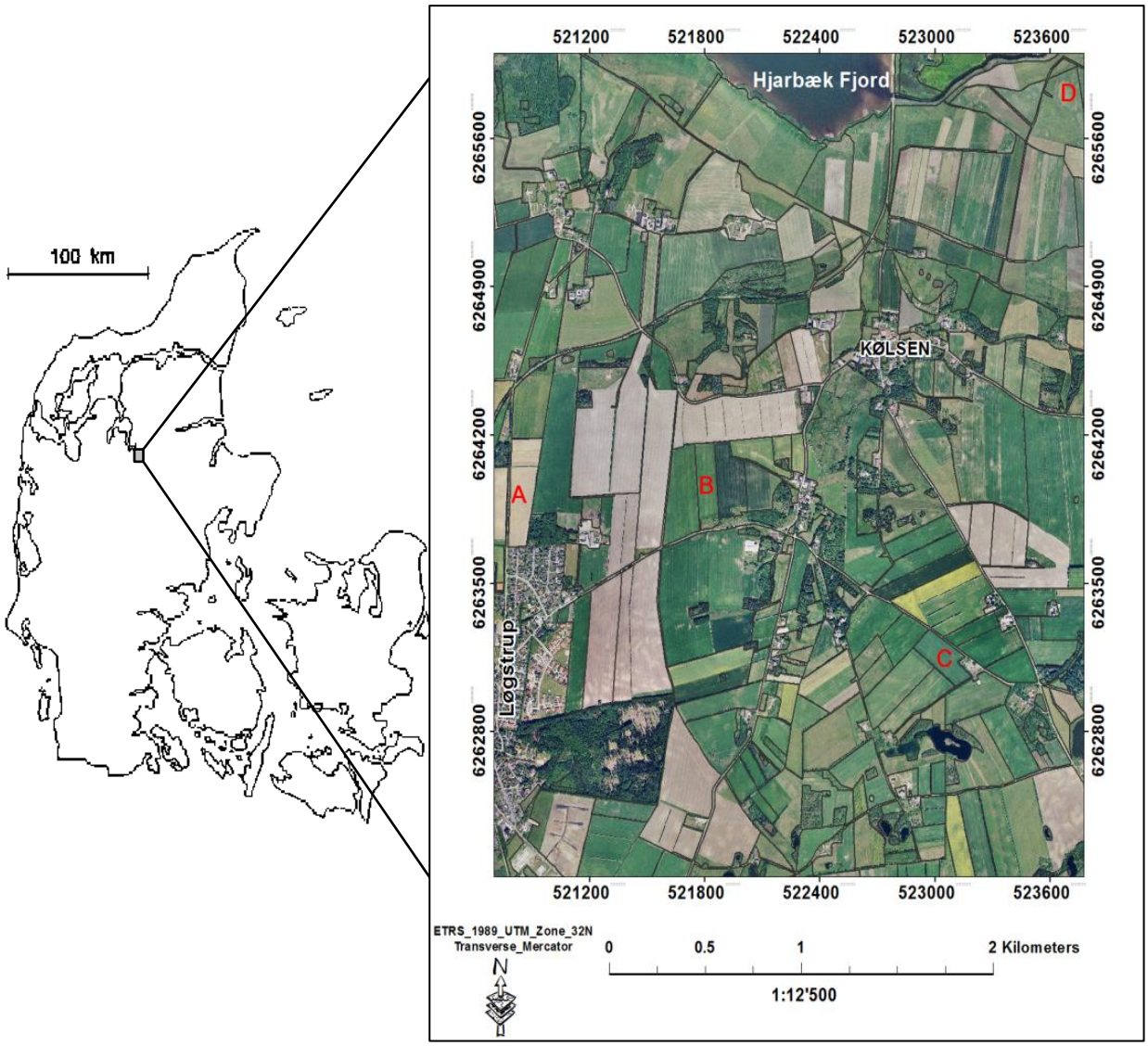

Figure 2.2. Location of study area and four main study sites

A: Loamy sand class 1, B: Loamy sand class 2, C: Loamy sand class 3, D: Organic soil

Despite these protection measures, local scale wind erosion occurs on very specific fields in this region. The annual crop calendar for common crops is obtained by conducting interview with the farmer in September 2012 as shown in Table 2.1. Four main crops are dominantly used for cultivation, including barley, winter wheat, maize and grass with different rotation systems. Based on in-farm observation which was described by the farmer, the critical time for wind erosion is the end of April when the lands are ploughed and they are still without vegetation cover. As can be seen in the cropping calendar, this critical time period is especially important for the cultivation of barley and maize crops. During this time of the year the fields are ploughed and a seedbed is prepared, so that for a relatively long period of time the surface is bare and thus, unprotected against wind erosion.

Table 2.1. Annual calendar for common crops grown in study area; Gray box showing the critical time for the wind erosion due to lack of vegetation cover hand crop residue.

Month / Crop	Rotation (year)	Jan	Feb	Mar	Apr	May	Jun	Jul	Aug	Sep	Oct	Nov	Dec
Barley	2	G&L	G&L	G&L	**P.L**	**S**	C.L	C.L	C.L	HR & CR	CR	CR&G	CR&G
Winter wheat	1	C.L	C.L	C.L	C.L	C.L	C.L	C.L	C.L	HR & CR	CR	P.L / S	C.L	C.L
Maize	1	CR&G	CR&G	CR&G	CR&G	**P.L**	**S**	C.L	C.L	C.L	C.L	HR & CR	CR	CR	CR&G
Grass	3	-	-	P.L	S	C.L	C.L	HR	C.L	C.L	HR	C.L	HR	-	-

C.L= Cultivated land P.L= Ploughed land G&L= Grass and legumes CR&G= crop residue and grass

S= Seeding CR= Crop residue HR & CR= Harvesting and crop residue

2.2 Field data

In this part, the soil sampling design in the study area is described. The soil samples were taken according to the simulation and modelling requirements. Wind data of Foulum synoptic weather station was available for a 14-year period (2000 – 2013).

2.2.1 Soil sampling

To measure the specific soil and soil surface parameters, which are essential for the application of the wind erosion model, two perpendicular transects were located around a central measurement position. Seven main sampling positions were distributed along these transects in a systematic-logarithmic pattern (Figure 2.3, right). At each of the seven main sampling positions, five individual samples were taken. In total 35 soil samples were taken from the topsoil layer (0-5 cm) for each test site. In addition, approximately 70 kg of soil from the topsoil layer of each field were collected, to be able to accomplish the wind tunnel simulations.

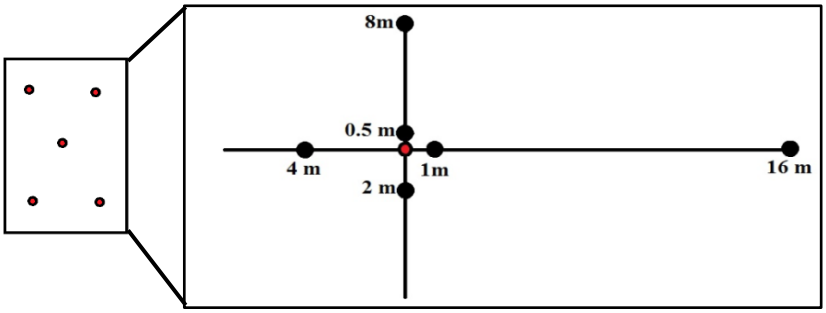

Figure 2.3. Schematic figure of positions of individual sample points (left) and general pattern of main sampling positions around central point (right)

2.2.2 Meteorological Data

The closest synoptic meteorological weather station to the test sites is Foulum weather station. It is located between 56° 29' 35" N latitude, 9° 34' 15" E longitude about 58 meters above sea level. Meteorological data were obtained for the period from 2000 to 2013.

In order have data about the volumetric water content in the soil, a Decagon 10HS soil moisture probe was placed into the 10 cm of top soil layer at field A (loamy sand class 1) for a one year period, starting from September 2012 (Figure 2.4). The sensor was pre-calibrated to measure the dielectric permittivity of the soil and it was part of a fully automatic weather station that was mounted in the study area.

Figure 2.4. Decagon's 10HS soil moisture sensor

2.3 Experimental setup of wind tunnel simulations

The main reasons for carrying out experimental simulations with a wind tunnel were to test the erodibility of the soils, measuring the nutrient loss of sediments and evaluation of effects of tillage direction on wind erosion rates. This experimental approach, therefore, aimed on finding a relationship between the enrichment ratio of the different particle sizes and the amounts of eroded nutrients. Most importantly, the experimental data made it possible to evaluate the modelling results. Simulations for this research were performed using a straight line push type wind tunnel at the Erosion Laboratory, Witterswil campus, near Basel in Switzerland.

2.3.1 Description of wind tunnel

The samples of soils were placed and shaped into a wind tunnel which has been developed at the University of Trier in Germany. A detailed description of the tunnel is given in Fister and Ries, (2009). In brief, the air flow was generated by a 4 kW push-type electrical fan with 163 cm^3 and 0.7 m diameter. The transition section is made of strong PVC plastic sheets (thickness 0.5 mm) is 4 m long and leads the turbulent rotating airflow to a honeycomb. The airflow passes through a 15 cm long flow straightener, which is made of 289 PVC tubes with a diameter of 4 cm. Upstream of the honeycomb, a double layer of wire mesh with open spacing of 0.5 cm and a blend are attached. The blend is made of plywood and is used to deflect the airflow from the upper 20 cm downwards to reduce wind velocities on the tunnel roof (Figure 2.5). The wind tunnel has a 300 cm long rectangular shaped working section, 70 cm wide and 70 cm high, but the experimental plot of soil samples into the working section has 200 cm long (proportion between width to the length of soil plot scale =1:2.85). The boundary layer thickness was estimated to be (δ) about 20 mm (Fister and Ries, 2009).

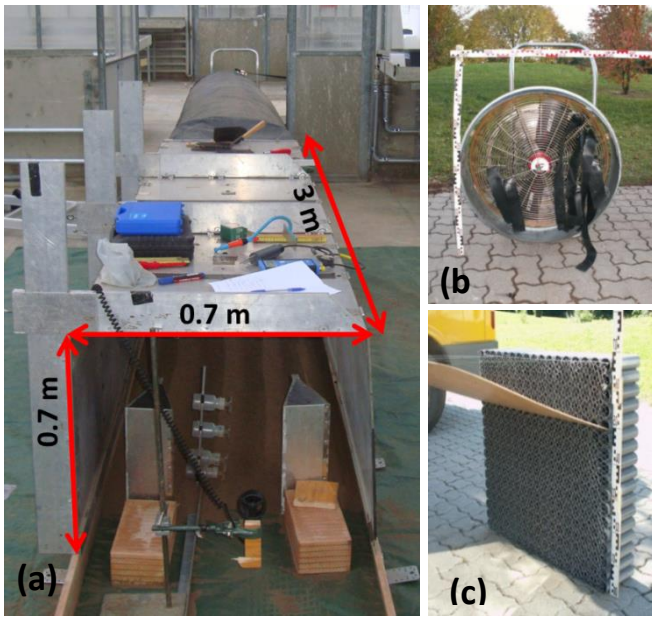

Figure 2.5. Wind tunnel and its structure (a), fan (b), honeycomb (c)

2.3.2 Soil surface scenarios

For the experiments, three different scenarios of soil surface were used (Figure 2.6): flat surface, parallel tillage and perpendicular tillage (the tillage rows in relation to the wind direction). The soil surfaces were shaped to reflect real surface conditions. Flat surfaces are often found after seedbed preparation and it was assumed that only random roughness elements exist. The sandbed thickness was kept constant at a depth of 5cm.

The dimensions of the ridges and furrows also reflect the common land management in Denmark. The ridge height, ridge spacing and ridge width were kept constant at 5 cm, 15 cm and 10 cm, respectively as the most effective ridge type to control wind erosion (Armbrust et al., 1964). In total 60 test runs were conducted for the four types of soils, three surface scenarios and five replicates for each surface scenario.

Figure 2.6. The soil surface scenarios

2.3.3 Experimental conditions and assumptions

In order to perform uniform simulations and for comparability reasons between the experiments, it is most important to create similar conditions for all experiments. Because of this necessity, the soil was always treated and prepared following the same protocol. Following is a list of the some basic requirements and assumptions that had to be made for the experiments:

Soils: The soils were air dried and afterwards sieved through a 5 mm mesh. Air dry soil conditions were chosen to have comparable conditions for all soils and to simulate the worst case scenario. Sieving was executed to reduce the amount of stones and large clods, which would have over-proportionally influenced the wind pattern on the surface, thus protecting small particles from the wind. After each test run, the soil surfaces were refreshed and reshaped to ensure comparable conditions for all repetitions.

- Replicates: Five replicate experiments were done for each soil surface scenario to be able to see if an experiment failed.

- Wind direction: Prevailing wind direction was assumed to be straight and parallel to the wind tunnel's plot length.

- **Soil moisture**: The average antecedence soil moisture was controlled by a handheld INFIELD 7 soil moisture sensor (UMS GmbH, München). The soil moisture content before every experiment was between 7.5 to 8 volume percent approximately.

- **Wind speed conversion**: For calculations of wind velocities in different heights and shear stress, it had to be assumed that the wind flow and boundary layer is in a steady and uniform condition (Goossens et al., 2000). Thus, the data could be fitted to logarithmic wind profile and expressed as (equation 2.1):

$$U_2 = U_1 \frac{\ln\left(\frac{H_2}{Z_0}\right)}{\ln\left(\frac{H_1}{Z_0}\right)} \qquad (2.1)$$

U_1 wind speed (m/s) at the weather station height ($H_1 = 10$ m)
U_2 measured wind speed (m/s)at the centre of the wind tunnel outlet ($H_2 = 0.30$ m)
Z_0 roughness length (m)

Therefore, based on logarithmic equation for the wind profile, the wind speed at 10 meter anemometer height was predicted of 12.61 m/s.
Wind velocity measurements were taken automatically using a PCE-007 air flow meter (PCE Instruments) in the centre of the wind tunnel outlet at 0.35 m above the tunnel floor. The measurement interval of the anemometer was one measurement every second (=1Hz). Each test run of the wind tunnel simulation lasted 5 minutes and during this time, the average wind speed was 7.5 m/s in the wind tunnel outlet (Figure 2.7).

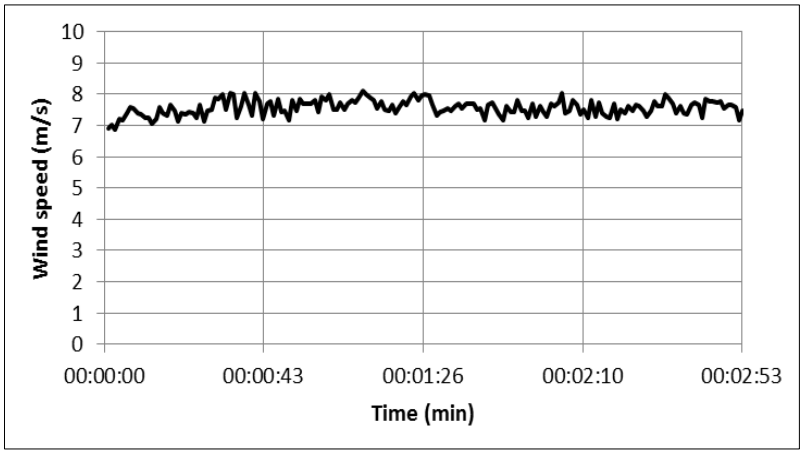

Figure 2.7. Exemplary graph of wind speed fluctuations in the center of the wind tunnel outlet

2.3.4 Sediment collection and calculation of sediment flux

In this study, for the measurements of wind-blown mass transport, two modified Guelph-Trent wedge shaped sediment traps (GTW, Nickling and McKenna Neuman, 1997, Fister and Schmidt 2008, Fister et al. 2012) were used to collect the aeolian sediment which is blown from the soil surface up to 50 cm height. The modified wedge shape (MWS) sediment trap as one of the direct quantification techniques for soil loss by wind is designed to measure the flux profile of blowing sediments into wind tunnel and classified into the passive and vertically integrating sediment trap groups (Figure 2.8). The soil creep, saltation and suspension loads have been estimated by weight of sediments which were collected by two MWS sediment traps that were located perpendicular to the wind path. They were positioned about 17.5 cm, from both sidewalls of the wind tunnel at the outlet. The collected sediment was emptied into measuring jars for weighing using a weighing balance. The weight of sediment was then converted to the mass of soil loss for each kind of the simulated scenario. These samples were used to analyze soil nutrient status in the laboratory to test for possible nutrient loss by wind erosion.

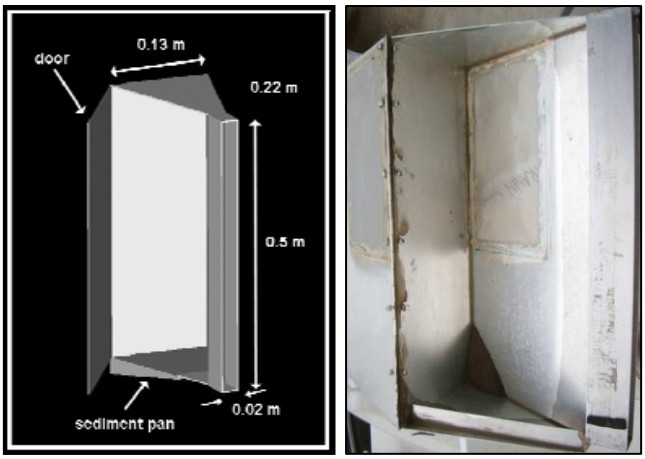

Figure 2.8. MWS sediment trap dimensions (Fister et al., 2008)

The sediment flux of erodible soil for each wedge-shaped sediment trap at 0 to 50 cm height (z) was calculated by equation 2.2 (Sankey et al., 2012):

$$q = mass * area^{-1} * time^{-1} \quad (2.2)$$

where q is sediment flux (g/m^2/min), mass is collected sediments (g), area is the inlet of wedge-shaped sediment (m^2) and time is simulation time (min).

2.4 Laboratory measurements

In this section, soil and sediment particle size distribution analysis were obtained by using a Malvern Mastersizer 2000 analyser. For soil and sediment samples, the total element contents of soil organic carbon (SOC), calcium carbonate ($CaCO_3$), nitrogen (N), phosphorus (P) and potassium (K) were analysed using standard laboratory techniques.

2.4.1 Soil and aggregate size distribution

The particle size distributions of the samples were determined by a Malvern Mastersizer 2000 particle size analyser (Figure 2.9). First, the samples were treated with 100 ml of 0.05 M $(Na\ PO_3)_6$ on an ultrasonic vibrator for 2 min to facilitate dispersion of particles before grain-size analysis and then, the Mastersizer 2000 automatically yields the median volumetric diameter and the percentages of the related size fractions of a sample with a relative error of less than 1% (Mastersizer 2000E, 2004). The percentage of different particle size and also dust indices (PM_{10} and $PM_{2.5}$) were calculated from the result of Mastersizer analyser (Table 2.2).

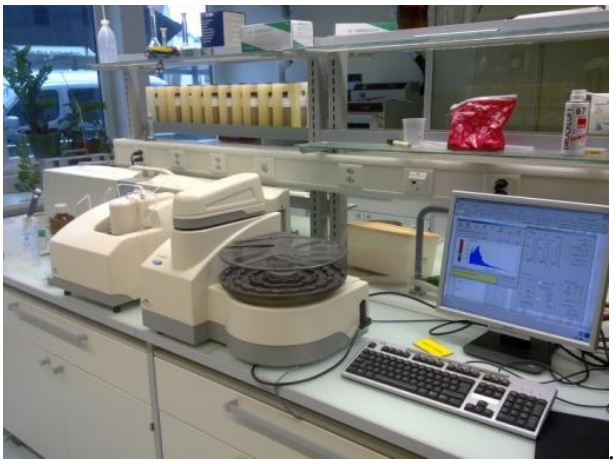

Figure 2.9. Measurement of soil and sediment particle-size using the Malvern Mastersizer 2000 analyzer

The texture of different soils are classified as three loamy sand soils and a sandy loam (organic soil), with 87.7 %, 79.2 %, 81.3 % and 51.4 % sand in the top-soil layer (Table 2.2) and with median particle (D50) sizes of 178.9 µm (field A), 199.9 µm (field B), 214.3 µm (field C) and 68.9 µm (field D) respectively. The averages and standard deviation (SD) of the measured and calculated soil properties are summarized in Table 2.2.

Table 2.2. Average (mean± SD*) particle size distributions of topsoil samples (n = 35 soil samples, *SD = standard deviation).

	Clay (%)	Silt (%)	Very Fine Sand (%)	Fine Sand (%)	Medium Sand (%)	Coarse Sand (%)	Very Coarse Sand (%)	D_{50} (µm)	$PM_{2.5}$ (%)	PM_{10} (%)
Loamy sand-Class 1	0.99	11.32	11.09	45.98	26.73	3.85	0.04	178.88	1.27	2.89
(Field A)	(0.02)	(2.5)	(3.0)	(2.1)	(3.6)	(2.1)	(0.01)	(19.8)	(0.3)	(0.5)
Loamy sand-Class 2	1.45	19.39	11.13	28.61	30.23	9.17	0.03	193.90	1.87	4.51
(Field B)	(0.2)	(2.0)	(1.4)	(2.8)	(2.1)	(3.3)	(0.01)	(24.1)	(0.03)	(0.05)
Loamy sand-Class 3	1.37	17.36	9.05	29.42	31.72	10.87	0.22	214.30	1.78	4.28
(Field C)	(0.3)	(2.0)	(1.3)	(2.6)	(2.2)	(4.4)	(0.05)	(20.3)	(0.4)	(0.8)
Organic soil	4.13	44.45	9.57	28.52	11.23	2.11	0.00	68.91	5.63	16.51
(Field D)	(0.9)	(9.4)	(1.9)	(6.4)	(7.5)	(0.03)	(0.0)	(25.4)	(1.2)	(3.4)

2.4.2 SOC and $CaCO_3$ analysis

Sediment and soil samples were analysed for nutrient concentration including SOC and $CaCO_3$ using LECO-RC 612 analyzer (Figure 2.10). SOC was measured based on a thermo-analytical analysis, which differentiates between the organic and inorganic carbon fractions by the specific temperature at which they oxidize. The release of organic carbon was measured at a constant temperature of 550°C. After the CO_2 concentrations dropped to <1 % of the peak intensity, the sample was further heated up to 950°C at a rate of 120° per minute to measure the release of the inorganic fraction. SOC concentrations were estimated through the time-integrated CO_2 concentrations (RC612, 2006).

Figure 2.10. Measurement of TOC and $CaCO_3$ using LECO-RC 612

2.4.3 Nitrogen (N) analysis

The Nitrogen (N) concentration was measured by dry combustion method using LECO CHN-628 elemental analyzer (Figure 2.11). Encapsulated samples were placed into the loading head of the machine, and then, the samples were transferred to the instrument's purge

chamber directly above the furnace, eliminating the atmospheric gases from the transfer process. The samples were then introduced to the primary furnace containing only pure oxygen, resulting in a rapid and complete combustion of the samples. In the final stage, the NOx gases were passed through a reduction tube filled with copper to reduce the gases to N and remove any excess oxygen present from the combustion process. The aliquot gas was then passed through Lecosorb and Anhydrone to remove CO_2 and the water generated during the CO_2 trapping process and onto a thermal conductivity cell utilized to detect N_2 (Leco CHN628 Series, Leco Corporation).

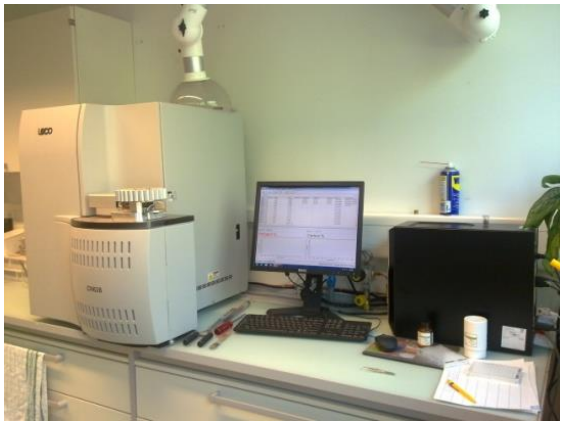

Figure 2.11. Measurement of N using LECO-CN 628

2.4.4 Phosphorus (P) and Potassium (K) analysis

The nutrients including Phosphorus (P) and Potassium (K) were measured using an ICP Spectrometer (Spectro Ciros Vision, Spectro GmbH, Kleve). To determine the elements, 5 g of soil and sediment were sieved through a 2 mm mesh. Samples were shacked for one hour with 50 ml CO_2-saturated water. Then, the resulting soil extract was filtered through a filter paper and measured on ICP (Figure 2.12).

Figure 2.12. Measurement of P and K using ICP Spectro Ciros Vision

Table 2.3 shows the results of the average nutrient concentration in the top soil samples which is obtained from various techniques mentioned above.

Table 2.3. Nutrient concentration (mean± SD) in soil samples

	K (mg/l)	P (mg/l)	N (%)	TOC (%)	$CaCO_3$ (%)
Loamy sand-Class 1	3.44	2.08	0.113	1.24	0.24
(Field A)	(1.63)	(0.33)	(0.01)	(0.18)	(0.04)
Loamy sand-Class 2	5.28	2.85	0.152	1.57	0.30
(Field B)	(1.34)	(0.28)	(0.02)	(0.20)	(0.03)
Loamy sand-Class 3	2.90	1.72	0.128	1.47	0.26
(Field C)	(1.54)	(0.71)	(0.04)	(0.32)	(0.07)
Organic soil	2.93	0.68	0.980	12.10	0.51
(Field D)	(0.70)	(0.18)	(0.26)	(3.14)	(0.14)

2.5 Calculations of indices and parameters and statistical analysis

In this section, the calculations of nutrient loss, dust and nutrient enrichment ratios are given based on eroded sediments of wind tunnel simulations. These results were statistically compared for each soil type and surface scenario. Also, separation of dry periods from total wind data and then calculation of erosive winds and its probability distribution in dry period are described.

2.5.1 Calculation of nutrient loss, dust and nutrient enrichment ratios

The amount of nutrient loss by horizontal sediment flux was calculated with following formula (equation 2.3):

$$q_n = N_{sediment} * q \tag{2.3}$$

where q_n is total loss in nutrients (mg/m^2/min); q is horizontal mass flux (g/m^2/min); $N_{sediment}$ is nutrient content of sediment (mg/g)

Since wind erosion is a selective process, usually, increasing erosion rates are associated with increasing loss of nutrients and finer particles. Therefore, it is necessary to take into account the nutrient enrichment ratio (NER) when agricultural fields are the subject of a wind erosion study. The NER was calculated by dividing the nutrients in the sediment from the nutrient concentration in origin soil. Hence, based on the nutrient measurements for soil and sediment

carried out in the laboratory, an index of enrichment was determined for each experiment and each nutrient.

In this study, according to the NER index, a new index for the two main dust indices i.e. PM_{10} and $PM_{2.5}$ was calculated based on the results gained from the mastersizer by the following formula (equation 2.4). Indeed, dust enrichment ratios were calculated as the ability of different soil surface scenarios to produce rich dust sediment. It is defined as ratio of the $PM_{2.5}$ and PM_{10} (dust indices) concentration in trapped sediments to their concentration in top soil layer:

$$DER = \frac{sedc}{sodc} \tag{2.4}$$

sedc is dust particles ($PM_{2.5}$ and PM_{10}) concentration in sediment

sodc is dust particles ($PM_{2.5}$ and PM_{10}) concentration in the top soil layer

2.5.2 Basic statistical analyses

Data analysis was done using Minitab software (version16.0). Nutrient and particle enrichment ratios in soil and sediment samples were analysed using Pearson correlation with a significance level of 0.05.

2.5.3 Separation of erosive wind in dry periods

Soil moisture is one of the most important influencing parameters on wind erosion. Studies by Naeini (2015) and Hagen (2007) showed that using wind time series without soil moisture influence most likely leads to an overestimation of wind erosion risk. In order to overcome the lack of soil moisture data in this study, a wet/dry separation model was used, which was developed by Naeini (2015). The accuracy of the model separate between wet and dry times is 78%. The model is based on some easy to access weather elements to estimate the soil wetness during observed wind data times (Ravi et al., 2006; Shang .et al., 2007; Naeini, 2015). As shown in Figure 2.13, four stages can be considered in the proposed method:

1. Estimating initial time of precipitation by threshold of precipitation amount (≥ 6mm per day);
2. Calculating the duration of rainfall effect on the soil surface by relative humidity (> 85%);
3. Estimating solid state times of precipitation by temperature (< 0°C);
4. Prediction of dew formation time by nightly relative humidity (100%).

Given that the soil surface moisture, which is used by this method is higher than field capacity (generally saturated), it can be assumed that there is no occurrence of wind erosion in these times. Based on this method, the detected wet periods were excluded from the wind speed calculations in this research.

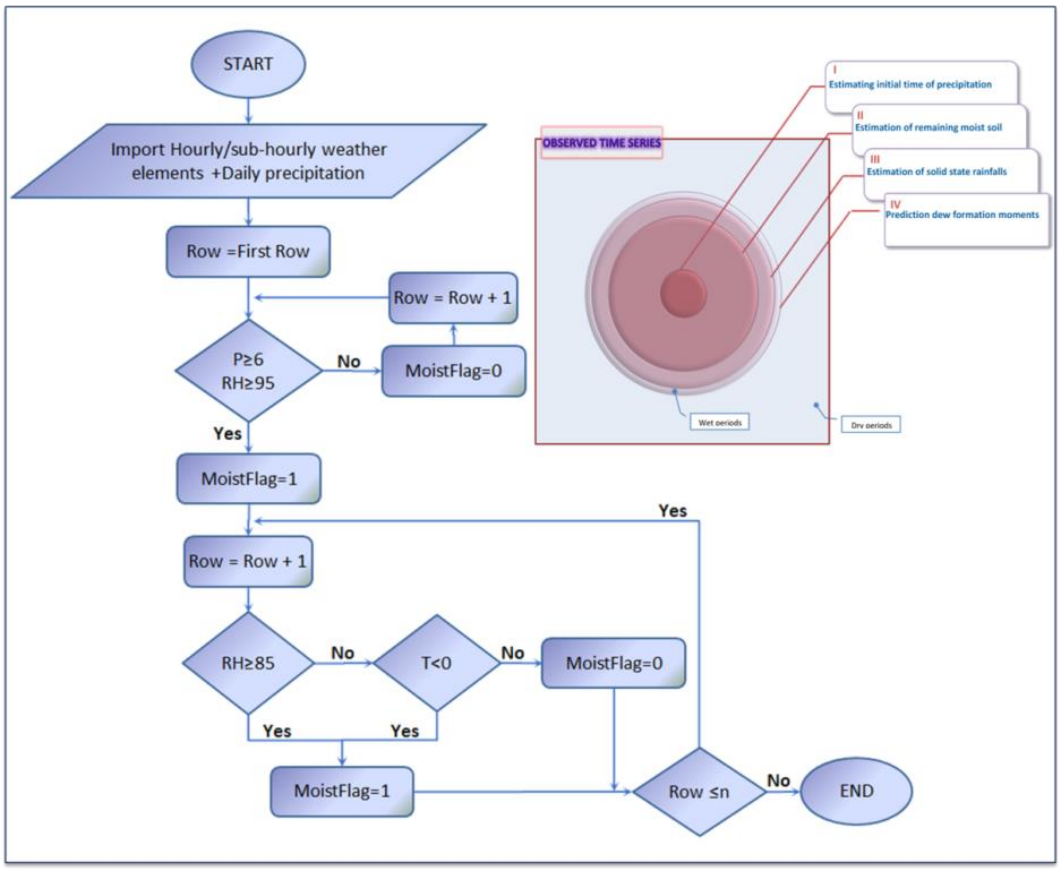

Figure 2.13. Conceptual flowchart of Wet/dry time separation method

RH: relative humidity, T: temperature, P: precipitation, n: number of observed wind data

2.5.4 Probability distribution of erosive winds in dry period

Erosive winds were selected from the total for dry periods when the wind velocity exceeded the threshold of 11 m/s (defined by SWEEP model calculations) for at least one hour. The Weibull distribution is the most widely used probabilistic model representing wind speed distributions (Hagen, 2004). To estimate the probability of erosive winds in dry periods, three parameters were calculated for a Weibull cumulative wind speed distribution F(u) and the probability density function f(u) by the following formulas (equation 2.5 and 2.6). Then the probabilities were classified for each daily average wind speed to calculate the risk values as described in section 2.8 (Hagen, 1996).

$$F(u) = 1 - exp\left[-\left(\frac{u}{c}\right)^{k}\right] \quad (2.5)$$

$$f(u) = \left[\frac{k}{c}\right]\left[\frac{u}{c}\right]^{k-1} exp\left[-\left(\frac{u}{c}\right)^{k}\right] \quad (2.6)$$

u is wind speed

c is a scale factor (units of velocity),

k is a shape factor (dimensionless)

2.6 Wind erosion modelling using SWEEP

In this research a repeatable and easily adjustable model was applied for predicting single event wind erosion and dust emission on agricultural lands. Therefore, the SWEPP model as a computer simulation model and dynamic simulation software for short periods over a user-defined simulation region was chosen for the modelling part of this study.

2.6.1 Introduction to Single-event wind erosion evaluation program (SWEEP)

SWEEP is a single-event wind erosion evaluation program released in 2007 by the Wind Erosion Research Unit (WERU) of the United States Department of Agriculture (USDA) and Agricultural Research Service (ARS) in Manhattan, Kansas, USA. SWEEP as a process-based model can predict and simulate wind erosion for a single-day with erosive winds under different conditions of soil, surface, and management (Feng and Sharratt, 2009). There are a limited number of studies which have evaluated SWEEP in simulating soil loss subject to different tillage practices and soil surface conditions under storm events by Feng and Sharratt (2009), Jia et al., (2014), Liu et al., (2014), Pi et al., (2014) and Gao et al.,(2014). The SWEEP model is actually the erosion sub-model of the Wind Erosion Prediction System (WEPS) with a graphical user interface that calculates soil loss and deposition for sub-hourly periods when friction velocity exceeds the static threshold friction velocity (Hagen, 2004). Required input variables for running the SWEEP model include wind speed, wind direction, wind duration, and soil parameters of particle size distribution, soil moisture and surface characteristics.

In this research, we have considered all subroutines of the SWEEP model which represented in the individual farm lands without plant biomass (flat or standing) and crop residues. We assumed that lands are fully under ploughing with two tillage orientations (parallel and

perpendicular tillage). The soil loss by saltation/creep and PM_{10} loss were considered for fields that were protected by a wind barrier as well as fields without barrier.

The simulation procedure of the SWEEP model has several steps (Funk et al., 2004). First, the SWEEP predictions start with the calculation of static threshold friction velocity at which the erosion begins for each test site. The SWEEP model calculates the friction velocity based upon the aerodynamic roughness of the log-law wind speed profile. In agricultural land, due to an existing tillage-based relief, the friction velocity can be characterized by the ridge dimensions such as height, spacing, orientation, and top bed width by following equation 2.7 (Hagen, 1996):

$$\frac{WZ0_{rg}}{SZ_{rg}} = \frac{1}{-64.1 + 135.5\frac{SZ_{rg}}{SXP_{rg}} + \frac{20.84}{\sqrt{\frac{SZ_{rg}}{SXP_{rg}}}}}, \qquad SZ_{rg} > 0 \tag{2.7}$$

$WZ0_{rg}$ is aerodynamkc roughness of ridges (mm)

SZ_{rg} is ridge height (mm)

SXP_{rg} is ridge spacing parallel to the wind (mm)

The ridge spacing parallel to the wind direction is determined by equation 2.8 (Hagen, 1996):

$$SXP_{rg} = \frac{SX_{rg}}{abs\left[sin\left(\frac{3.1416}{180}\left(AWA_{dir} - SA_{rg}\right)\right)\right]}, \quad if\ denominator > 0.2 \tag{2.8}$$

SX_{rg} is ridge spacing (mm)

AWA_{dir} is daily wind direction (degrees)

SA_{rg} is ridge orientation(degrees), clockwise from north and parallel to the ridge

The calculation of friction velocity in SWEEP at the sub-region as an important physical parameters that govern wind erosion model, has two steps:

1) At first, the friction velocity is calculated for the wind measurements at the weather station by equation 2.9 (Hagen, 1996):

$$WUF = \frac{0.4\,WU}{\ln\frac{WZ}{WZZ0}} \tag{2.9}$$

WUF is friction velocity at weather station (m/s)
WU is wind speed at the weather station (m/s)
WZ is anemometer height at weather station (mm)
WZZ0 is aerodynamic roughness at the weather station; assumed 25 mm in SWEEP model

2) Then the maximum friction velocity is determined using the daily maximum wind speed. If there is no standing biomass, it is calculated based on the ratio of soil surface aerodynamic roughness of the field divided by the aerodynamic roughness at the weather station multiplied with the friction velocity at the weather station (see equation 2.10, Hagen, 1996):

$$WU_* = WUF\ (\frac{WZ0}{WZZ0})^{0.067} \tag{2.10}$$

WU_* is friction velocity used to drive the erosion simulation (m/s)

2.6.2 Static threshold friction velocity

The threshold friction velocity for bare and tilled soil surfaces without vegetation cover is defined as the velocity at which aggregates begin to detach and is calculated based on a combination of surface conditions: soil aggregate geometric mean diameter and geometric standard deviation, minimum and maximum aggregate size, aggregate density, clod/crust cover, loose material on crust, surface roughness, soil surface water content, tillage geometric parameters and soil wilting point water content. If friction velocity exceeds threshold friction velocity, the model initiates to compute the soil loss for the characterized regions by equation 2.11 (Hagen, 1996).

$$SF_{cv} = [(1 - SF_{cr})(1 - SF_{84}) + SF_{cr} - SF_{los}][1 - SV_{roc}] + SV_{roc} \tag{2.11}$$

SF_{cv} is soil fraction covered by clod, crust and rock (it does not emit)
SF_{cr} is soil fraction covered by crust (excluding the fraction of rock − covered area)
SF_{84} is soil fraction covered with aggregates < 0.84 mm on the noncrusted area
(excluding the fraction of rock − covered area)
SF_{los} is soil fraction covered with loose, erodible soil on the crusted area
SV_{roc} is rock volume fraction > 2mm, (m^3/m^3)

The latter term is calculated from the modified lognormal aggregate size distribution as equations 2.12 and 2.13 (Hagen, 1996):

$$SLT = \frac{(0.84 - SL_{agn})(SL_{agx} - SL_{agn})}{(SL_{agx} - 0.84)SL_{agm}} \tag{2.12}$$

$$SF_{84} = 0.5\left[1 + erf\left[\frac{\ln(SLT)}{\sqrt{2}\ln(SO_{ags})}\right]\right] \tag{2.13}$$

SL_{agn} is lower limit of size distribution(mm)

SL_{agx} is upper limit of size distribution(mm)

SL_{agm} is geometric mean of size distribution (mm)

SO_{ags} is geometric standard deviation of size distribution

In order to determine the threshold friction velocities for bare soil, the equation below has been used in SWEEP based on the best fitted regressions to the wind tunnel data by equations 2.14 and 2.15 (Hagen, 1996):

$$WUB_{*ts} = 1.7 - (1.35)exp[-(b2)SF_{cv}] \tag{2.14}$$

$$b2 = \frac{1}{-0.076 + \frac{1.111}{\sqrt{WZO}}} \tag{2.15}$$

WUB_{*ts} is static threshold friction velocity of bare surface (m/s)

The soil surface moisture content is assumed to be constant during individual event simulation (Feng and Sharratt, 2009). For the wet surfaces, threshold friction velocities increase as equations equation 2.16 (Hagen, 1996):

$$WUCW_{*ts} = 0.48\ \frac{HR0_{wc}}{HR15_{wc}}, \qquad if\ \frac{HR0_{wc}}{HR15_{wc}} > 0.2 \tag{2.16}$$

$WUCW_{*ts}$ is increase in static threshold friction velocity from surface wetness (m/s)

$HR0_{wc}$ is surface soil water content (kg/kg)

$HR15_{wc}$ is surface soil water content at 1.5 MPa (kg/kg)

Therefore, the static threshold velocity with wetness on bare soil is calculated using equation 2.17 (Hagen, 1996):

$$WU_{*ts} = WUB_{*ts} + WUCW_{*ts} \quad (2.17)$$

2.6.3 SWEEP input parameters

The wind erosion hazard and risk assessment in this study focuses on un-crusted fields without vegetation or crop cover. The input parameters, which are related to these conditions, were, therefore, excluded from the modelling. Hence, the computations were only based on changes in soil properties, soil moisture and characteristics of tillage ridges of the fields in relation to the prevailing direction of erosive winds during dry periods of the year. Since the biomass information layer was also excluded, the SWEEP input parameters in this study include:

1) **Dimensions, shape and boundary definition of the simulated field**

In order to be able to compare the modelling results from all four different fields, a theoretical rectangular field with a dimension of 285m × 100 m was used. It is approximately 142 times larger than the work section of the wind tunnel. To simulate the influence of a windbreak, a single hedge row the simulated field was implemented into the calculations. The wind break network was characterized by 35% porosity, 3.5 meter height, and 3 meter width and is representative for existing common single row windbreaks in the study area (Figure 2.14).

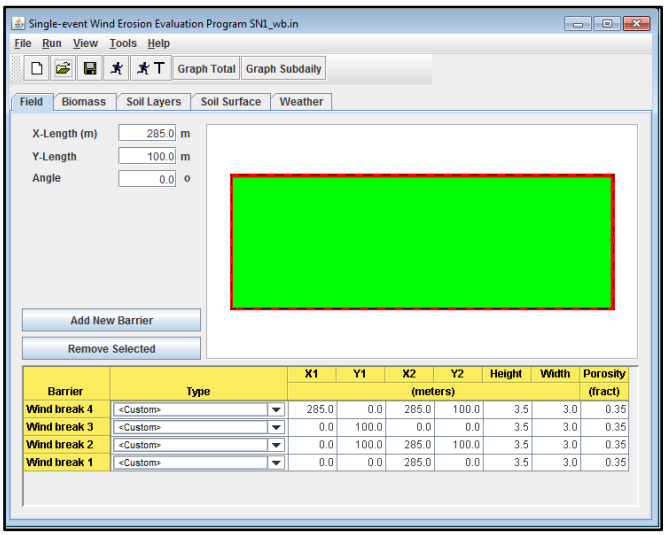

Figure 2.14. The main SWEEP screen showing simulation region including field and barrier coordinate

2) Soil type characteristics

The soil input file of SWEEP includes the number and thickness (mm) of soil layers, detailed particle size distribution (specific fractions), dry bulk density, average dry aggregate stability (ln(J/kg), aggregate density (Mg m^{-3}), aggregate size distribution (fraction), its geometric characteristics and soil water content, more specifically the soil wilting point (Figure 2.15).

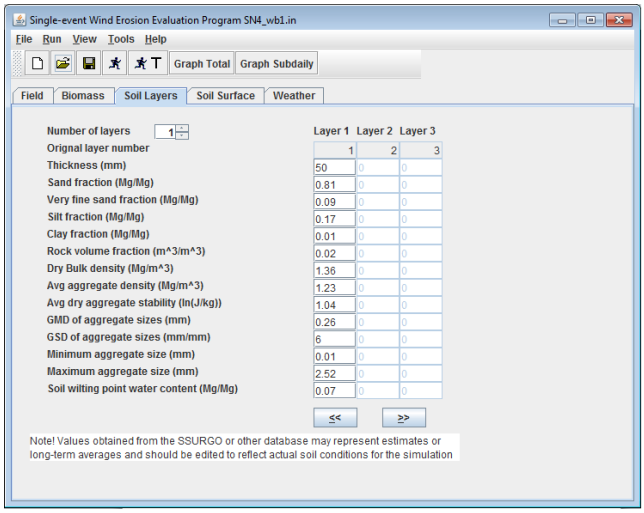

Figure 2.15. The main soil layer screenshot showing the input soil properties to run the SWEEP model

Most of the soil layer properties entered as input data for the SWEEP model were calculated based on results of grain size distribution and some other derived soil properties such as geometric mean diameter (GMD), geometric standard deviation (GSD), and maximum aggregate size (agmax). Dry aggregate stability was estimated based on the fractions of different aggregate sizes on top soil layer properties according to a log-normal function and the empirical formulas in the SWEEP user guide (USDA, ARS Wind Erosion Research Unit, 2008) as shown in Table 2.4.

Table 2.4. The parameters of soil layer and its related equations and measuring techniques (USDA, 2008)

	Parameter	Description
1	Bulk density	The oven dry weight of the less than 2 mm soil material per unit volume of dry soil in Mg/m^3.
2	Sand fraction	Mineral particles 0.05 to 2.0 mm in equivalent diameter as a weight fraction of the less than 2.0 mm fraction in kg/kg. Estimated by: sand = 1.0 - (silt + clay)
3	Very fine sand fraction	Mineral particles 0.05 to 0.1 mm in equivalent diameter as a weight fraction of the less than 2 mm fraction, kg/kg.
4	Silt fraction	Mineral particles 0.002 to 0.05 mm in equivalent diameter as a weight fraction of the less than 2.0 mm fraction in kg/kg. Estimated by: silt = 1.0 - (sand + clay)
5	Clay fraction	Mineral particles less than 0.002 mm in equivalent diameter as a weight fraction of the less than 2.0 mm fraction in kg/kg. Estimated by: clay = 1.0 - (silt + sand)
6	Rock volume fraction	The volume fraction of the layer occupied by the 2.0 mm or larger (20 mm or larger for wood fragments) on a whole soil basis in m^3/m^3.
7	Avg aggregate density	The oven dry weight of the less than 2 mm soil aggregates per unit volume of dry soil aggregates in Mg/m 3. Estimated by: ag den = 2.01 *(0.72 + 0.00092 * layer depth) for layer depth =< 300 mm, ag den = 2.0 for layer depth > 300 mm
8	Avg dry aggregate stability	Mean of natural log of aggregate crushing energies in ln(J/kg). Estimated by: ag stab = 0.83 + 15.7 * clay - 23.8 * $clay^2$
9	GMD of aggregate sizes	Soil aggregate geometric mean diameter of the modified log-normal distribution in mm. Estimated by: ag gmd = exp(l.343 - 2.235 * sand - 1.226 * silt - 0.0238* sand/$clay^3$+ 33.6 * om + 6.85*$CaCO_3$)*(1.0 +0.006*layer depth)
10	GSD of aggregate sizes	Soil aggregate geometric standard deviation of the modified log-normal distribution, dimensionless. Estimated by: ag gsd = 1.0 / (0.0203 + 0.00193(aggr. gmd) + 0.074 / $(aggr.gmd)^{0.5}$)
11	Minimum aggregate size	Lower limit of the modified log-normal aggregate size distribution in mm. Estimated by: ag min = 0.01
12	Maximum aggregate size	Upper limit of the modified log-normal aggregate size distribution in mm. Estimated by: ag max = (ag gsd) * (ag gmd) + 0.84^p where p = 1.52 * $(ag\ gsd)^{-0.449}$
13	Soil wilting point	The amount of soil water retained at 15 bars (1500 kPa), expressed as a percentage of the less than 2 mm, oven-dry soil by volume in Mg/Mg.

Soil samples were taken using a soil bulk density ring (cylinder) with a 5 cm diameter and height (98.17 cm^3). The porosity of the soil, and thus also the soil wilting point for each soil type was measured using a small pressure chamber (Figure 2.16). The density rings with the samples were placed on a permeable plate. By sucking the air out of the pressure chamber, the reduced pressure causes drainage of water out of the soil. The remaining water content at 15

atmospheres pressure (-15 bar) is the so called permanent wilting point. This method is based on the method by Saxton, et al. (1986).

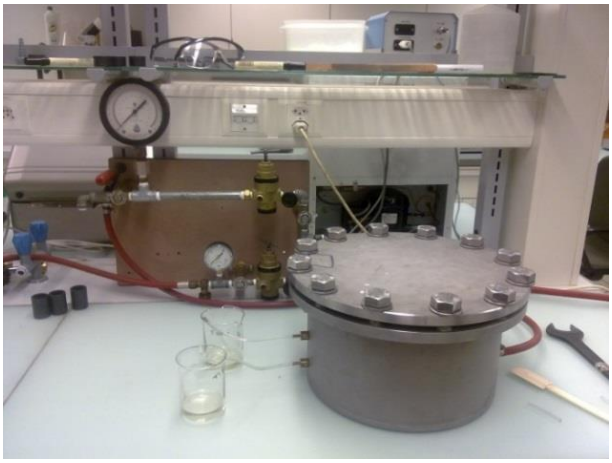

Figure 2.16. Pressure plate used to measure the volumetric content of a soil at wilting point

3) Soil surface characteristics

The soil surface is described within SWEEP by random and oriented roughness values, fraction of surface that is crusted, and the amount of loose, erodible material on a fully crusted surface (Figure 2.17). In this study, based on our aims for evaluating the role of ridge geometric specifications and soil surface water content, these two parameters were chosen to analyze the effect of scenario combinations on the wind erosion hazard and risk. Soil water content was assessed volumetrically in the upper 100 mm of the soil profile by a 10HS soil moisture probe (Decagon). Following Table 2.5 contains the description of soil surface parameters which were responsible for the modelling of wind erosion in this study.

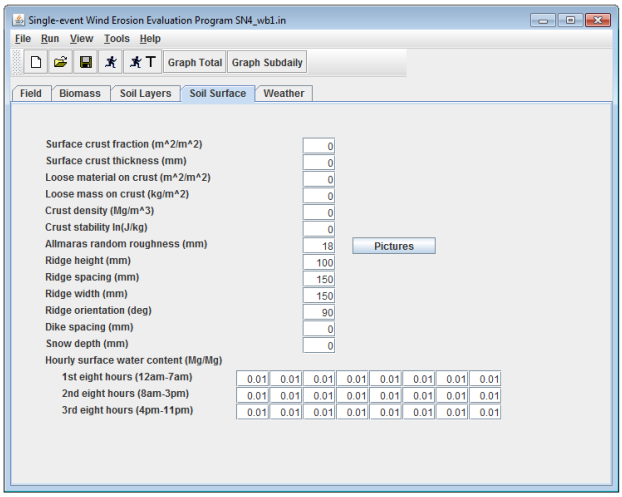

Figure 2.17. The main soil surface screen - SWEEP model

Table 2.5. The parameters of soil surface which is used for the hazard and risk assessment (USDA, 2008)

	Parameter	Description
1	random roughness	The standard deviation of elevation from a plane of a random soil surface
2	Ridge spacing	Spacing between ridge tops in mm. If no ridges, then specify 0.0.
3	Ridge height	The height of soil ridges from bottom of furrow to top of ridge in mm.
4	Ridge width	Width of the top of the ridge in mm.
5	Ridge orientation	Direction parallel to the tillage ridge, clockwise from true North in degrees.
6	Hourly surface water content	The near surface water content for each hour of the day in Mg/Mg.

4) Wind input parameters

The weather tab describes the weather parameters for the simulation location (Figure 2.18). As the wind simulator provides a single wind direction for each erosive day, the prevailing wind direction was chosen from west to east (275°). Wind speed was set at a 10 m height with an aerodynamic roughness of 0.01 m for the average hourly of erosive days in dry periods.

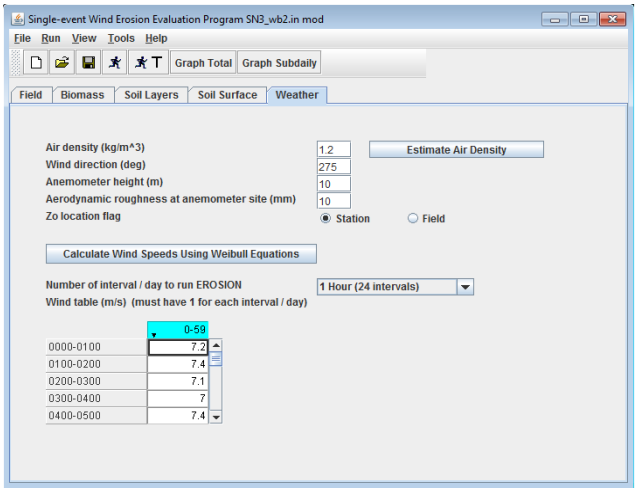

Figure 2.18. The main soil surface screen to run the SWEEP model

Table 2.6 shows the required input parameters for the weather tab in the SWEEP model. For each average of erosive day that were selected in 2.5.3 section, a 24 hour wind speed data were extrapolated.

Table 2.6. Required input parameters for the weather tab in the SWEEP model (USDA, 2008)

	Parameter	Description
1	Air density	The average density of the air at the simulation location for the day in kg/m3.
2	Wind direction	Wind direction (degrees) of the day with the fastest wind speeds, measured clockwise from North.
3	Anemometer height	The height of the anemometer above the soil surface at which the wind speeds were measured in m.
4	Aerodynamic roughness at anemometer site	Aerodynamic roughness at the site where wind speeds were measured in mm.
5	Number of intervals	The number of time steps erosion is calculated for each day including:
6	Wind table	Wind speeds for the time interval of the entire day in m/s. Wind data are typically averages for the period.

As described above, simulations were performed for a rectangular agricultural field on a sub-hourly basis. Soil loss and deposition was propagated on the basis of different inputs parameters including wind speed, soil surface characteristics, soil conditions, and field orientation. The output of SWEEP is represented as total soil loss and it is subdivided into components and reported as saltation/creep, total suspension, and fine particulate matter (PM_{10}) as component of suspension loss. (Figure 2.19).The graphical user interface provides an environment to evaluate the impacts that alternate practices and conditions might have on reducing that hazard and risk of wind erosion under various scenario combinations.

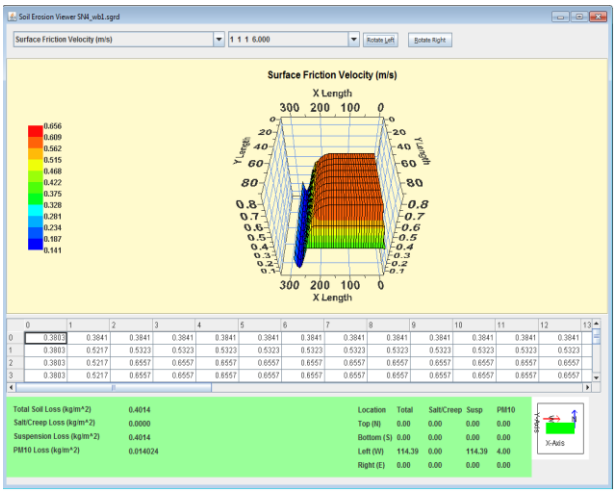

Figure 2.19. Graphical user interface of SWEEP output showing soil loss parameters

2.7 Model evaluation and sensitivity analysis

In order to evaluate the quality of model predictions, its results were compared with the simulation results of the wind tunnel experiments. Finally, to choose the important input

parameters that had the most effects on wind erosion balance in the study area, a relative sensitivity index was selected.

The uncertainty in input parameters, model structure, and output values of models are considered as the most important reasons for differences between model predictions and measured values in laboratory. Therefore, conformity of modeled results with real experiments should be analyzed and validated using efficiency criteria techniques (Refsgaard et al., 2007). In order to evaluate the quality of model predictions, the results were compared with the simulation results of the wind tunnel experiments. Some recommended model evaluation techniques (Feng and Sharratt, 2007) were used for comparison and described below. In a final process, a sensitivity analysis of the parameters was performed to evaluate their importance on the wind erosion process.

2.7.1 Model efficiency criteria techniques

The model evaluation statistics used in this study for testing the goodness-of-fit of the wind erosion models included: Root Mean Square Error (RMSE), Correlation Coefficient (R^2) and Index of agreement (d).

- **Root Mean Square Error (RMSE)**

RMSE is known as one of the most frequent formulas employed to measure differences between simulated values by a model and real observed values gained by experiments. This index describes the degree of approximate linear relationship between predicted and observed values (Moriasi et al., 2007). RMSE is defined as equation 2.18:

$$\mathrm{RMSE} = \left[\sqrt{\frac{\sum_{i=1}^{n}\left(Q_i^{pre} - Q_i^{obs}\right)^2}{n}}\right] \tag{2.18}$$

where,

Q_i^{obs} is observed (measured) values,

Q_i^{pre} is predicted (modeled) outputs,

and n equals the number of values

- **Coefficient of determination ($\mathbf{R^2}$)**

The coefficient of determination R^2 is defined as the squared value of the coefficient of correlation according to Bravais-Pearson. The coefficient of determination or r^2 shows the

explained variation in a regression. It ranges between 0 and 1 (Dodge 2008). It is calculated as equation 2.19:

$$r^2 = \left[\frac{\sum_{i=1}^{n} (Q_i^{obs} - Q_{mean}^{obs})(Q_i^{pre} - Q_{mean}^{pre})}{\sqrt{\sum_{i=1}^{n} (Q_i^{obs} - Q_{mean}^{obs})^2} \sqrt{\sum_{i=1}^{n} (Q_i^{pre} - Q_{mean}^{pre})^2} } \right]^2 \quad (2.19)$$

where,

Q_{mean}^{obs} is the mean of observed (measured) values,

Q_{mean}^{pre} is the mean of predicted (modeled) outputs

- **Index of agreement (d)**

The index of agreement is considered as a standardized measure of the degree of model prediction error in order to the quotient of potential error and mean square error (Willmot 1984). The range of the index of agreement lies between 0 and 1. If the computed value was closer to 1, it would indicate a perfect agreement between the observed and predicted values and 0 shows no agreement at all (equation 2.20).

$$d = 1 - \left[\frac{\sum_{i=1}^{n} (Q_i^{pre} - Q_i^{obs})^2}{\sum_{i=1}^{n} (|Q_i^{pre} - Q_{mean}^{obs}| + |Q_i^{obs} - Q_{mean}^{obs}|)^2} \right] \quad (2.20)$$

2.7.2 Relative sensitivity analysis

For testing the model accuracy, a sensitivity analysis can represent the nature of interrelations between important input parameters and fluctuations of the output values. The relative sensitivity analysis denotes a comparison between sensitivities of the hypothetical input parameters change to a normalized change in output that allows different orders of magnitude (Hagen et al., 1999).

In this study, a linear relative sensitivity model was selected to find the most important input parameter that control the soil loss hazard. The relative sensitivity of input parameters was calculated using equation 2.21:

$$SS = \left| \frac{\frac{O_2 - O_1}{O_{12}}}{\frac{I_2 - I_1}{I_{12}}} \right| \quad (2.21)$$

I_1 , I_2 = minimum and maximum value of input respectively

I_{12} = average value of I_1 and I_2

O_1 , O_2 = associated output for the two input values

O_{12} = average value of O_1 and O_2

Based on the purpose of this study, the maximum and minimum of each input parameter were considered for sensitivity testing (Table 2.7). For this reason, only one parameter was changed with each model execution and all other parameters were kept constant on the base values. By this procedure, sensitivity values were calculated and ranked for a number of parameters that could most likely affect the SWEEP model output for specified scenarios. The findings of the sensitivity analysis, more precisely the knowledge of the most important parameters, it could be possible to select the best possible management protection methods to control the wind erosion in the research area.

Table 2.7. List of maximum and minimum values of model input parameters, which are used in SWEEP for the sensitivity test

Input Parameter and its units	Loamy sand 1 (Field A)		Loamy sand 2 (Field B)		Loamy sand 3 (Field C)		Organic soil (Field D)	
	Low	high	Low	high	Low	high	Low	high
Field length (m)	100	285	100	285	100	285	100	285
Field width (m)	100	285	100	285	100	285	100	285
Bulk density (Mg m^{-3})	1.36	1.48	1.34	1.42	1.27	1.43	0.68	1.05
Sand content (kg kg^{-1})	0.80	0.92	0.75	0.83	0.75	0.84	0.31	0.72
Very fine sand (kg kg^{-1})	0.07	0.18	0.08	0.14	0.07	0.13	0.06	0.14
Silt content (kg kg^{-1})	0.08	0.18	0.16	0.24	0.15	0.23	0.26	0.64
Clay content (kg kg^{-1})	0.01	0.02	0.01	0.02	0.01	0.02	0.02	0.06
Rock volume fraction (m^3 m^{-3})	0.00	0.01	0.01	0.05	0.01	0.03	0	0
Aggregate density (Mg m^{-3})	1.23	1.38	1.20	1.28	1.13	1.36	0.38	0.75
Aggregate stability (ln[J kg^{-1}])	0.94	1.08	1.00	1.12	0.99	1.18	1.15	1.64
Aggregate geometric diameter (mm)	0.03	0.35	0.21	0.49	0.16	0.50	3.95	29.10
Minimum aggregate size (mm)	0.006	0.01	0.006	0.01	0.006	0.01	0.006	0.01
Maximum aggregate size (mm)	0.91	5.00	2.05	5.00	1.66	5.00	3.00	5.00
Aggregate geometric standard deviation (mm mm^{-1})	2.36	6.86	5.51	7.88	4.87	7.97	11.09	16.06
Random roughness (mm)	7	18	7	18	7	18	7	18
Soil wilting point water content (Mg Mg^{-1})	0.03	0.07	0.08	0.09	0.05	0.10	0.27	0.41
Surface water content (Mg Mg^{-1})	0.01	0.15	0.01	0.15	0.01	0.15	0.01	0.15
Ridge height (mm)	50	100	50	100	50	100	50	100
Ridge orientation (°)	180	275	180	275	180	275	180	275
Wind speed (m s^{-1})	7.5	11.5	7.5	11.5	7.5	11.5	7.5	11.5
Wind direction (°)	180	275	180	275	180	275	180	275

2.8 Hazard and risk assessment of soil and nutrient loss by wind erosion

Three main factors play a key role in assessing wind erosion hazard and risk which include: soil erodibility, wind erosivity and land management. In order to be able to accomplish this task, the results from above described analysis of weather data, the scenario modelling using SWEEP, and the wind tunnel simulations have been used. Figure 2.20 presents a schematic flow chart of the analysis process. The wind erosivity was calculated based on a 14 year time record (2000-2013) from Foulum climatic weather station (NOAA-NCDC, 2013). Since the soil in Denmark is most prone to wind erosion during dry periods between March and July (no crop cover, dry soil surface), the calculation of erosive winds, prevailing wind direction (275°, west to east) as well as frequency and probability distribution was conducted only for this time period.

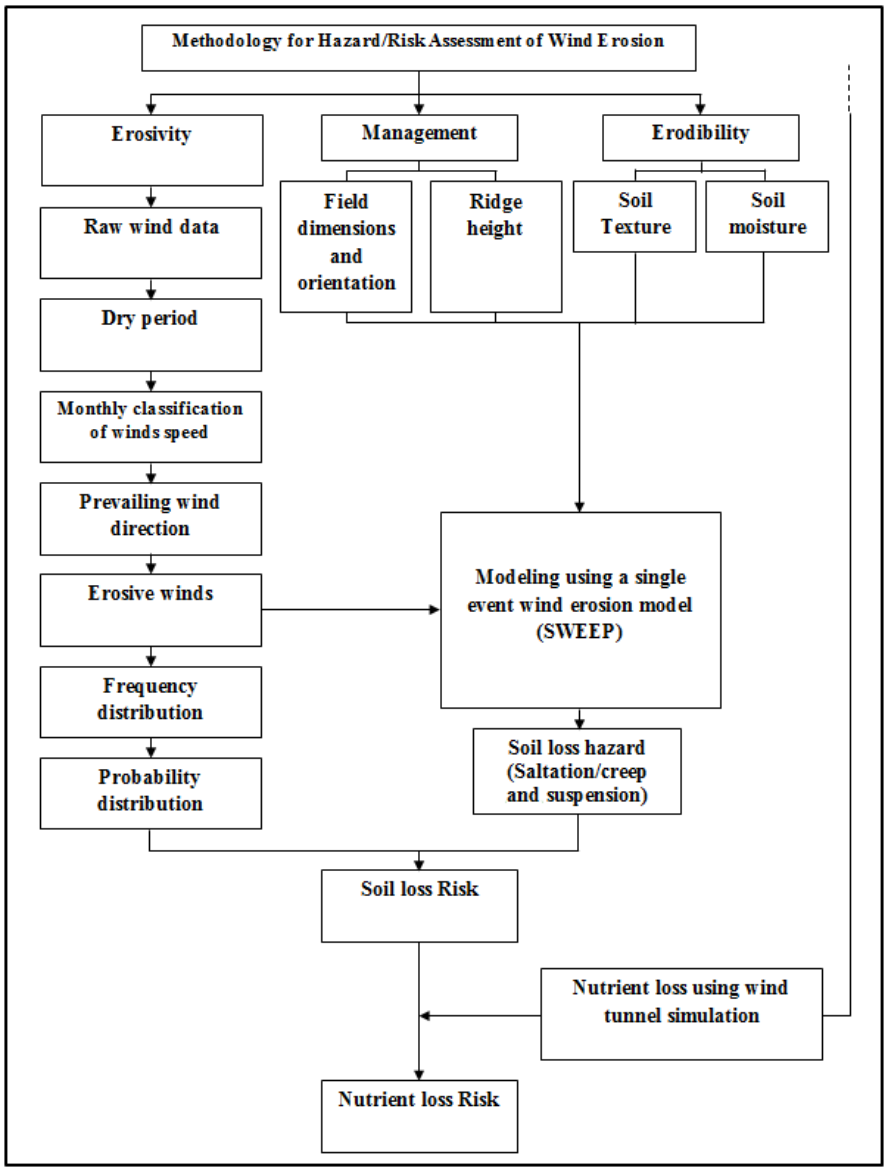

Figure 2.20. Flow chart of methodology for assessing hazard/risk of soil and nutrient loss based on probability distribution of erosive winds in dry periods

Different scenarios for soil erodibility and land management were used to calculate the hazard of soil loss by creep, saltation, and suspension using the SWEEP model (see table 2.8). Soil moisture content has a significant effect on threshold wind velocity by reducing or increasing the adhesion forces in the soil. Because of its importance, two soil moisture scenarios were included into the modelling. The specific threshold values were selected based on soil moisture measurements at a portable weather station, was installed close to research field A (Figure 2.21). The first scenario threshold with 0.15 Mg/Mg water content reflects the average measured water content during the four months period. The second threshold can be seen as 'worst case' and reflects the minimum water content (0.01 Mg/Mg) during that time period.

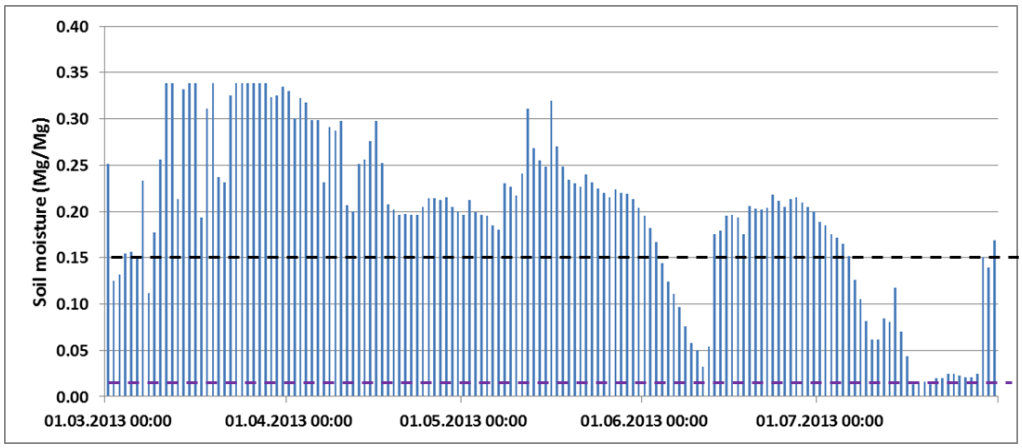

Figure 2.21. Temporal variation of soil-water content was measured at a depth of 10 cm from March to July 2013.

In order to evaluate management scenarios that influence wind erosion, dust emission and nutrient loss, two kinds of field orientation were considered. One field was elongated from North to South and the other field was oriented from West to East. In the other words, due to the incidence of prevailing wind direction from west to east, the first simulated field was perpendicular and the second one was parallel to the prevailing wind direction. Since, ploughing practices are dominantly implemented along the maximum length of the fields, tillage orientation was considered to be perpendicular to the prevailing wind direction for the north-south fields and parallel for the west-east fields. On conventionally managed fields, tillage ridges are the only soil roughness element that contributes to reduce wind erosion during springtime, before the plants can cover and protect the soil surface. Another management scenario which has been considered in this study was, because of that, related to the ridge height. Two common types of conservation tillage were selected by 50 mm and 100 mm ridge height as the most important reduced tillage to control wind erosion (Armbrust et

al., 1964). Therefore, these two ridge heights were selected as additional management scenario. Table 2.8 shows the list of different scenarios and its various classes which are categorized as scenario combinations for the hazard and risk assessment.

Table 2.8. Scenario characteristics for the wind erosion, dust emission and nutrient loss hazard/risk assessment

Scenario description		Scenario Class	Scenario Symbol	Scenario Combinations	
Erosivity	Daily Average Wind Speed	[7-8] m/s	S1	S1, S5, S7, S9	S1, S5, S7, S10
				S2, S5, S7, S9	S2, S5, S7, S10
		[8-9] m/s	S2	S3, S5, S7, S9	S3, S5, S7, S10
				S4, S5, S7, S9	S4, S5, S7, S10
		[9-10] m/s	S3		
		[>10] m/s	S4	S1, S5, S8, S9	S1, S5, S8, S10
				S2, S5, S8, S9	S2, S5, S8, S10
Erodibility	Soil surface moisture	0.15 (Mg/Mg)	S5	S3, S5, S8, S9	S3, S5, S8, S10
				S4, S5, S8, S9	S4, S5, S8, S10
		0.01 (Mg/Mg)	S6		
Management	Field dimension and orientation	X (100 m), Y(285 m) N-S	S7	S1, S6, S7, S9	S1, S6, S7, S10
				S2, S6, S7, S9	S2, S6, S7, S10
				S3, S6, S7, S9	S3, S6, S7, S10
		X (285 m), Y(100 m) W-E	S8	S4, S6, S7, S9	S4, S6, S7, S10
	Ridge height	100(mm)	S9	S1, S6, S8, S9	S1, S6, S8, S10
				S2, S6, S8, S9	S2, S6, S8, S10
		50 (mm)	S10	S3, S6, S8, S9	S3, S6, S8, S10
				S4, S6, S8, S9	S4, S6, S8, S10

As described in the introduction chapter, field sizes in northern Europe seem to increase and shelterbelts are being removed, which are the main reasons for increasing wind erosion risk in these areas (Funk et al., 2004; Kristensen, 2001). In order to investigate how the erosion risk and hazard would change with or without the influence of a protective wind barrier, all of the above scenario combinations were also modelled with a wind barrier. The applied barrier reflected the most commonly observed barrier in the study area (a single row windbreak with 35% porosity, 3.5 meter height and 3 meter width).

In order to determine the risk values for different scenario combinations, the following equation was used (equation 2.22):

$$R = P * H \tag{2.22}$$

P= probability of daily average wind speed class for the days in dry periods with at least one hour wind speed greater than threshold (11 m/s)

H= soil, PM_{10} and nutrient loss hazard for each scenario

In total 32 different scenario numbers were chosen with changing combinations of the described wind velocity, soil moisture, and land management scenarios. Table 2.9 shows the representative parameters which are modelled for each scenario number to assess the potential soil, dust, and nutrient hazard. The erosivity factor was represented by different daily average erosive wind speeds in dry periods in erosive months (March to July). The erodibility was represented by soil surface moisture content for two scenario classes in the erosive months, including average and minimum soil moisture content in 2013. The management variable was represented by two scenarios including field dimension and orientation and ridge height.

Table 2.9. Representative parameters (S_i) which are operated for each scenario number (SN_i) are presented with the grey boxes

	Erosivity				Erodibility		Management			
	Wind Speed				Moisture		Field size		Ridge	
	S1	S2	S3	S4	S5	S6	S7	S8	S9	S10
SN1										
SN2										
SN3										
SN4										
SN5										
SN6										
SN7										
SN8										
SN9										
SN10										
SN11										
SN12										
SN13										
SN14										
SN15										
SN16										
SN17										
SN18										
SN19										
SN20										
SN21										
SN22										
SN23										
SN24										
SN25										
SN26										
SN27										
SN28										
SN29										
SN30										
SN31										
SN32										

University of Basel

Hazard and Risk Assessment of Wind Erosion and Dust Emissions in Denmark - A Simulation and Modelling Approach

Results

"Wonder is the seed of knowledge"

Francis Bacon (1561-1626)

CHAPTER 3

3. Results

According to the objectives of this study, the results are presented in eight sections.

1) Wind data analysis: wind data analysis is performed to determine the frequency, wind velocity, and wind direction of erosive wind events during the critical time between March and July, in which soil cover by plants is lowest. Since the risk assessment is based on the probability distribution of erosive winds in dry periods, the first step is to extract the dry periods from the annual dataset. In the second step, the probability of occurrence is determined for each wind speed class.

2) Grain size distribution of soil and eroded sediment: Comparing the grain size distributions of soil and sediment with each other, offered an approach to distinguish the most erodible particle size fraction and to evaluate the effects of different surface scenarios. For this purpose, the wind tunnel experiments were set up.

3) Soil loss and dust enrichment ratio: the wind tunnel simulations were employed to measure the total soil and nutrient loss, in order to calculate the enrichment ratios of dust particles at different test soils and surface scenarios.

4) Nutrient loss and its enrichment ratio: wind tunnel tests and chemical analysis were used to measure the nutrients concentration in the soils and eroded sediments under different surface scenarios. The nutrient losses and nutrient enrichment ratios were calculated to determine the susceptibility of the nutrients to wind erosion from selected soils under different surface scenarios.

5) Modelling, calibration, and sensitivity analysis: the observed total soil losses from wind tunnel simulations were compared with the predicted values computed by the SWEEP model. Through this comparison, the accuracy and reliability of the model results was evaluated. In order to determine the most important and most sensitive parameters of the model, a relative sensitivity analysis was applied.

6) Hazard assessment based on scenario analysis: the results of the hazard assessment are presented for soil, PM_{10}, and nutrient losses. The assessment was based on the analysis of different potential risk scenarios for ploughed fields with no crop cover. In addition, the effect

of wind barriers as wind erosion control was evaluated by modelling different scenarios for sheltered and unsheltered farmlands.

7) Risk assessment based on scenario analysis: results from the hazard assessment that were greater than zero were multiplied by the corresponding probability of occurrence of days with at least one hour of recorded wind above the threshold of 11 m/s. Like for the hazard assessment, risk values were calculated for soil, PM_{10}, and nutrient loss in different potential risk scenarios for unsheltered and sheltered lands by wind break.

8) Hazard and risk assessment based on current conditions of field sites: the results of the scenario analysis for the actual field conditions provides a means to evaluate the effectivity of current land management and to improve our understanding of soil, PM_{10} and nutrient loss hazards and risks in the presence or absence of windbreaks.

3.1 Wind data analysis

The hourly wind velocity and direction data were obtained from the nearest synoptic weather station in Foulum, North Viborg, Denmark. The results show that, out of 2136 days of wind records, during the five months critical period (March to July) for a 14-year time series (2000-2013), 1917 days were classified into dry days. In other words, only 219 days or about 10% of the total days were classified as wet days. Figure 3.1 shows the number of dry days according to different wind speed classes. It can be seen that the most frequent wind speed belongs to the class of 3-4 m/s, in the total 488 days.

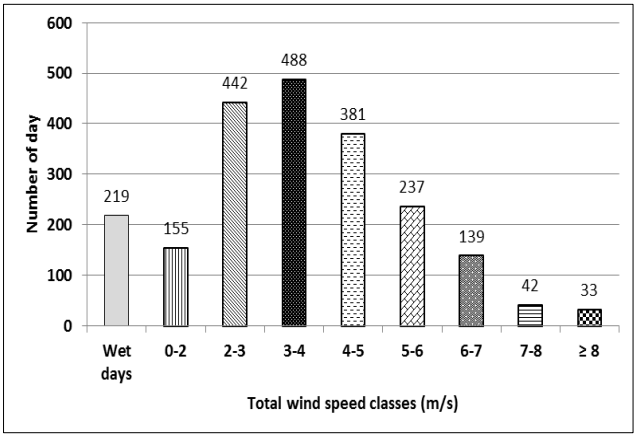

Figure 3.1. Relationship between the number of dry days and wind speed classes for (March-July) during a 14-year period (2000-2013)

Figure 3.2 displays that, out of the 1917 dry days, 49 days (about 2.5%) can be classified as erosive days, with at least one hour of wind velocities above the wind erosion threshold of 11 m/s. It can also be seen that March experienced most of the erosive winds (30 days), followed

by April, May, June, and July with 10, 6, 2, and 1 days respectively. Based on the wind data analysis, the highest probability for wind erosion events is during March to April.

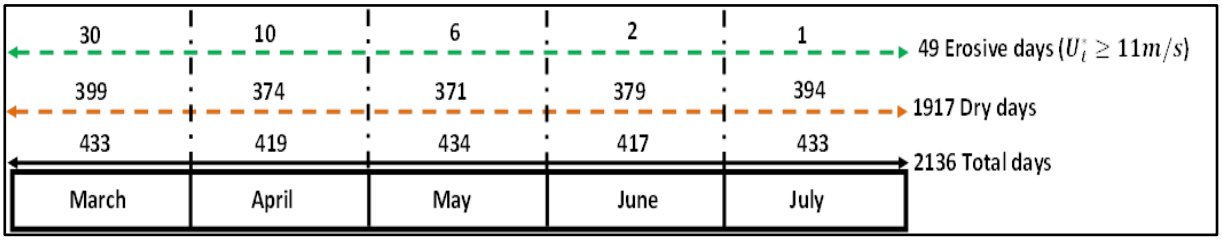

Figure 3.2. Distribution of daily wind speed for total, dry and erosive days (data periods 2000-2013)

If the erosive days per month are plotted over the years (Figure 3.3), no distinctive annual trend can be found. The variability of the erosive days over the years is so high that in 2005, 2006, and 2010 not one single erosive day occurred, whereas in 2000 the maximum of nine erosive days occurred.

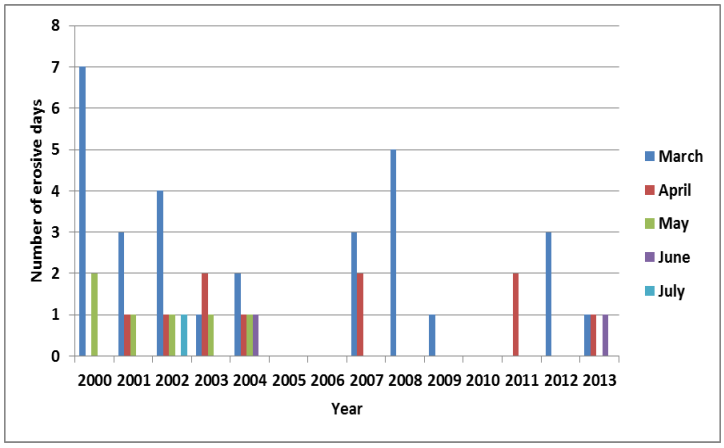

Figure 3.3. Monthly distribution of erosive wind speeds in the dry periods (2000-2013).

Figure 3.4 shows the main wind direction of erosive winds in dry periods. The most frequent direction of erosive winds during dry periods is the North-West. The wind comes less frequently out of North-East and East directions. The erosive winds from the North-East to South-West and East to the West are respectively indicating the less frequent erosive wind directions.

The results demonstrate that the main wind direction for all winds is west, whilst the prevailing direction for erosive winds is North-West. Most of the fields in this region are oriented from North to South. The test fields A and B are generally well oriented perpendicular to the prevailing wind direction. Regarding predominant direction for erosive winds, their orientation is still satisfactorily. The picture is quite different for the fields C and

D, which have their longer direction in the direction of the prevailing winds, both for all days and dry days.

The analysis of variation trends of daily average wind velocities indicates that erosive winds have the highest probability of occurrence between 12:00 p.m. and 15:00 p.m. Generally, the wind velocities start to increase at about 6:00 a.m. and subside at about 18:00 p.m.

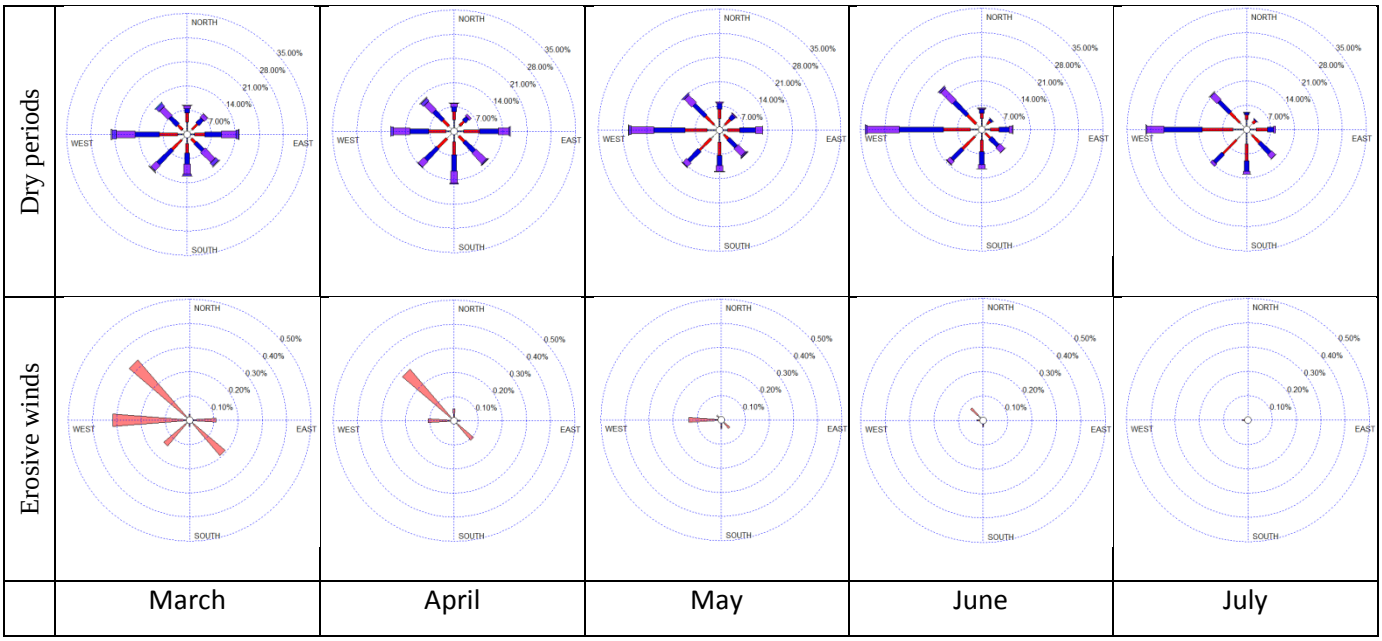

Figure 3.4. Wind direction changes for erosive winds and in dry periods

The probability distribution for erosive wind velocities is calculated using Weibull distribution. Figure 3.5 shows the cumulative distribution function fitted to daily average of erosive wind for the Foulum synoptic weather station. The scale factor of the Weibull distribution is 8.74 and the shape factor is 5.26. The best fitted line shows high values of coefficient of determination (~95%). The results of daily average wind speed and probability of erosive winds were used as input wind speed for the modeling and the risk assessment. The figure on the right (probability density) indicates that most of the erosive winds have a daily average wind velocity between 7 and 9.5 m/s.

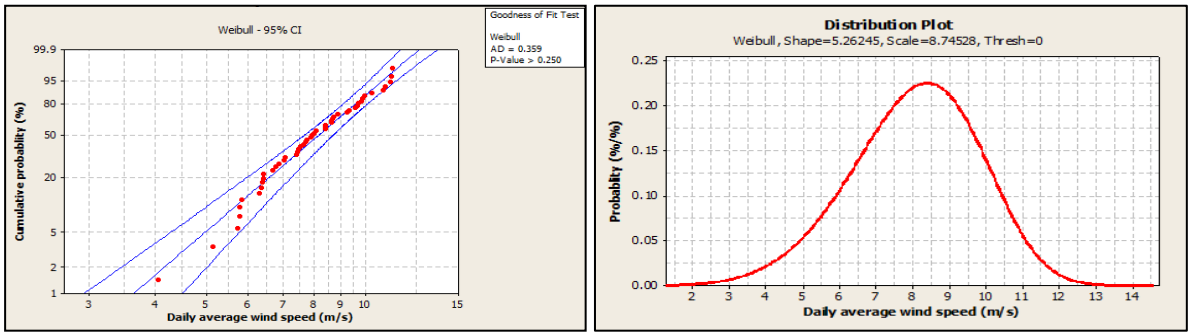

Figure 3.5. Cumulative probability (left) and probability density (right) of measured wind speed data and the fitted Weibull distribution function for erosive wind speed in dry periods

3.2 Grain size distribution of soil and eroded sediment

3.2.1 Comparison of grain size distributions

The cumulative grain size distributions for parent soils and windblown sediments are shown in Figure 3.6 and Figure 3.7 respectively. All particle size distributions represent a bimodal distribution for soil and sediment samples. The median (D_{50}) values for the soils are 178.9 µm, 199.9 µm, 214.3 µm and 68.9 µm for loamy sand class 1, loamy sand class 2, loamy sand class 3 and organic soil respectively. The organic soil from field D has clearly the highest contents in fines, followed by loamy sand class 2 (field B) and 3(field C), While loamy sand class 1 (field A) has the lowest silt content.

The comparison between parent soil grain size distributions and the ones from the eroded sediment clearly show a significant increase ($P < 0.05$) of fine particles and a decrease of everything larger than the fine sand fraction. Especially the fine sand size fraction increased on average about 15% for the loamy sand soils and 7.5% for the organic soil. This difference is caused by the preferential mobilization of fine particles by winds. Only the clay content, which is in all four soils very low, does not differ between parent soil and eroded sediment. Based on these results, the fine sand size fraction has the highest risk of erodibility, regardless of soil type.

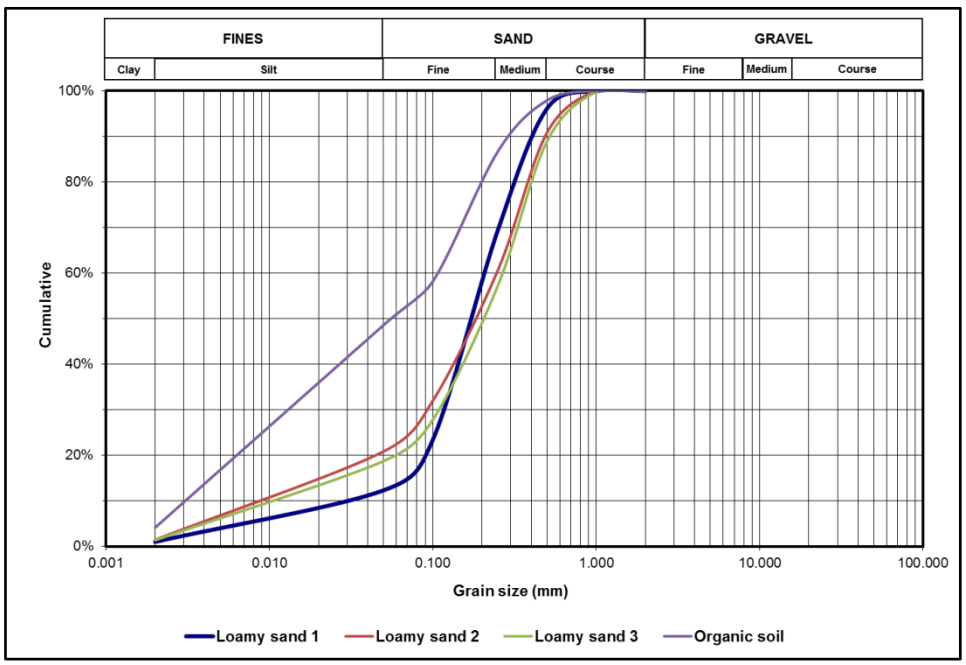

Figure 3.6. The cumulative soil grain size distribution for different soil types

(n = 35 soil samples, 5 for each soil type)

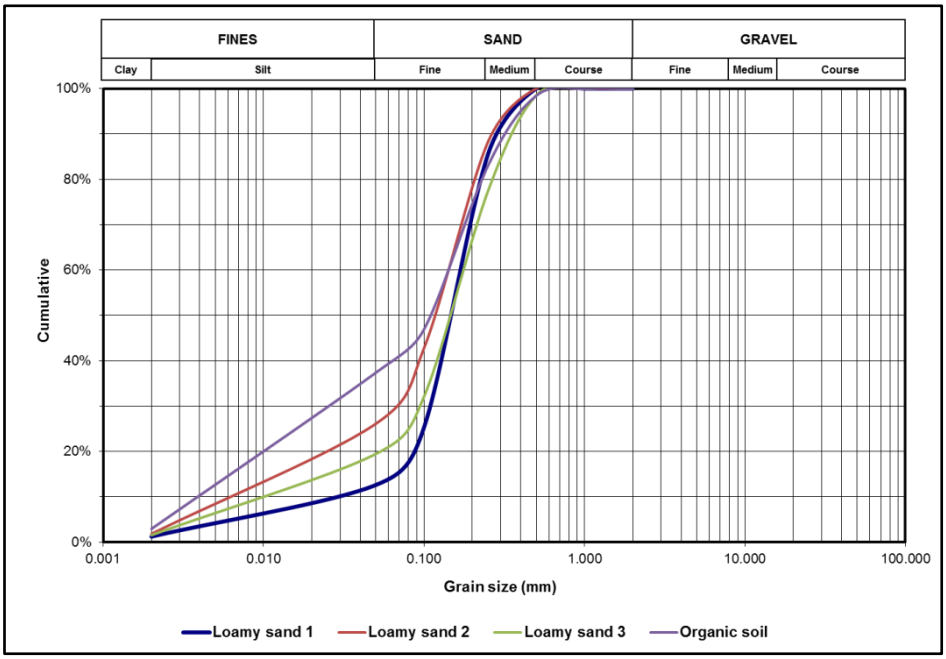

Figure 3.7. The cumulative sediment grain size distributions for different soil types collected by the sediment trap during the wind tunnel simulations. (n = 15 sediment samples for each soil type)

A detailed particle-size analysis of windblown sediments under different surface scenarios, resulting from 5 replicates of wind tunnel simulations, is presented in Figure 3.8. The results reveal that with parallel tillage, all grain size distributions follow a similar curve, with maximum amounts of fine sand (48-60%) and silt (10-25%). However with flat conditions and perpendicular tillage they show a much more diverse status. The biggest differences can be seen for perpendicular tillage, which seems to have a special sorting effect on the eroded sediment. In the flat surface and perpendicular tillage experiments, the organic soil shows much higher silt content in the eroded sediments than the other soils, which correlates well with the initial silt content of the soils (Figure 3.7). However, despite the high initial silt content, the amount of silt in the sediment, for longitudinal tillage, is much lower and almost similar to the other soils.

Symmetric graph in Figure 3.8-b is resulted by sediment grain size distribution in parallel tillage scenario. This indicates that the most sediment particles are transported through the tillage rows which are aligned to the wind direction. Whereas sediment analysis for flat surface (Figure 3.8-a) and especially for perpendicular tillage (Figure 3.8-c) demonstrated that the asymmetric graphs are due to increasing in silt and very fine sand contents especially for loamy sand class 2 and to some extent for loamy sand class 3 under perpendicular tillage practice.

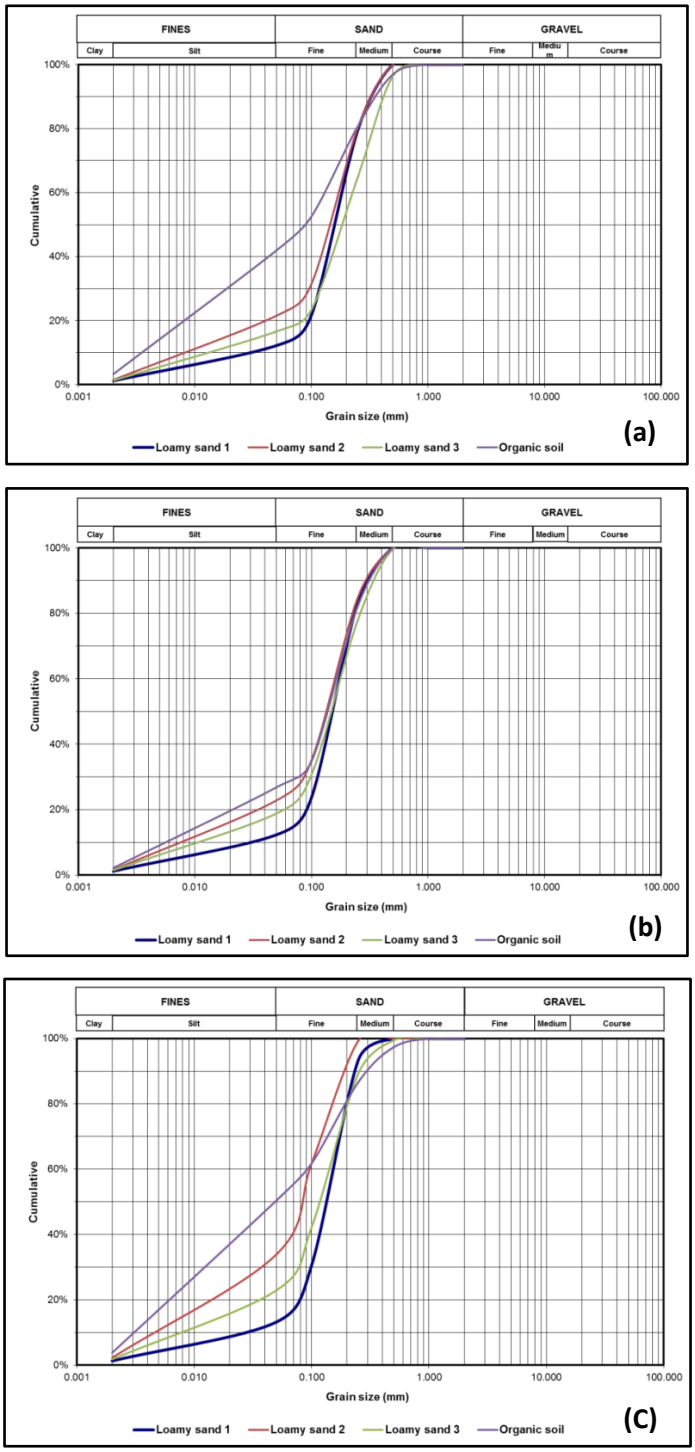

Figure 3.8. The cumulative sediment grain size distribution in different soil types and three soil surface scenarios a) Flat surface, b) Parallel tillage, c) Perpendicular tillage (n = 5 sediment samples for each soil and management)

3.2.2 Frequency of dust particles in soil and sediment

The average of PM_{10} and $PM_{2.5}$ particle content in the parent loamy sand soils (1, 2, 3) is less than 5 percent (Figure 3.9). However in organic soil, due to its silty texture, there are 5.6 and 16.5 % of $PM_{2.5}$ and PM_{10} content in parent soil respectively. Among all loamy sand soils,

loamy sand class 1 contains the lowest amounts of dust particles and classes 2 and 3 do not show any significant differences in dust particles ($P< 0.05$).

The amount of dust particles in eroded sediments is for all soils and management practices strongly attributed to the particle size distribution of the parent soils (Figure 3.10). For example all loamy sand classes do not show any difference between parent soil and sediment for neither PM_{10} nor $PM_{2.5}$ in the scenarios flat and parallel tillage. In the perpendicular scenario, however, a clear enrichment can be found for all loamy sand classes 2 and 3 (up to 3% increase for PM_{10} and 1% for $PM_{2.5}$), but surprisingly not for class 1.

The organic soil behaves very different from the loamy sand soils, most probably because of the high dust content in the parent soil. Generally, the organic soil shows the biggest differences between parent soil and sediment for both, PM_{10} and $PM_{2.5}$. For PM_{10}, the sediment in the parallel tillage scenario is reduced to about half of the fines that were present in the parent soil and in the flat scenario the decrease is about 4-5%. Same behavior, but less explicit differences can be found for $PM_{2.5}$ in these two scenarios.

Again, like for the loamy sands, the perpendicular scenario shows completely different behavior. Instead of a clear decrease in the percentage of PM_{10} and $PM_{2.5}$, almost the same amounts in the parent soil can be found. Generally, it can be summarized that the perpendicular tillage management seems to have a solid effect on dust erosion by wind and the flat as well as the parallel tillage do not seem to have a big influence on the loamy sand soils, but a reducing one for organic soil.

Sediment grain size distribution results for PM_{10} and $PM_{2.5}$ particles under different soil types and surface scenarios indicate that potential values of dust particles in the sediments are strongly attributed to the frequency of their particle size distributions in the origin soils. In organic soil where more silt are in parent soil compared with different classes of loamy sand soils, there is a certain amount of PM_{10} and $PM_{2.5}$ particles in sediment materials under all surface scenarios (Figure 3.10).

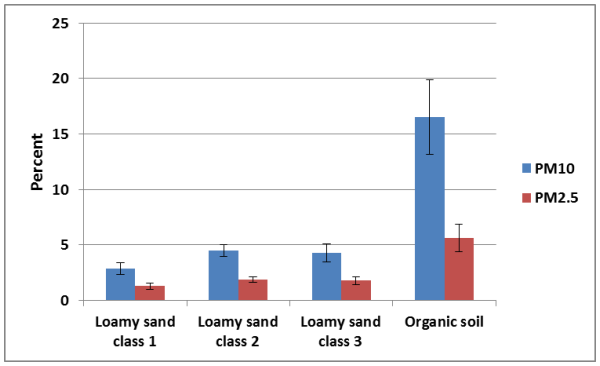

Figure 3.9. Potential PM_{10} and $PM_{2.5}$ particles in different soil types (n = 35 soil samples for each soil)

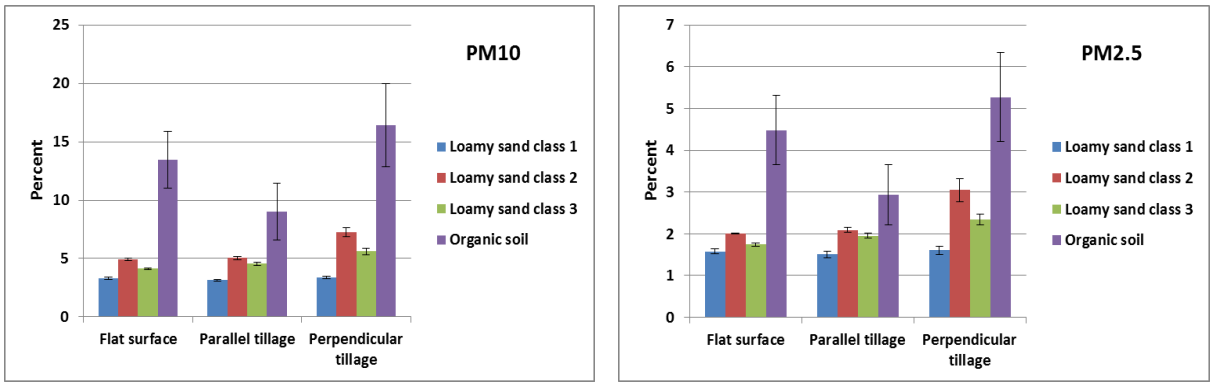

Figure 3.10. PM_{10} and $PM_{2.5}$ contents in sediments under different soil types and soil surface scenarios (n = 5 samples for each scenario)

3.3 Erosion rates (q)

3.3.1 Total soil loss

Results from wind tunnel simulations based on different soil surface scenarios show that the total mass of sediment transported at the height of 0–50 cm is largest for parallel tillage for all soil types (Figure 3.11).. Maximum erosion rates of almost 201g/m^2/min were reached for loamy sand class 1, which is in all management scenarios the most susceptible to wind erosion. The difference between erosion from parallel tillage and flat surface for this particular soil is not as distinct as it is for all other management scenarios. For example loamy soil classes 2 and 3 show twice as much erosion on parallel tillage than it was observed from flat surfaces. No significant ($P < 0.05$) difference could be found between the erosion values of loamy soil classes 2 and 3 for all scenarios, fits quite well to the relatively small differences in particle size distribution. Very interesting is that the perpendicular tillage shows by far the lowest soil erosion rates over all land managements and that the organic soil is the least susceptible soil, although it has the finest texture. The low erosion rates from perpendicular managed surfaces are important, because it somehow contradicts the promotion of dust particle deflation, which was found in section 3.2.2.

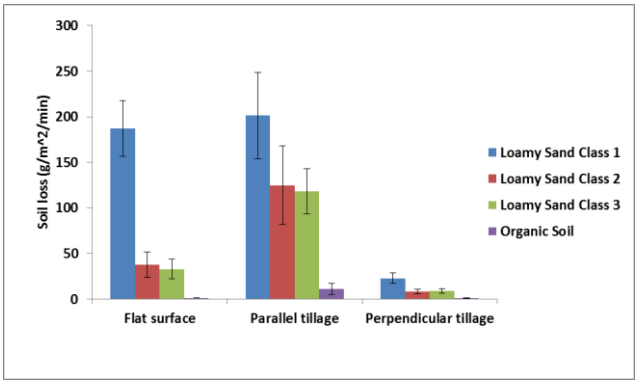

Figure 3.11. Total sediment loss (q) in different soil types and surface scenarios

3.3.2 Dust enrichment ratio (DER)

The dust enrichment ratio for all soils and managements types shows similar results as section 3.2.2 (frequency of dust). Very clearly, the low values for PM_{10} and $PM_{2.5}$ for organic soil indicates a negative enrichment on flat surfaces and parallel tillage, or in other words, a depletion of dust in sediment in comparison to parent soil. All three loamy sand classes are, with the exception of one, dominated by enrichment of PM_{10} and $PM_{2.5}$, which was expected, based on the selective process of wind erosion. The soil treatment perpendicular tillage shows for all soils by far the highest enrichment ratios (Figure 3.12 and 3.13).

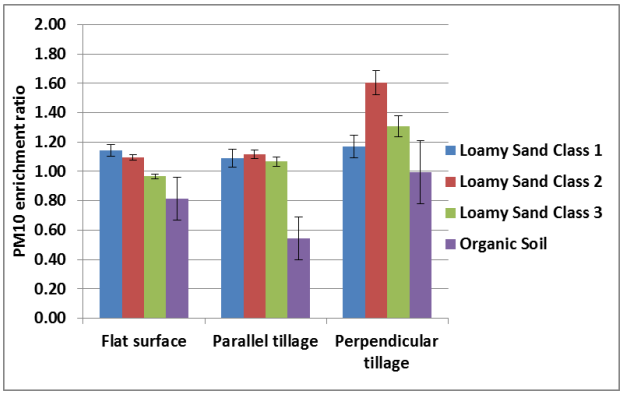

Figure 3.12. PM_{10} enrichment ratio for different soil types under different surface scenarios (n = 5 samples for each scenario)

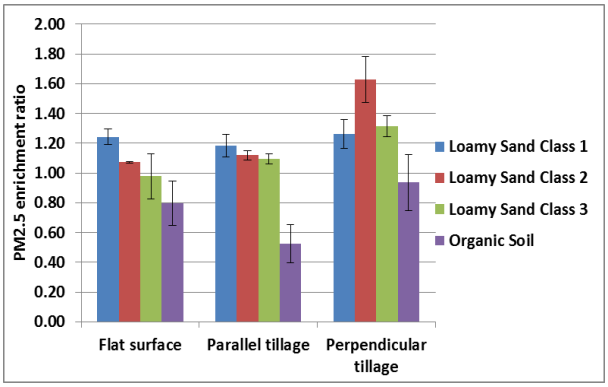

Figure 3.13. $PM_{2.5}$ enrichment ratio for different soil types under different surface scenarios (n = 5 samples for each scenario)

3.4 Nutrient loss (q_n)

3.4.1 Total nutrient loss

Soil and sediment samples were analysed for nutrient concentration including TOC, $CaCO_3$, N, P and K. Nutrient concentrations in the windblown sediment were multiplied by the sediment loss for each soil type under different surface scenarios to get the total nutrient loss ($mg/m^2/min$) as shown in Table 3.1. Since nutrient loss is a function of total soil loss, it can

be expected that the highest nutrient loss occurs from parallel tilled surfaces, followed by flat surfaces and perpendicular tillage.

Among all nutrients, TOC and $CaCO_3$ show the highest amounts of nutrient loss and P the lowest ones for all scenarios. Due to highest erosion rates of loamy sand class 1, this soil has the highest nutrient loss for all soil surface scenarios as well. The above mentioned general rule does only work for soils with similar nutrient contents in the initial soil, which are in our case the three loamy sand soils. For the organic soil the case is different, since it has a different nutrient composition. For some nutrients, for example N quite considerable losses can be found, but for other nutrients, the loss is very low or negligible (K, $CaCO_3$). The nutrient enrichment ratio is, because of this comparability problem, a better parameter to evaluate the different soils and management practices with regards to their nutrient loss.

Table 3.1. The average nutrient loss discharge (q_n) in different soil types and surface scenarios ($mg/m^2/min$)

soil types	soil surface scenario	K	P	N	TOC	$CaCO_3$
Loamy Sand Class 1 (field A)	Flat Surface	8.15	0.35	162.26	1853.19	496.31
	Parallel Surface	7.93	0.36	188.62	2187.19	539.96
	Perpendicular Surface	1.25	0.06	25.16	287.04	71.58
Loamy Sand Class 2 (field B)	Flat Surface	2.87	0.13	55.56	597.72	144.84
	Parallel Surface	8.84	3.54	189.18	2069.79	497.09
	Perpendicular Surface	0.70	0.24	17.91	195.87	45.41
Loamy Sand Class 3 (field C)	Flat Surface	1.18	0.51	39.82	464.19	91.49
	Parallel Surface	4.36	1.92	133.31	1605.28	352.77
	Perpendicular Surface	0.47	0.14	15.00	177.73	39.99
Organic Soil (field D)	Flat Surface	0.06	0.01	14.08	168.76	19.63
	Parallel Surface	0.39	0.07	94.87	1116.76	129.68
	Perpendicular Surface	0.06	0.01	12.86	143.90	13.55

3.4.2 Nutrient enrichment ratio

To identify the most susceptible soil and management scenario to nutrient loss, the nutrient enrichment ratios were calculated based on the nutrient losses obtained by wind tunnel simulations (section 3.4.1) in comparison to the chemical composition of the parent soils. The average nutrient enrichment ratios under different surface scenarios and soil types are shown in Figure 3.14.

The nutrients $CaCO_3$ and K have the highest enrichment ratios and they are the only nutrients that show enrichment under all management techniques. For most of the nutrients enrichment can be observed for perpendicular tillage surfaces, which corresponds very well with the previous mentioned enrichment ratio of dust particles for perpendicular tillage. This

phenomenon can be attributed to preferential attachment of nutrients to finer particles. The lowest enrichment ratio for almost all nutrients and scenarios can be detected for loamy sand class 1.

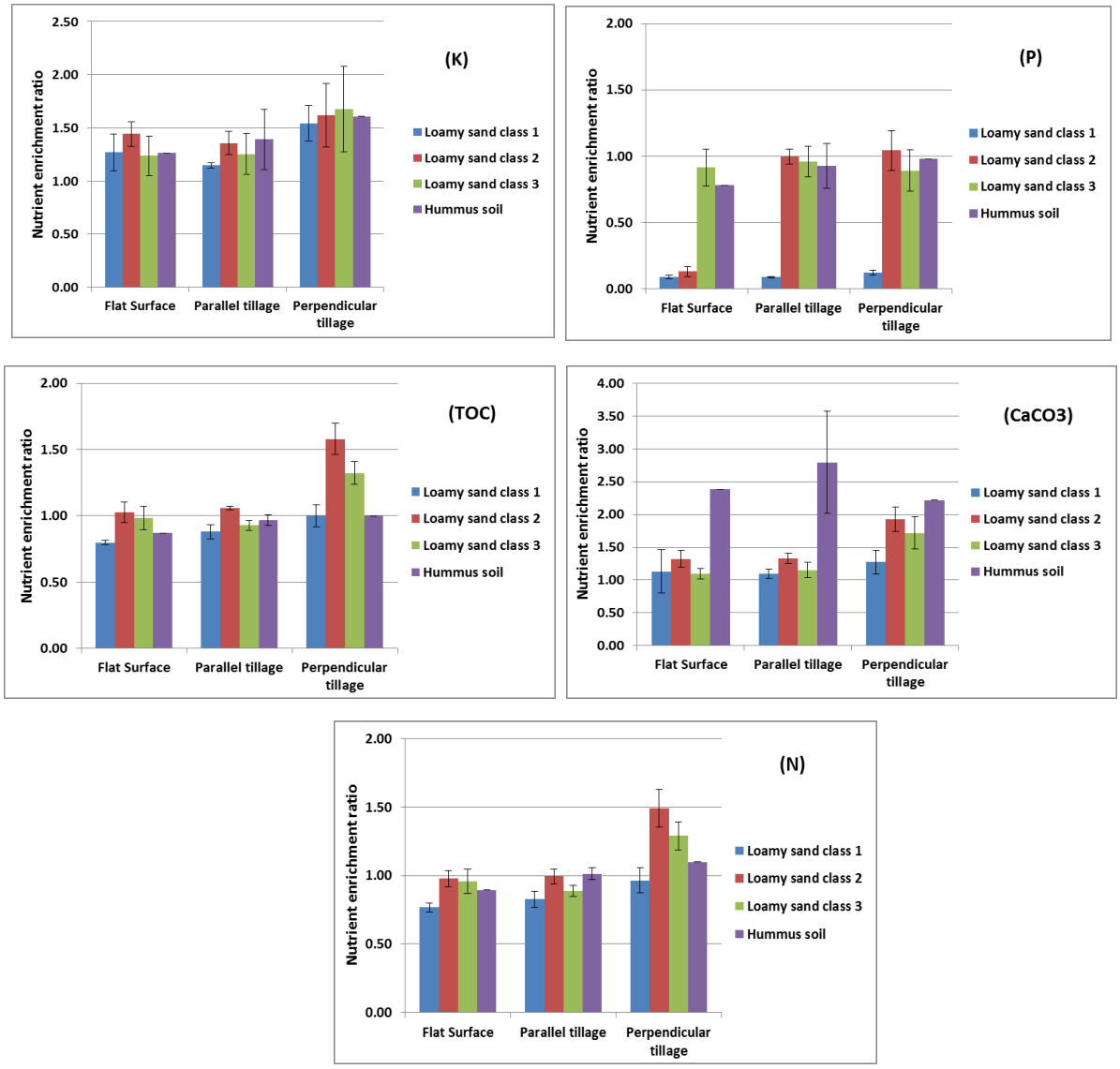

Figure 3.14. Nutrients enrichment ratio for various soil types and different surface scenarios

Tables 3.2-3.5 include the Pearson correlation ($P<0.05$) between nutrient and particle enrichment ratio which confirms that the nutrient is mostly attached to fine particles. In particular, $CaCO_3$, N and TOC in loamy sands class 2 and 3 represent a strong correlation with PM_{10} and $PM_{2.5}$ enrichment ratios. Since eroded particle sizes are more represented in the erodible portion of the parent soil (Nickling, 1983; Sharratt, 2011), results indicated a strong correlation between dust enrichment ratios with clay and silt particles. In loamy sand class 1 and organic soil, there is no observed significant correlation between particle sizes and nutrient contents.

Table 3.2. Pearson correlation between nutrient and particle enrichment ratio in loamy sand class 1

	K	P	N	TOC	CaCo3	PM2.5	PM10	Clay	Silt	Very Fine Sand	Fine Sand
P	0.97										
N	0.52	0.66									
TOC	0.63	0.77	0.81								
CaCo3	0.50	0.47	0.46	0.52							
PM2.5	0.35	0.28	0.16	0.05	-0.02						
PM10	0.44	0.36	0.30	0.05	0.00	0.90					
Clay	0.34	0.27	0.14	0.05	-0.02	1.00	0.89				
Silt	0.52	0.54	0.49	0.42	0.05	0.79	0.81	0.79			
Very Fine Sand	0.56	0.64	0.65	0.75	0.19	0.44	0.41	0.45	0.77		
Fine Sand	0.28	0.40	0.64	0.52	0.20	-0.33	-0.09	-0.34	0.12	0.48	
Medium Sand	-0.53	-0.64	-0.76	-0.74	-0.21	-0.19	-0.30	-0.19	-0.63	-0.92	-0.79

Table 3.3. Pearson correlation between nutrient and particle enrichment ratio in loamy sand class 2

	K	P	N	TOC	CaCo3	PM2.5	PM10	Clay	Silt	Very Fine Sand	Fine Sand
P	0.24										
N	0.41	0.54									
TOC	0.50	0.56	0.98								
CaCo3	0.59	0.51	0.93	0.97							
PM2.5	0.55	0.58	0.89	0.91	0.89						
PM10	0.46	0.55	0.92	0.93	0.89	0.98					
Clay	0.56	0.59	0.88	0.90	0.89	1.00	0.98				
Silt	0.41	0.58	0.94	0.95	0.90	0.94	0.98	0.93			
Very Fine Sand	0.37	0.59	0.95	0.94	0.88	0.88	0.92	0.87	0.97		
Fine Sand	-0.42	-0.42	-0.92	-0.96	-0.92	-0.83	-0.89	-0.82	-0.94	-0.92	
Medium Sand	-0.34	-0.67	-0.90	-0.88	-0.81	-0.90	-0.93	-0.90	-0.95	-0.97	0.82

Table 3.4. Pearson correlation between nutrient and particle enrichment ratio in loamy sand class 3

	K	P	N	TOC	CaCo3	PM2.5	PM10	Clay	Silt	Very Fine Sand	Fine Sand
P	-0.39										
N	0.38	-0.14									
TOC	0.48	-0.13	0.96								
CaCo3	0.47	-0.37	0.87	0.87							
PM2.5	0.56	-0.21	0.80	0.81	0.90						
PM10	0.56	-0.22	0.83	0.84	0.92	1.00					
Clay	0.55	-0.21	0.79	0.80	0.89	1.00	0.99				
Silt	0.48	-0.17	0.82	0.84	0.90	0.99	0.98	0.99			
Very Fine Sand	0.46	-0.11	0.79	0.79	0.82	0.96	0.94	0.96	0.97		
Fine Sand	0.43	0.06	0.17	0.18	0.33	0.62	0.56	0.63	0.57	0.66	
Medium Sand	-0.50	0.09	-0.74	-0.75	-0.79	-0.96	-0.94	-0.96	-0.96	-0.99	-0.75

Table 3.5. Pearson correlation between nutrient and particle enrichment ratio in organic soil

	K	P	N	TOC	CaCo3	PM2.5	PM10	Clay	Silt	Very Fine Sand	Fine Sand
P	0.96										
N	0.56	0.60									
TOC	0.58	0.68	0.95								
CaCo3	-0.77	-0.64	-0.20	-0.12							
PM2.5	0.34	0.08	-0.04	-0.24	-0.45						
PM10	0.40	0.15	0.00	-0.20	-0.49	1.00					
Clay	0.33	0.08	-0.04	-0.25	-0.45	1.00	1.00				
Silt	0.39	0.13	-0.01	-0.22	-0.52	1.00	1.00	1.00			
Very Fine Sand	0.15	-0.11	0.06	-0.20	-0.49	0.83	0.80	0.83	0.84		
Fine Sand	-0.30	-0.05	0.11	0.31	0.47	-0.99	-0.98	-0.99	-0.99	-0.85	
Medium Sand	-0.38	-0.15	-0.33	-0.04	0.57	-0.82	-0.83	-0.82	-0.85	-0.87	0.78

3.5 Modelling and calibration of the SWEEP model

3.5.1 Input parameters and mean soil erosion loss

The SWEEP model requires hourly wind speed data and additional input parameters for soil properties to run wind erosion simulations and predict the average total soil loss. The total soil loss can be differentiated into sum of saltation + creep, suspension, and PM_{10} as the part of the suspension mode. The necessary input values of soil properties, which were used as input data for the SWEEP model for the selected soils, are listed in Table 3.6.

Table 3.6. List of intrinsic soil properties used by SWEEP for various soil types
(Mean ± standard deviations, Sample size (N) = 35 samples)

Parameter	unit	Loamy sand class 1 (field A)	Loamy sand class 2 (field B)	Loamy sand class 3 (field C)	Organic Soil (field D)
Bulk density	Mg/m^3	1.42 ± 0.04	1.38 ± 0.02	1.36 ± 0.05	0.83 ± 0.09
Sand fraction	kg/kg	0.88 ± 0.03	0.79 ± 0.02	0.81 ± 0.02	0.51 ± 0.11
Very fine sand fraction	kg/kg	0.11 ± 0.03	0.11 ± 0.01	0.09 ± 0.01	0.10 ± 0.02
Silt fraction	kg/kg	0.11 ± 0.03	0.19 ± 0.02	0.17 ± 0.02	0.44 ± 0.10
Clay fraction	kg/kg	0.01 ± 0.00	0.01 ± 0.00	0.01 ± 0.00	0.04 ± 0.01
Rock volume fraction	m^3/m^3	0.003 ± 0.00	0.02 ± 0.01	0.02 ± 0.01	0.00 ± 0.00
Avg aggregate density	Mg/m^3	1.30 ± 0.04	1.24 ± 0.02	1.23 ± 0.06	0.54 ± 0.08
Avg dry aggregate stability	ln(J/kg)	0.98 ± 0.03	1.05 ± 0.03	1.04 ± 0.04	1.44 ± 0.13
GMD of aggregate sizes	mm	0.12 ± 0.08	0.31 ± 0.09	0.26 ± 0.07	19.07 ± 6.21
GSD of aggregate sizes	-	4.09 ± 1.08	6.49 ± 0.73	6.00 ± 0.68	13.47 ± 1.51
Minimum aggregate size	mm	0.01 ± 0.00	0.01 ± 0.00	0.01 ± 0.00	0.01 ± 0.00
Maximum aggregate size	mm	1.41 ± 0.56	2.99 ± 0.85	2.52 ± 0.65	5.00 ± 1.09
Soil wilting point water content	Mg/Mg	0.04 ± 0.01	0.08 ± 0.00	0.07 ± 0.01	0.34 ± 0.05

The output of model simulations for the test fields in Denmark are presented in Figure 3.15. In accordance to the results from the wind tunnel experiments, the SWEEP computations show that the loamy sand class 1 is the most susceptible soil to be eroded. About 10.2 Kg/m^2 of the total soil loss were calculated, whereas for the organic soil the lowest erosion rate was observed (2.2 Kg/m^2). The statistical analysis of the soil losses for loamy sands class 2 and 3 indicates that there is no significant difference between the soils. This is again in agreement with the wind tunnel results. Although the results show that suspension is the main mode of erosion and transport regardless of the soil type, the PM_{10} loss is very low in relation to the

total soil loss. Main reason for this is most probably the low initial content of dust in the parent soils.

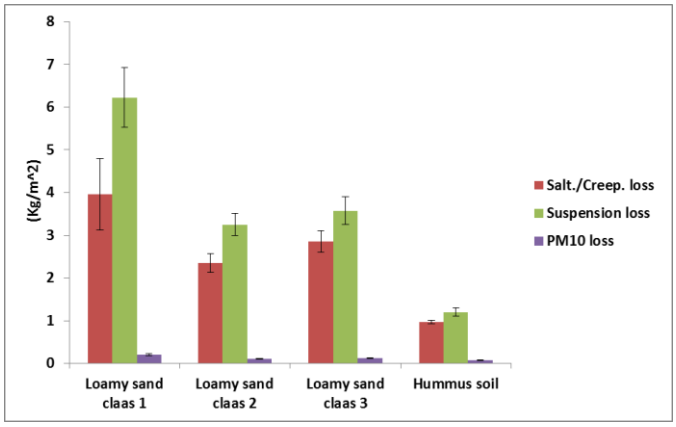

Figure 3.15. Average soil loss

3.5.2 Model performance evaluation

In order to assess the performance of the SWEEP model, the computed predictions for total soil loss were compared with experimental results using the wind tunnel. Table 3.7 presents a summary of the model performance evaluation according to the introduced calibration coefficients (section 2.7.1) and comparison plot for the different soil types. All selected statistical criteria underline the visual observation from the plot.

The results show that there is a relatively good correlation for loamy sand class 3 and the organic soil with R^2-values of 0.96 and 0.82, RMSE of 2.19 and 2.87, respectively. The sandy class 2 has also a good correlation coefficient of 1.16, but the R^2-value is only 0.44. A possible reason for the low R^2-value is that the coefficient of determination (R^2) is oversensitive to outliers. The comparison plots confirm the appraisal via the correlation coefficients (CC), because the curve pattern of predicted and measured values are very similar to each other for loamy sand class 2, 3, and organic soil. In contrast, the index of agreement (d) indicates a good correlation between observed and simulated for loamy sands class 2 and 3 by 0.61 and 0.75 values respectively. All soil types illustrated a relatively low RMSE, except loamy sand class 1 which indicated a poor agreement between observed and predicted total soil loss (RMSE= 44.21). Therefore, only for loamy sand class 1 a significant difference between predicted and observed values can be noted. This indicates that the SWEEP model under estimates the total soil loss in the prediction for loamy sand class 1.

Table 3.7. Calibration coefficients, model evaluation statistics and plots of comparison in different soil types

Soil types	Total soil loss (Kg/m^2)		Average calibration coefficient	Model evaluation statistics			Plots of comparison
	Observed	Predicted		R^2	RMSE	d	
Loamy sand class 1	21.58 31.49 28.97 32.66 33.61	8.89 10.61 8.17 10.98 12.29	2.93	0.46	44.21	0.27	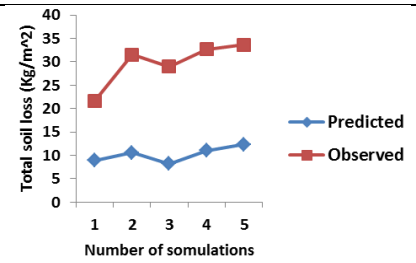
Loamy sand class 2	6.85 7.34 4.97 8.01 5.39	5.13 5.88 5.00 6.27 5.76	1.16	0.44	2.87	0.61	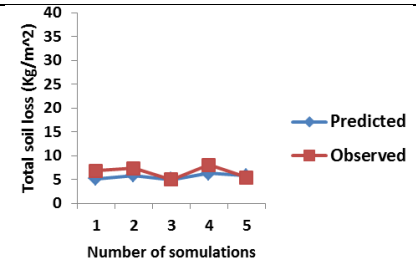
Loamy sand class 3	4.27 6.32 5.64 4.60 7.22	5.79 6.74 6.23 5.99 7.38	0.87	0.96	2.19	0.75	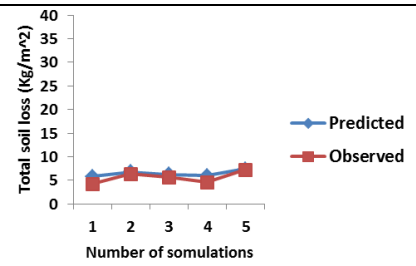
Organic soil	0.18 0.20 0.22 0.24 0.25	1.99 2.05 2.18 2.40 2.26	0.10	0.82	3.54	0.03	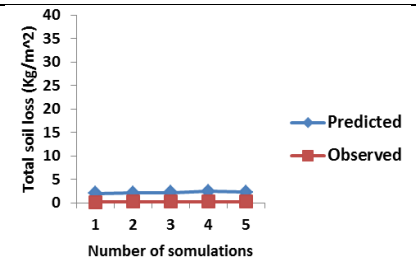

3.5.3 Sensitivity analysis

The sensitivity analysis is employed to understand the magnitude of changes in the outputs of SWEEP model in relation to changes in the value of input parameters to find the most sensitive ones. For this reason, the effect of each input parameter was studied by changing its minimum and maximum values among the four types of soil, while keeping the other parameters constant.

The most influential parameter in the SWEEP model is the ridge orientation in relation to the prevailing wind direction (relative sensitivity index = 4.79). This statement is only valid for ploughed soils with no crop cover. The second ranked parameter is random roughness

(sensitivity index of 2.27). Wind speed, ridge height, aggregate density, soil surface water content, sand content, rock volume fraction, aggregate stability, aggregate geometric diameter, aggregate geometric standard deviation, Soil wilting point water, field length and width are respectively the other most sensitive parameters, varying between 0.01 and 1.87 (Table 3.8). The least sensitive input parameters include very fine sand, silt content, clay content, bulk density, minimum and maximum aggregate size, which all have a relative sensitivity index of zero.

Table 3.8. The relative sensitivity values of the input parameters to the model output

Input Parameter and its units	Input values		Sensitivity index	Importance of the parameters (%)
	Low	high		
Field length (m)	100	285	0.01	0.066
Field width (m)	100	285	0.01	0.066
Bulk density (Mg m^{-3})	0.68	1.48	0.00	0
Sand content (kg kg^{-1})	0.31	0.92	0.01	0.066
Very fine sand (kg kg^{-1})	0.06	0.18	0.00	0
Silt content (kg kg^{-1})	0.08	0.64	0.00	0
Clay content (kg kg^{-1})	0.01	0.06	0.00	0
Rock volume fraction (m^3 m^{-3})	0.00	0.05	0.26	1.4
Aggregate density (Mg m^{-3})	0.38	1.38	1.27	6.8
Aggregate stability (ln[J kg^{-1}])	0.94	1.64	0.04	0.2
Aggregate geometric diameter (mm)	0.03	29.10	0.43	2.3
Minimum aggregate size (mm)	0.006	0.01	0.00	0
Maximum aggregate size (mm)	0.91	5.00	0.00	0
Aggregate geometric standard deviation (mm mm^{-1})	2.36	16.06	0.07	0.4
Random roughness (mm)	7	18	2.27	12
Soil wilting point water content (Mg Mg^{-1})	0.03	0.41	0.17	0.9
Surface water content (Mg Mg^{-1})	0.01	0.15	1.14	6.1
Ridge height (mm)	50	100	1.63	8.7
Ridge orientation (°)	180	275	4.79	25.5
Wind speed (m s^{-1})	7.5	11.5	1.87	10
Wind direction (°)	180	275	4.79	25.5

3.6 Hazard and risk assessment of total soil, dust and nutrient loss based on scenario analysis

Hazard and risk analysis of wind erosion for the total soil loss and dust (PM_{10}) loss were performed by SWEEP model and classified based on 32 hypothesized scenarios and their representative parameters for each soil type (see chapter 2). The results for different nutrient loss hazards were obtained by multiplying the total soil loss in each scenario by average nutrient loss for its representative tillage surface obtained from the wind tunnel experiments. The risk values were calculated by multiplying the amounts of different hazards (soil, dust and nutrient losses) to the representative erosive wind speed probability for each of daily average classes.

3.6.1 Hazard assessment of total soil loss

All scenario numbers with the average amount of soil surface water content of 0.15 Mg/Mg, do not show any soil loss regardless of soil type. Accordingly, a wind erosion event during the period from March to July can only happen, when the soil moisture content is less than average. It is evident, that only 9 scenarios out of the 32 scenario numbers show at least a minimum amount of total soil and PM_{10} loss for the loamy sand soils. Consequently, PM_{10} loss could only be observed for the scenarios SN12, SN15, SN16, SN27, SN28, SN29, SN30, SN31, and SN32 (Figure 3.16). For field D, which is covered by organic soil, there is only one scenario (SN32) which presents a hazard for the soil.

In all fields, SN12 (10cm height of the ridges in perpendicular tillage) shows the lowest hazard among the ones with any erosion. The other scenarios with erosion are related to perpendicular tillage with a 5 cm ridge height (SN27 and SN28), parallel tillage with a 10 cm ridge height (SN15 and SN16), and parallel tillage with a 5 cm ridge height (SN29, SN30, SN31 and SN32). Among all of the scenario numbers, the highest hazard for the total soil loss can be found for SN32 (5cm parallel ridges, wind velocity > 10 m/s), regardless of the soil type (Figure 3.16).

Among the different soils, the loamy sand class 3 is the one with highest susceptibility to wind erosion in the most of the possible scenarios, although there is no general significant difference between hazard values for loamy sands class 3 and class 2. The scenarios with 5cm parallel tillage orientation can be classified as the worst case scenarios (including SN29,

SN30, SN31 and SN32), all of which have erosion hazards above 20 ton/ha on unsheltered fields.

In addition, a clear reduction of soil loss hazard can be seen for the simulations including a standard, single row wind break (Figure 3.17, right). The reduction coefficient is roughly 80 percent for all soil types. Scenario numbers SN12, SN27, and SN28, all of which are perpendicular tilled surfaces do not show any hazard of erosion anymore.

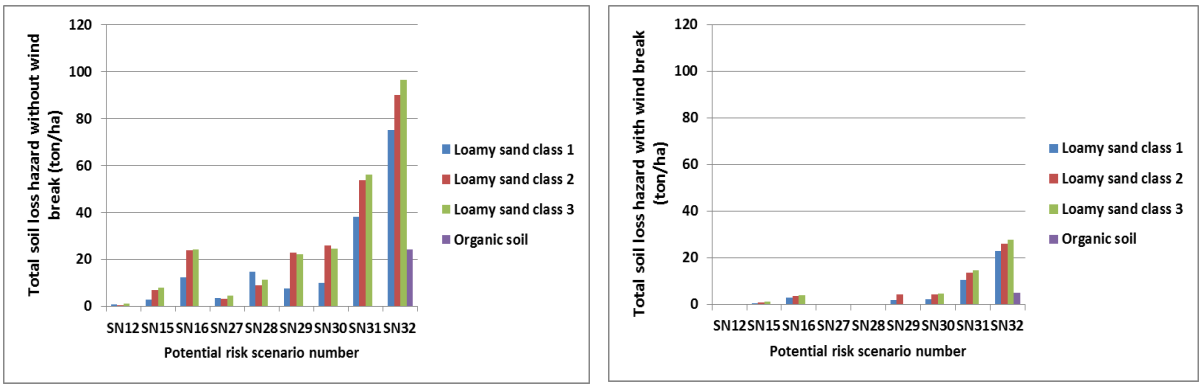

Figure 3.16. Comparison of total soil loss hazard without (left) and with (right) wind break for different soil types under potential scenarios

SN12= Perpendicular tillage, ridge height: 10 cm, Daily average wind speed: ≥ 10 m/s
SN15= Parallel tillage, ridge height: 10 cm, Daily average wind speed: 9-10 m/s
SN16= Parallel tillage, ridge height: 10 cm, Daily average wind speed: ≥ 10 m/s
SN27= Perpendicular tillage, ridge height: 5 cm, Daily average wind speed: 9-10 m/s
SN28= Perpendicular tillage, ridge height: 5 cm, Daily average wind speed: ≥ 10 m/s
SN29= Parallel tillage, ridge height: 5 cm, Daily average wind speed: 7-8 m/s
SN30= Parallel tillage, ridge height: 5 cm, Daily average wind speed: 8-9 m/s
SN31= Parallel tillage, ridge height: 5 cm, Daily average wind speed: 9-10 m/s
SN32= Parallel tillage, ridge height: 5 cm, Daily average wind speed: ≥ 10 m/s

3.6.2 Hazard assessment of dust (PM_{10}) loss

Figure 3.17 shows the comparison of different amounts of PM_{10} loss hazard in sheltered and unsheltered fields. In the worst case scenario (SN32), establishing a wind break around fields A, B and C with loamy sand soils classes 1, 2 and 3 respectively, could decrease the intense dust (PM_{10}) loss by up to more than 2.5 times. For organic soils, results show that a single row of wind break network is able to reduce PM_{10} loss hazard by 4 times compared to when obstacles have been removed around field D.

As results reveal, loamy sand class 3 produces more dust but there is no significant difference between this soil and loamy sand class 2 regarding to dust emission in the most evaluated scenarios.

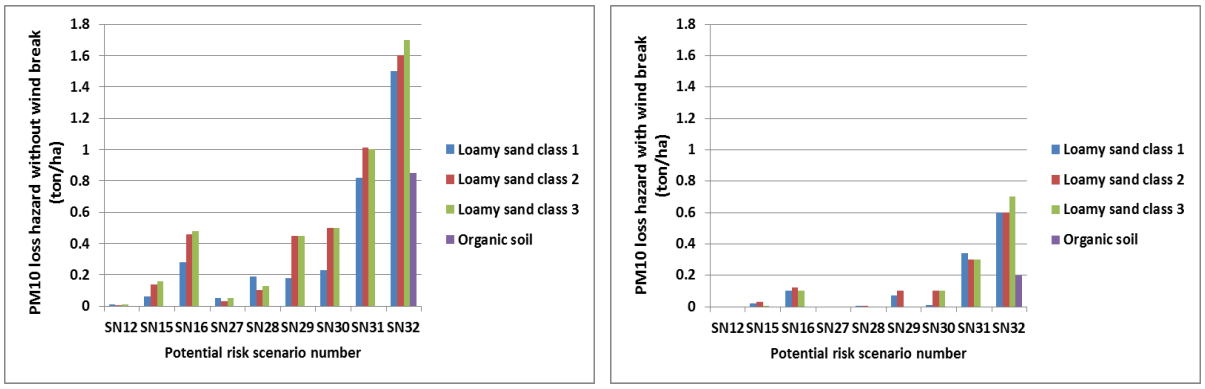

Figure 3.17. Comparison of PM_{10} loss hazard without (left) and with (right) wind break for different soil types under potential scenarios

3.6.3 Hazard assessment of nutrients loss

There is a significant difference between the amounts of nutrient loss hazard for TOC and $CaCO_3$ due to higher concentration of these nutrients in the sediments. Among nutrient loss hazard for K, P and N, results show that K commonly represent the highest hazard values in all fields (Figure 3.18). For unsheltered fields with loamy sand class 1, TOC, $CaCO_3$, and K represent the highest amount of nutrient loss hazard in SN32 by 817, 200, and 3 Kg/ha respectively. In comparison to loamy sand class 1 (field A), the field with loamy sand class 2 shows much higher nutrient loss hazards. For Potassium (K), TOC, and $CaCO_3$ it is about 2 times as higher than field A. A more significant increase can be seen in the amount of phosphorus loss hazard, in comparison between loamy sand class 1 and 2. It is partly related to the higher concentration of P in the origin soil, which is caused the phosphorus to be in the fourth rank of different nutrient loss hazards after TOC, $CaCO_3$ and K in loamy sand class 2 (Figure 3.18).

Due to similar conditions of total soil loss rates in fields B and C, the amounts of nutrient loss hazard tend to follow the pattern of soil loss, except when the concentration of nutrient content in the parent soils are different. As shown in Figure 3.19, the worst case scenarios are related to SN31 and SN32 where the soil surface is Ploughed parallel to the erosive wind with a 5 cm ridge height. As in field B, the highest nutrient loss hazard is present in the worst case scenario (SN32). The result show that the nutrient losses for TOC and $CaCO_3$ are1315 and 288 Kg/ha, respectively in field C.

As shown in Figure 3.19, there are no calculated nutrient loss rates for the most scenarios in field D due to inherent resistance of organic soil to wind erosion. Results display that the highest amount of nutrients loss hazard in organic soil can be observed for SN32, which

represents the scenarios with highest daily average wind speed (≥ 10 m/s) and lowest ridge height (5 cm) with parallel orientation to the direction of erosive winds.

In summary, loamy sand class 2 has a higher potential nutrient loss hazard than loamy sands class 1 and 3. However, the organic soil showed highest hazard for SN32, all other scenario numbers do not show any nutrient loss hazard in field D, so the loamy sand class 2 can, therefore, be considered as the most threatened soil by nutrient loss.

Drastic reduction of total soil loss and PM_{10} by site protection using a supposed single row wind break (see Figure 3.18 and 3.19) resulted in decreasing nutrients loss hazard up to 3 times in each scenario because of attaching more nutrients to fine particles. As shown in Figure 3.19 due to the establishment of wind break, the amounts of nutrient loss hazard for TOC, $CaCO_3$ and K as the most eroded nutrients in SN32 can be considered as the worst case scenario decreased by 250, 61, 0.91 Kg/ha respectively in field A.

Figure 3.19 indicates the effect of using a single row windbreak to reduce loss hazard of nutrients under different potential scenarios in field B (loamy sand class 2). As it was shown for field A (loamy sand class 1), the establishment of shelterbelts led to a clear reduction of nutrient loss hazard in potential scenarios with perpendicular tillage, including SN12, SN27 and SN28.

The comparison between TOC loss hazard, the nutrient with highest deflation probability, in unsheltered (Figure 3.18) and sheltered (Figure 3.19) conditions, verify the positive impact of wind breaks for use as wind erosion protection (worst case scenario (SN32) on field C (1315 versus 377 Kg/ha). In field D, the significant role of wind breaks again led to a 4.8 folds reduction of nutrient loss for organic soil in comparison to the hazard values in unsheltered area.

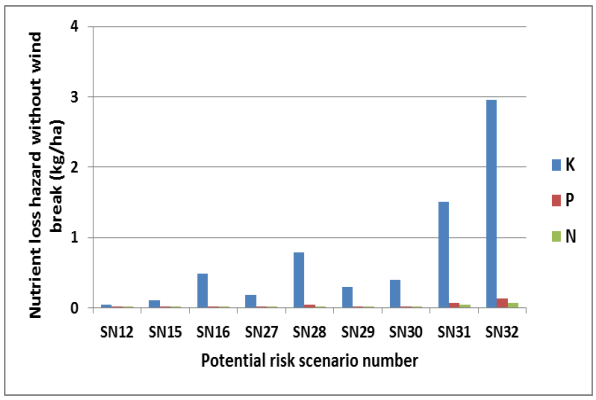

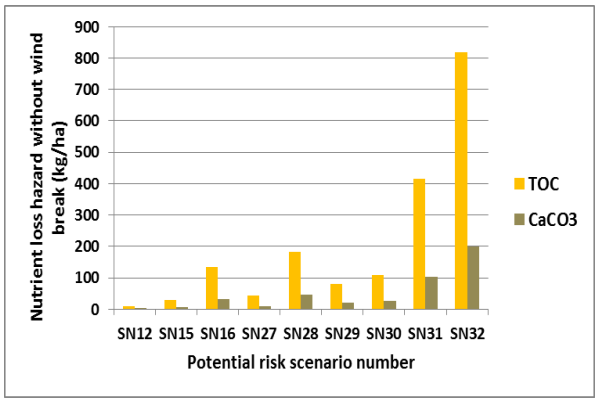

Loamy sand class 1 (field A)

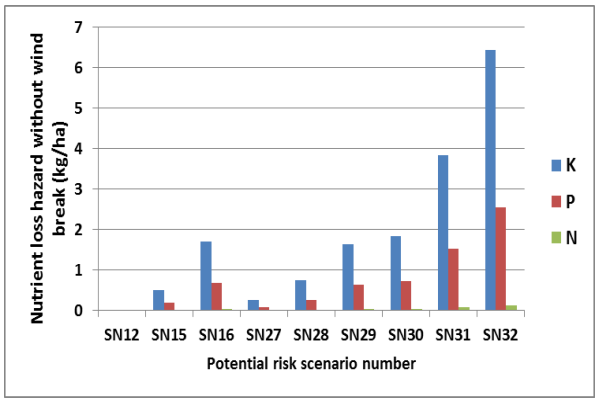

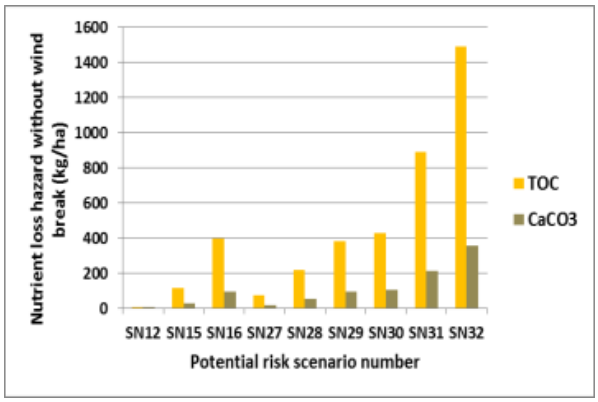

Loamy sand class 2 (field B)

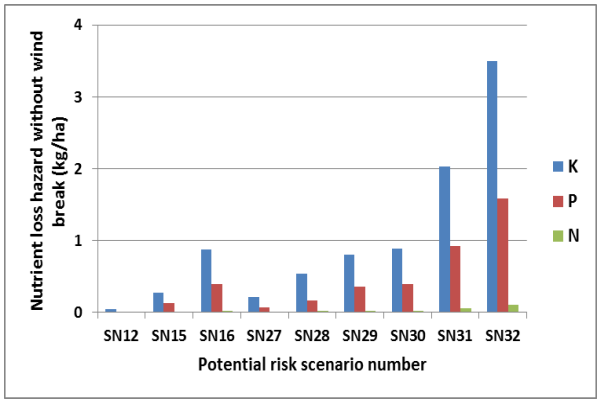

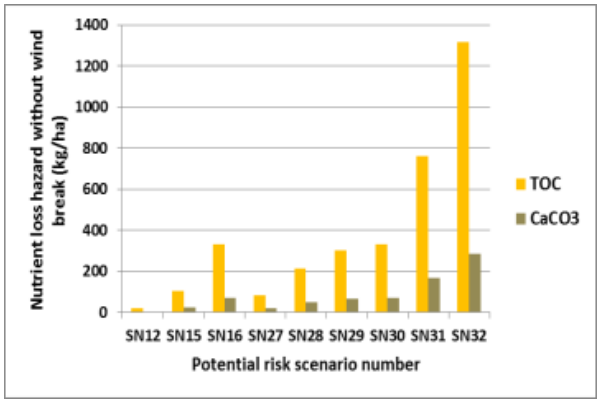

Loamy sand class 3 (field C)

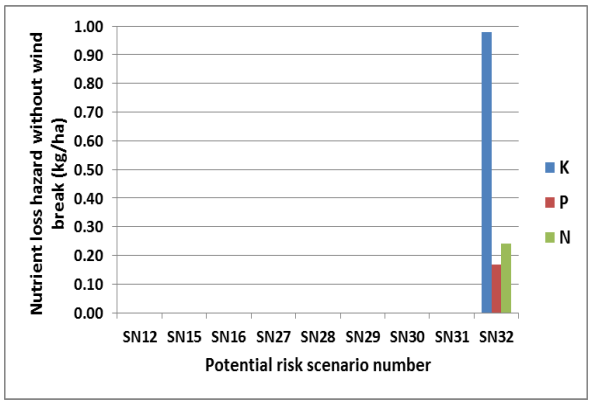

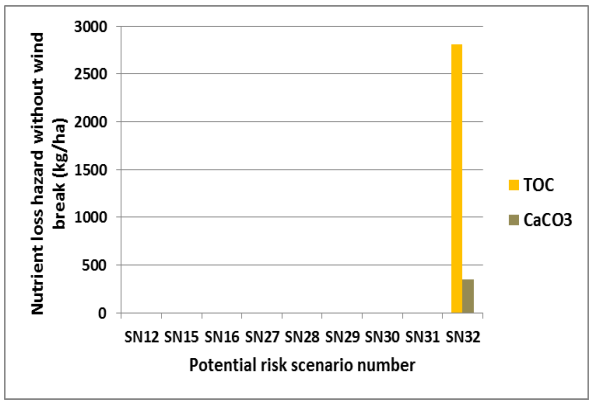

Organic soil (field D)

Figure 3.18. Nutrient loss hazard assessment in unsheltered fields

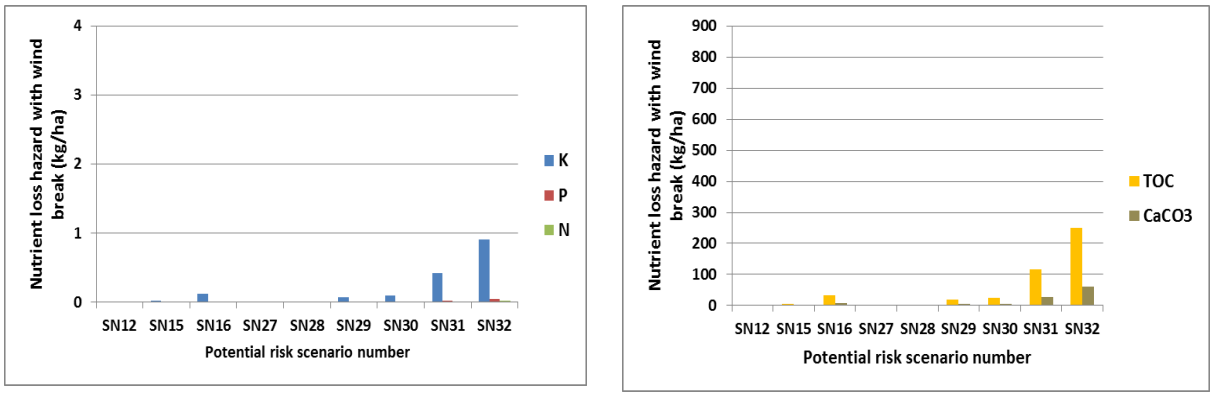

Loamy sand class 1 (field A)

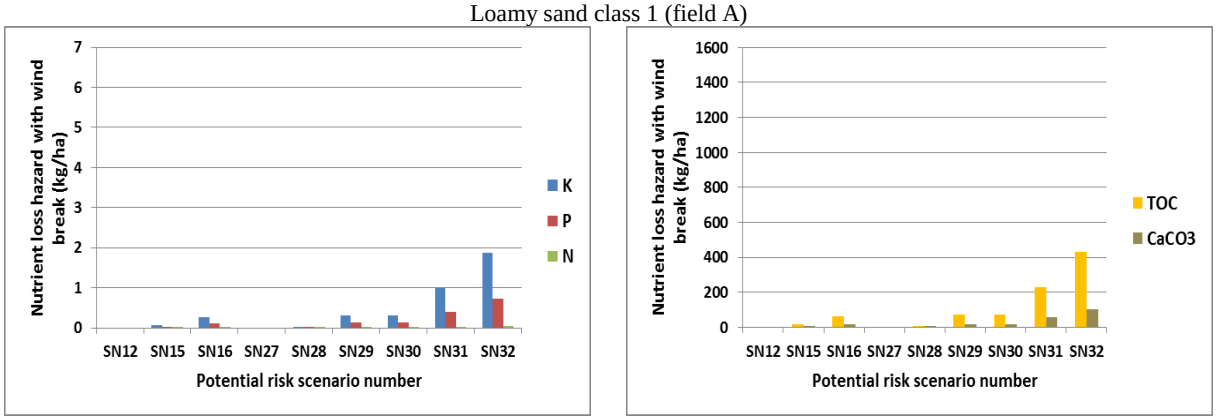

Loamy sand class 2 (field B)

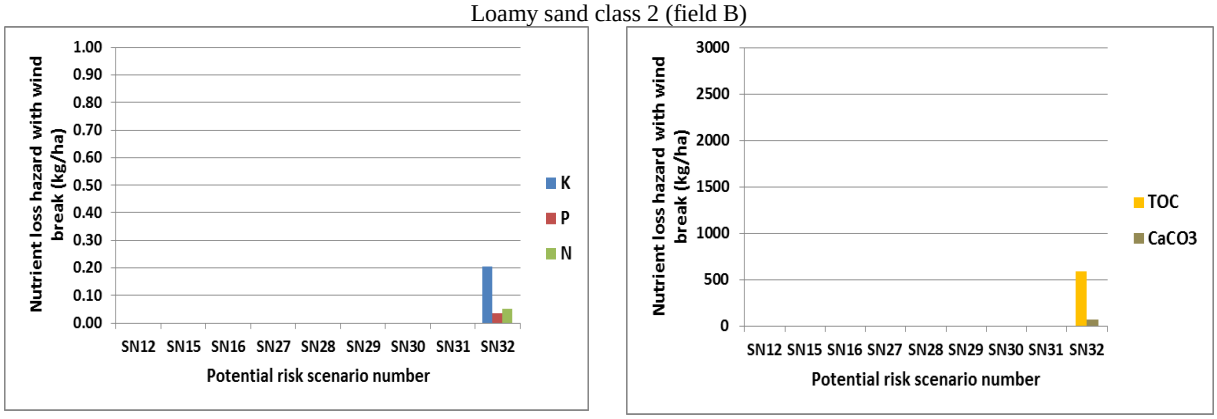

Loamy sand class 3 (field C)

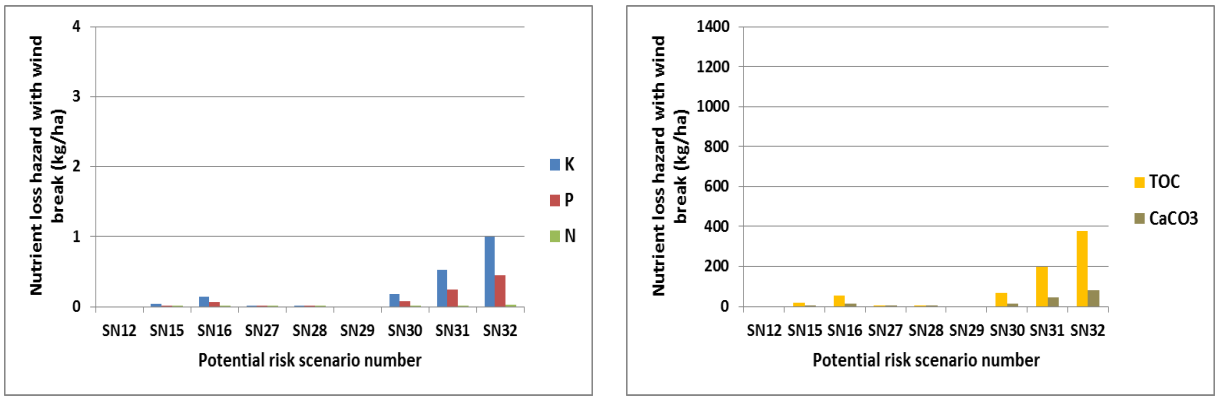

Organic soil (field D)

Figure 3.19. Nutrient loss hazard assessment in sheltered fields

3.6.4 Risk assessment of nutrients loss

The values of risk of nutrients loss are gained by multiplying the risk values of total soil loss in each scenario number by the representative amount of nutrient loss for each surface scenario. Hence, only scenarios with a hazard of nutrient loss also have an associated risk value.

As shown in Figure 3.20 and TOC and $CaCO_3$ represent the highest values of nutrient loss of 74.90 and 18.30 respectively, in unsheltered areas of field A. Since, loamy sand class 2 (field B) represented the highest amounts of total soil and nutrient loss hazard, accordingly the highest risk values for nutrient loss will be observed in this soil type. Compared to the field A, the risk value of TOC loss as the highest amount of nutrient risk in the worst case scenario (SN31) indicates more than a 50 % risk value in field B (74.90 versus 159.26).

As shown in Figure 3.20, like loamy sand class 2, the nutrient risk values follow a similar trend in field C with the exception that in loamy sand class 3, the average values of risk is 14 % less than loamy sand class 2 which is referred to more nutrient loss hazard in field B.

The potential risk scenarios of nutrient loss risk in Field C show that compared to the other soil types, although organic soil indicates the maximum potential of TOC loss hazard, but due to low occurrence probability of daily average wind speed which is responsible to create SN32, this soil presents the minimum values of nutrient loss risk among all soil types.

A wind break could significantly reduce the nutrient loss risk by more than 90% in field. As shown in Figure 3.21, the establishment of a wind break could decrease all of the nutrient loss risk in the worst case scenario by 74 % in field B and C. In most cases, except for scenarios which represent a parallel tillage with a 5 cm ridge height (SN29, SN30, SN31 and SN32), there is no considerable risk present anymore after the implementation of a wind break. In field D, there is a remarkable reduction (a 4 times decrease) in risk values for nutrient loss resulting from the establishment of a single row wind break which prevents the negative effect of soil and nutrient loss for only one possible risk scenario in organic soil.

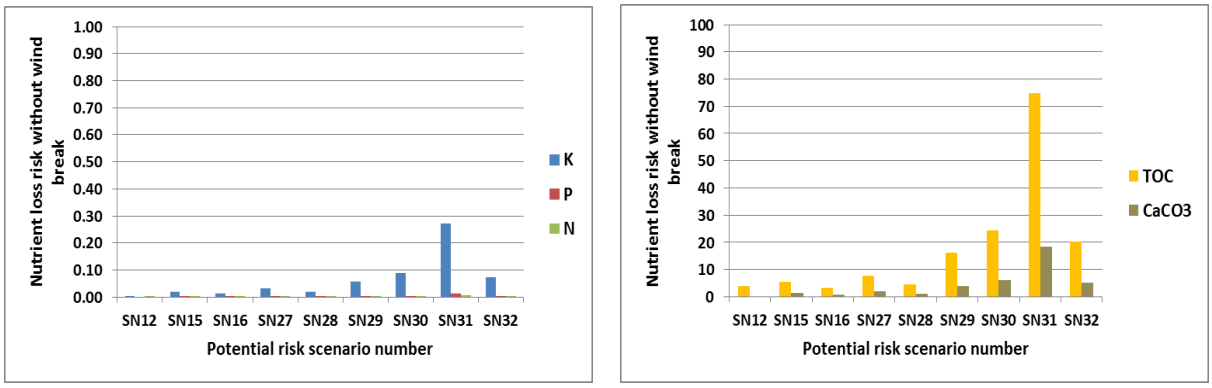

Loamy sand class 1 (field A)

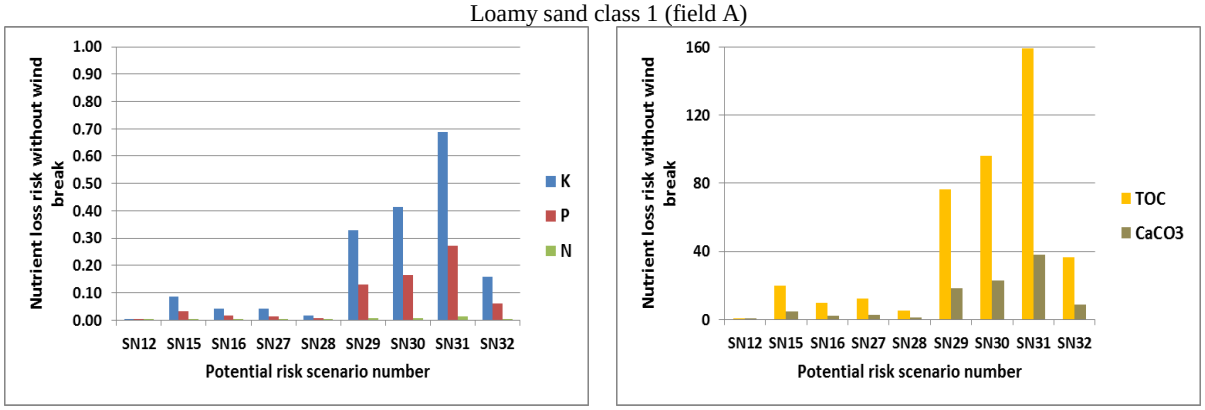

Loamy sand class 2 (field B)

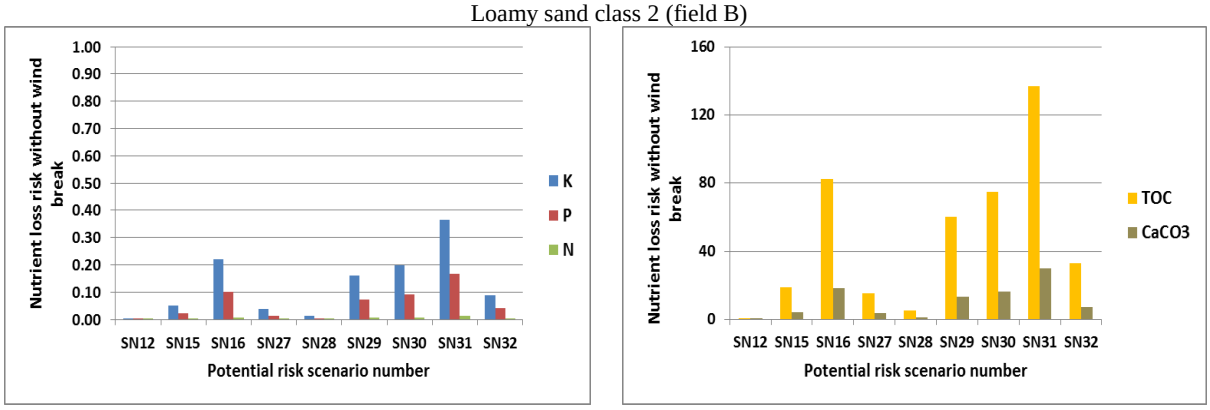

Loamy sand class 3 (field C)

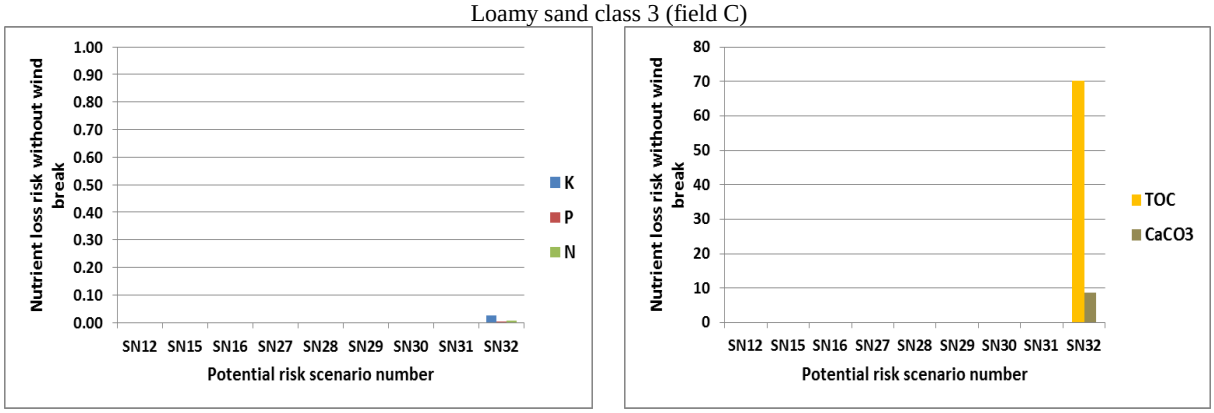

Organic soil (field D)

Figure 3.20. Nutrient loss risk assessment in unsheltered fields

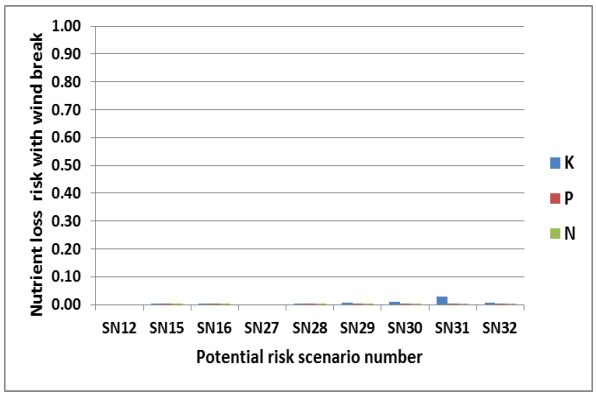

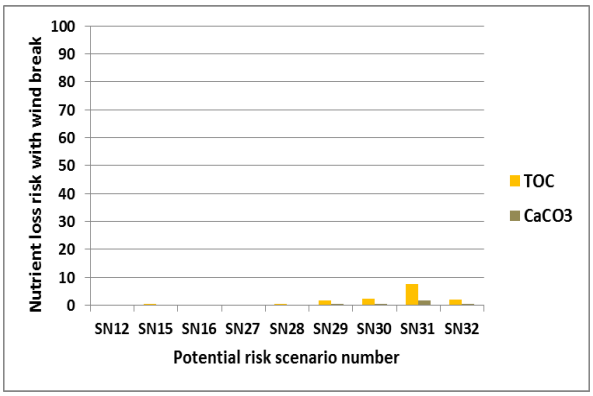

Loamy sand class 1 (field A)

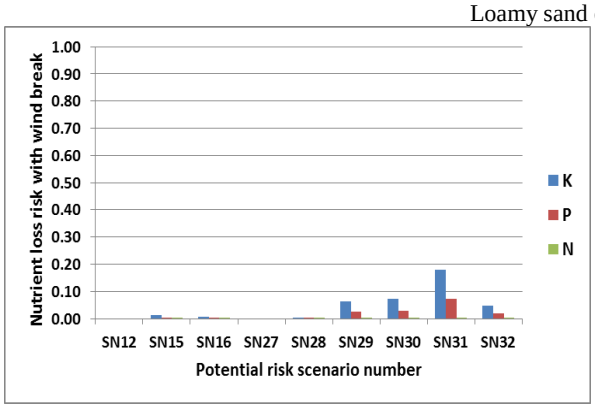

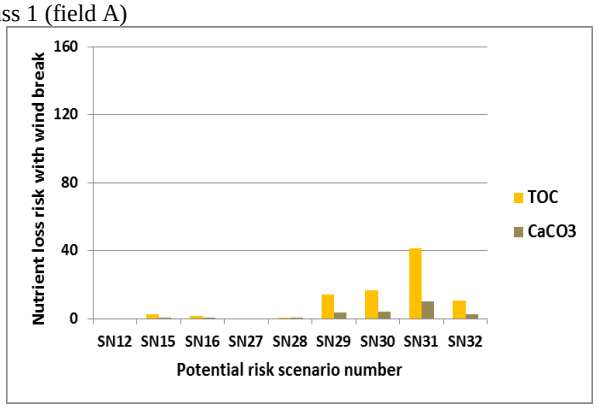

Loamy sand class 2 (field B)

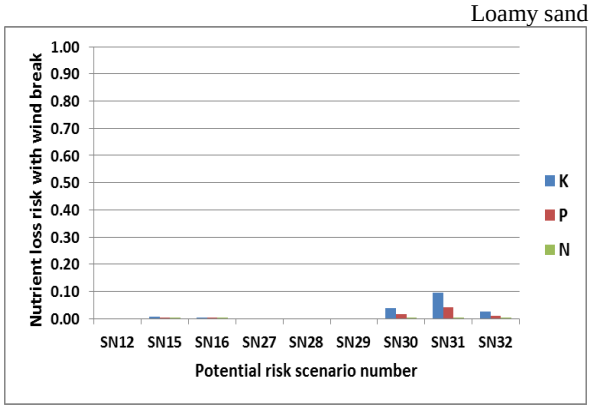

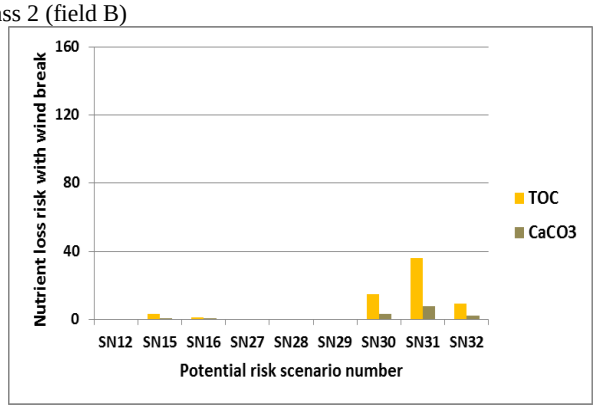

Loamy sand class 3 (field C)

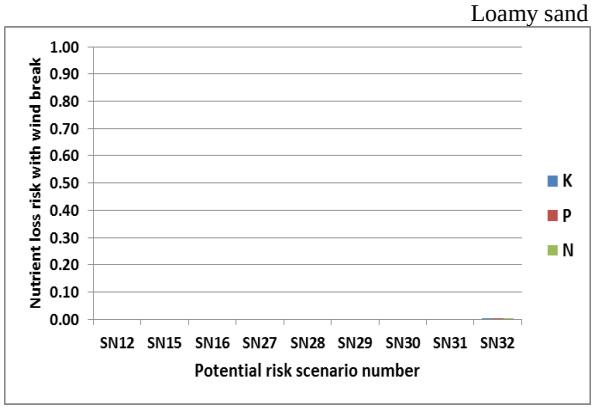

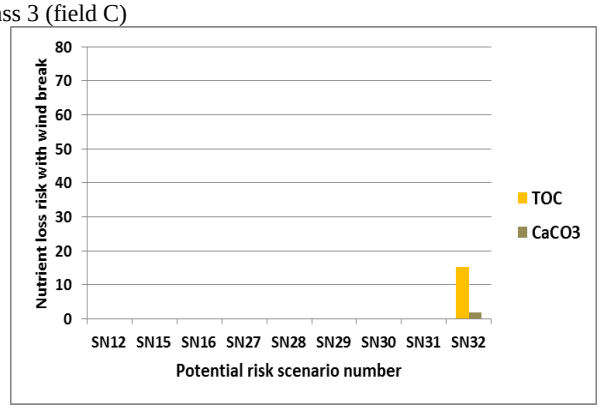

Organic soil (field D)

Figure 3.21. Nutrient loss risk assessment in sheltered fields

3.7 Hazard and risk assessment based on current condition of study sites

Fields C and D (loamy sand class 3 and organic soil) are currently ploughed in parallel direction to the erosive wind, and fields A and B (loamy sands class 1 and 2) are ploughed in perpendicular direction. Accordingly, the modelling of hazards and risks are done based on scenarios resembling these conditions.

3.7.1 Hazard and risk assessment of soil loss in current condition

As shown in Table 3.9 and 3.10, the highest hazards for total soil loss and PM_{10} loss occur in fields A and B and they are related to SN28. Lowest hazard can be observed for SN12 at both fields. Also under present field conditions it can be seen that a wind barrier reduces the actual soil, dust and PM_{10} loss very well to negligible amounts. The results illustrate that the hazard of SN28 in loamy sand class 2 is almost three times greater than SN27, if the land is unsheltered. In contrast, SN27 shows the greatest risk values for total soil and PM_{10} losses in reviewed potential scenarios (Table 3.10). The risk value for SN27 is about two times higher than SN28 (0.61 versus 0.37 in field A and 0.54 versus 0.22 in field B). In addition, SN12 with a 10 cm perpendicular ridge height displays negligible amounts of soil and PM_{10} loss hazard and risk values.

The results show that using a single row wind break around field A and B leads to considerable reduction of observed risk for total soil and PM_{10} losses in all of the possible scenarios. However, if the wind barrier is removed around the farm boundaries, the amounts of hazard and risk values could be increased by more than 90 %.

Comparisons between SN12 and SN28 which represent the perpendicular tillage with a 10 and 5 cm ridge height respectively under the same wind regime (daily average $\geq$ 10 m/s), demonstrate that a 5 cm increase of ridge height could reduce the hazard of all the parameters by more than 95 percent. In SN27 and SN28 (ploughed perpendicular; 5 cm ridge height) there is a significant difference between the results of hazard and risk values, because of different daily average wind speed regimes (9-10 versus $\geq$ 10 m/s respectively). Accordingly, SN28 shows the greatest hazard of all possible scenarios in this soil type. On the other hand, due to a high probability of occurrence in daily average of erosive wind speed in dry periods for SN27 (18 percent) compared to the SN28 (2.5 percent), results indicate that SN27 has the highest potential risk values in fields A and B. However, by implementing perpendicular ploughing to erosive wind direction and establishment of a wind break network, the potential hazards and risks could be reduced to almost zero.

In field C, as shown in Tables 3.9, the greater amounts of hazard occurred for SN32 (96.30 t/ha of total soil loss) where the soil surface is parallel Ploughed with a 5 cm ridge height and with daily average erosive wind greater than 10 m/s. Although, in all scenarios, a single row wind break could decrease various hazard values by at least 3.5 times in field C. However, in most cases under sheltered condition, there are still some amounts of total soil and PM_{10} losses except in SN29 due to lower daily average wind speed.

A comparison between SN15 and SN31, which represent the worst case scenarios with a10 cm and 5 cm ridge height respectively, demonstrates that a 5 cm increase of ridge height in unsheltered areas can lead to a 7 times reduction of soil loss hazard (55.80 versus 7.70 t/ha) and risk values (10.04 versus 1.39). In addition, the implementation of wind barriers also reduces the wind erosion threat significantly in field C, but it seems that, unlike the other loamy sands, this reduction does not completely succeed (no erosion anymore) because of the alignment of tillage rows with the erosive wind direction.

Like field C, the organic soil (field D) is currently ploughed (with 3 years rotations) parallel to the erosive wind direction. However, because of the inherent resistance to wind erosion as previously mentioned, only one scenario produces minimal values of hazard and risk (SN32). All other potential scenarios do not show any hazard and consequently risk values for total soil dust losses. In this field, the hazard and risk values could even further be reduced by about four times, if wind barriers would be implemented.

Table 3.9. Comparison of total soil loss hazard and risk for without and with wind break in current condition

Scenario number	**Total soil loss hazard (t/ha)**		**Total soil loss risk**	
	Without wind break	With wind break	Without wind break	With wind break
Loamy sand class 1 (field A)				
SN 12	0.80	0.00	0.02	0.00
SN 27	3.40	0.00	0.61	0.00
SN 28	14.70	0.10	0.37	0.00
Loamy sand class 2 (field B)				
SN 12	0.30	0.00	0.01	0.00
SN 27	3.00	0.00	0.54	0.00
SN 28	8.70	0.04	0.22	0.00
Loamy sand class 3 (field C)				
SN 15	7.70	1.20	1.39	0.22
SN 16	24.20	4.00	0.61	0.10
SN 29	22.10	0.00	4.42	0.00
SN 30	24.30	4.80	5.47	1.08
SN 31	55.80	14.60	10.04	2.63
SN 32	96.30	27.60	2.41	0.69
Organic soil (field D)				
SN 32	24.00	5.00	0.60	0.10

Table 3.10. Comparison of PM_{10} loss hazard and risk for without and with wind break in current conditions

Scenario number	**PM_{10} loss hazard (t/ha)**		**PM_{10} loss risk**	
	Without wind break	With wind break	Without wind break	With wind break
Loamy sand class 1 (field A)			Loamy sand class 1 (field A)	
SN 12	0.01	0.00	0.00	0.00
SN 27	0.05	0.00	0.01	0.00
SN 28	0.19	0.00	0.00	0.00
Loamy sand class 2 (field B)				
SN 12	0.00	0.00	0.00	0.00
SN 27	0.03	0.00	0.01	0.00
SN 28	0.10	0.00	0.00	0.00
Loamy sand class 3 (field C)				
SN 15	0.16	0.00	0.03	0.00
SN 16	0.48	0.10	0.01	0.00
SN 29	0.45	0.00	0.09	0.00
SN 30	0.50	0.10	0.11	0.02
SN 31	1.00	0.30	0.18	0.05
SN 32	1.70	0.70	0.04	0.02
Organic soil (field D)				
SN 32	0.85	0.20	0.02	0.01

3.7.2 Hazard and risk assessment of nutrient loss in current condition

As showed in the previous section, the results of the hazard and risk assessment for field C illustrate quite different than for fields A and B, because field C is currently ploughed parallel to the erosive wind direction with various potential scenarios in case of total soil, PM_{10} and nutrient losses including SN15, SN16, SN29, SN30, SN31 and SN32. Whilst, there are only three possible scenarios which is currently act in field A and B including SN12, SN27 and SN28. In addition, the comparison between sheltered and unsheltered fields regarding to nutrient hazard and risk values indicate that a single row barrier can reduces these values more than 70 percent (Table3.11 and Table 3.12).

The highest amount of nutrient loss hazard is related to the SN32 in field C with 1315 Kg/ha hazard. However in sheltered area this value could reduce up to 3.5 times in this field. In Fields A and B by establishing the wind break, the hazard values of different nutrient loss could be reduced to almost zero (Table3.11).

The highest hazard values of nutrient loss occurs in SN 32 in the field C for TOC and $CaCO_3$ by 1314.88 and 287.62 kg/ha respectively. These values are about five times greater than the worst case scenarios in fields A and B. However, like hazard assessment of soil and PM_{10} losses by implementing a single row wind break the amounts of hazard and be reduced by 3.5 times. Whilst, simultaneous application of perpendicular tillage and windbreaks around fields A and B lead to more than 99% reduction of nutrient loss hazard in these fields (Table3.11).

Table 3.12 shows that in SN31, the highest risk of nutrient loss is related to TOC and $CaCO_3$ with 137.09 and 29.99 values respectively in field C. The wind breaks reduce the risk values by approximately four times in comparison with field A and B.

The amounts of hazard and risk values in unsheltered and sheltered field indicate that the establishment of a single row wind break could decrease the hazard and risk potential of soil and nutrient losses by 4 times. However, the scenario number 32 has the lowest percentage of probability of occurrence by 2.5% among all potential scenarios and consequently less risk values.

Table 3.11. Comparison of nutrient loss hazard assessment without and with wind break in current condition

Loamy sand class 1	Nutrient loss hazard without wind break (kg/ha)					Nutrient loss hazard with wind break (kg/ha)				
	K	P	N	TOC	$CaCO_3$	K	P	N	TOC	$CaCO_3$
Loamy sand class 1 (field A)										
SN 12	0.04	0.00	0.00	9.92	2.49	0.00	0.00	0.00	0.00	0.00
SN 27	0.18	0.01	0.00	42.14	10.56	0.00	0.00	0.00	0.00	0.00
SN 28	0.78	0.04	0.02	182.19	45.67	0.01	0.00	0.00	1.24	0.31
Loamy sand class 2 (field B)										
SN 12	0.03	0.01	0.00	7.44	1.71	0.00	0.00	0.00	0.00	0.00
SN 27	0.26	0.09	0.01	74.38	17.14	0.00	0.00	0.00	0.00	0.00
SN 28	0.74	0.26	0.02	215.71	49.69	0.00	0.00	0.00	0.99	0.23
Loamy sand class 3 (field C)										
SN 15	0.28	0.13	0.01	105.14	23.00	0.04	0.02	0.00	16.38	3.58
SN 16	0.88	0.40	0.03	330.43	72.28	0.15	0.07	0.00	54.62	11.95
SN 29	0.80	0.36	0.03	301.75	66.01	0.00	0.00	0.00	0.00	0.00
SN 30	0.88	0.40	0.03	331.79	72.58	0.17	0.08	0.01	65.54	14.34
SN 31	2.03	0.92	0.06	761.89	166.66	0.53	0.24	0.02	199.35	43.61
SN 32	3.50	1.59	0.11	1314.88	287.62	1.00	0.45	0.03	376.85	82.43
Organic soil (field D)										
SN 32	0.98	0.17	0.24	2809.80	344.00	0.20	0.03	0.05	585.38	71.67

Table 3.12. Comparison of nutrients loss risk assessment without and with wind break in current condition

Loamy sand class 1	Nutrient loss risk without wind break					Nutrient loss risk with wind break				
	K	P	N	TOC	$CaCO_3$	K	P	N	TOC	$CaCO_3$
Loamy sand class 1 (field A)										
SN 12	0.00	0.00	0.00	3.81	0.00	0.00	0.00	0.00	0.00	0.00
SN 27	0.03	0.00	0.00	7.59	1.90	0.00	0.00	0.00	0.00	0.00
SN 28	0.02	0.00	0.00	4.55	1.14	0.00	0.00	0.00	0.50	0.12
Loamy sand class 2 (field B)										
SN 12	0.00	0.00	0.00	0.19	0.04	0.00	0.00	0.00	0.00	0.00
SN 27	0.04	0.01	0.00	12.40	2.86	0.00	0.00	0.00	0.00	0.00
SN 28	0.02	0.01	0.00	4.96	1.14	0.00	0.00	0.00	0.02	0.01
Loamy sand class 3 (field C)										
SN 15	0.05	0.02	0.00	18.92	4.14	0.01	0.00	0.00	2.95	0.65
SN 16	0.22	0.10	0.01	82.61	18.07	0.00	0.00	0.00	1.37	0.30
SN 29	0.16	0.07	0.01	60.35	13.20	0.00	0.00	0.00	0.00	0.00
SN 30	0.20	0.09	0.01	74.69	16.34	0.04	0.02	0.00	14.75	3.23
SN 31	0.36	0.17	0.01	137.09	29.99	0.10	0.04	0.00	35.91	7.85
SN 32	0.09	0.04	0.00	32.91	7.20	0.03	0.01	0.00	9.42	2.06
Organic soil (field D)										
SN 32	0.02	0.00	0.01	70.25	8.60	0.01	0.00	0.00	15.22	1.86

University of Basel

Hazard and Risk Assessment of Wind Erosion and Dust Emissions in Denmark - A Simulation and Modelling Approach

Discussion

"Never memorize something that you can look up"

Albert Einstein (1879-1955)

CHAPTER 4

4. Discussion

The results of this study have been discussed based on the research questions as follows:

1) What are the soil loss potentials under different tillage directions in comparison to flat surfaces (seedbed) in different soil types?

The use of conservation tillage is often recommended to control wind erosion in sensitive areas. This method is supposed to increase surface roughness of soils with the effect that the wind erosion susceptibility of the soil decreases. However, based on results obtained in this study for poorly aggregated soils in Denmark, this simplified picture is not universally applicable. The results from the wind tunnel experiments clearly show that tilled surfaces, if done parallel to the prevailing wind direction, tillage was performed, increasing soil surface roughness can, instead, lead to an increase of soil loss in comparison to flat surfaces. This observation could be made especially for the loamy sands class 2 and 3, which experienced more than twice the amount of soil loss from parallel tilled surfaces than from flat ones. Zobeck and Van Pelt (2011) observed in their investigation that oriented roughness has only limited effects on soil loss, if the wind blows in the direction parallel to the tillage ridges. A comparison of the effect of height differences of the ridges from parallel tilled surfaces in the SWEEP model showed, that an increase in ridge height of 5cm already decreases the soil loss by 14 times for loamy sand class 3, despite the fact that the ridges are parallel to the dominant wind direction(see section 3.7.1). This reduction of soil loss by increasing the ridge height were in agreement with Armbrust et al., (1964) and Kardous et al., (2005) wind tunnel simulations which showed that increasing of ridge height could reduce the horizontal fluxes exceeding 3.5 times. However, Armbrust et al., (1964) proved that the optimum ridge height to control the soil flux are between 5 and 10 cm, and higher tillage due to effect of drag velocity on particle transport process are not able to control soil flow rates.

As previous studies have examined, if the ridge tillage has an appropriate height and is perpendicularly orientated to the dominant wind direction, it can considerably decrease wind erosion rates (Armbrust et al., 1964; Lopez et al., 2000; Gomes et al., 2003; Liu et al., 2006). The results from both, the wind tunnel experiments and the SWEEP modeling are in accordance with these observations. The perpendicular ridge orientation has by far the lowest

soil loss in the experiments with on average 10 times lower rates than the two other treatments over all soils. The SWEEP modeling even suggests that perpendicular ridges would be able to reduce the soil loss in almost all tested scenarios and on all soils to zero or at least negligible amounts. The creation of a micro-relief that protects the surface by trapping sediment particles is the assumed actual process that causes this significant effect of soil loss reduction (Zobeck, 1991; Zobeck and Van Pelt, 2014). This issue was highlighted by Kardous et al., (2005) who suggested that ridged surfaces lead to an important relative reduction in horizontal sand fluxes (exceeding 60%) by trapping saltating particles.

The results proved that the average soil loss was typically lower for flat surfaces than for parallel tillage. This indicates that not only performing a parallel tillage in poorly-aggregated soil does not control the wind erosion, but it can also accelerate the soil loss hazard. It seems that the tillage direction can be considered as the most important agricultural management practice to avoid wind erosion in sandy soils.

2) What are the nutrients and dust enrichment ratios under different tillage directions and soil types?

The perpendicular orientation of the ridges had an important influence on the dust production in the wind tunnel simulations. For the slightly coarser loamy sands 2 and 3 (fields B and C) it could be seen that the perpendicular tillage led to an enrichment of the fine dust particles (PM_{10}, $PM_{2.5}$) in the eroded sediment by a factor of 1.6 and 1.3 for loamy sand class 2 and 3, respectively (see section 3.3.2). A likely reason why this dust enrichment occurred could be that, the larger particles, which were positioned on top of the tillage rows, roll down into the furrows and stay trapped there. The ridge tops are being ‘refreshed’, because the subsurface layer becomes exposed to the wind. Consequently, this would lead to an increase in sediment flux of fines, causing enrichment in the eroded sediment (Armbrust et al., 1964; Hagen and Armbrust, 1992).

Comparing particle and nutrient enrichment ratios between parent soil and eroded sediment proved that there is a strong correlation (> 80%) between N, TOC and $CaCo_3$ enrichment ratio with enrichment of composed dust particles ($PM_{2.5}$, PM_{10}, Clay, Silt, Very fine sand). From perpendicular to parallel tilled and flat surfaces, reduced nutrient enrichment ratios and dust enrichment ratios could be observed. This relation could be obtained with more clarity for loamy sands class 2 and 3. The results generally confirmed that finer particles tend to be more enriched by nutrients in comparison to coarser particles. This is in agreement with Sankey et al., (2012) and Webb et al., (2013), later one showing soil organic carbon enrichment of dust

emissions in Australia. Aimar et al., (2012) also found the relation of silt content with potential particulate matter (PM) emissions in Argentina.

The described selectivity of the wind erosion process in terms of its preferential deflation of fine particles and nutrients on the surface in combination with the rapid decline of nitrogen and organic carbon contents with soil depth (Larney et al., 1998), could affect not only the fertility of soil as suggested by Visser et al., (2005), but also decrease the aggregate stability (Fryrear et al., 1994; Colazo and Buschiazzo, 2010), change the water holding capacity (Weinan et al., 1996) and consequently, lead to an increase of soil erodibility to wind erosion and dust emission.

In contrast to this observation, a poor correlation was found between dust particles and the nutrients P and K. This observation could be related to lesser amounts of these nutrients in the parent soils (Buschiazzo et al., 2007; Buschiazzo and Funk, 2015) but it could also be attributed to greater concentrations of these nutrients in coarser and more stable particles, as reported by Sankey et al., (2012) for aeolian sediment in southeastern Idaho.

With regards to the initial research question, it can be concluded that the highest rate of soil protection does not necessarily coincide with lowest soil nutrient and dust enrichment ratios. For example, perpendicular tillage ridges very well protect the soil from erosion, but they promote dust and nutrient deflation from the soil. These contradicting results should, therefore, be taken into account for the evaluation of protection measures on different soil types in the study sites. It is important to differentiate and balance between their effectivity to reduce total soil erosion or dust emission and nutrient loss.

3) What is the reliability of wind erosion model results in comparison to results of wind tunnel simulations?

In this study, the performance of the SWEEP model was tested based upon three model evaluation statistics: Coefficient of Determination (R^2), Root Mean Square Error (RMSE), and index of agreement (d). These statistical indices were derived by comparing the predicted values from the SWEEP model and the observed values from the wind tunnel simulations. Although each of the comparison statistics has specific advantages and disadvantages, which have to be taken into account during model calibration, the overall agreement was satisfactory, especially for loamy sands class 2 and 3 and organic soil.

The loamy sand class 3 and the organic soil showed a very good correlation between predicted and observed values (loamy sand class 3 by 0.96, organic soil by 0.82). The high sensitivity of R^2 to outliers could be a reason, why the loamy sands classes 1 and 2 have

relatively poor R^2 values of 0.46 and 0.44, respectively (see table 3.7). The other reason given by Hagen (2001) it related to the uncertainties in soil surface conditions that affect the model validation and reduce correlation coefficients, he found an agreement of R^2 equal to 0.65 between measured and predicted soil loss using the WEPS model.

The index of agreement (d) indicated a good correlation between observed and simulated values for loamy sands class 2 and 3 with values of 0.61 and 0.75, respectively. Feng and Sharratt, (2007) have suggested that a value of $d > 0.5$ represents a satisfactory model performance. Loamy sand class 1 has the worst agreement between observed and predicted data from all soils. The RMSE was very high with a value of 44.21, whereas the other soils showed a relatively good agreement in RMSE.

Since the comparison by use of the above described statistical methods only returns an index without information on over- or underestimation of the actual erosion values, figures were plotted with the datasets for visual comparison (table 3.7). The only curves that differed very much from each other were the ones for loamy sand class 1. The clear underestimation of the predicted soil loss by the model with a factor of almost three times, can partly be attributed to the inherent susceptibility of this fine soil. It was discussed in literature that the parameter specification of the critical threshold wind velocity for finer and more susceptible soils in the SWEEP model, especially for velocities lower than 15 m/s, that could be the reason for the observed underestimation of erosion values (Van Donk and Skidmore, 2003; Hagen, 2004; Feng and Sharratt, 2007). Visser et al., (2005) and Feng and Sharratt, (2009) were in agreement to this and also argue that this underestimation of erosion values by the model could be due to an overestimation of the threshold friction velocity by SWEEP. This underestimation for loamy soil class 1 (finest sandy soil) is in agreement with presented model outputs for very erodible soils in China described by Liu et al., (2014).

The critical threshold wind velocity for the model simulations in this study was calculated by the model with 11 m/s. Hassenpflug et al., (1998) gave a threshold wind velocity of 7 m/s for sandy soils in northern Germany, which are very similar to the soils in Denmark. It seems to be obvious that the model would predict much higher erosion values, if the critical wind velocity threshold in the model would be lower. Skidmore (1986) suggested a 6 m/s as the threshold winds speed, although he mentioned that the threshold wind speed varies with the size and density of in the top soil layer.

The definite reason for this apparent difference between observed and predicted values in loamy sand class 1 is unclear but there are various possible causes that could influence the

model predictions and thus, be the reason for the underestimation of erosion values. Some of the possibilities are discussed below:

a) Soil bulk density

As shown in Figure 4.1, although there was a significant difference between average soil bulk densities in loamy sand class 1 compared to the other soils, where the higher value of bulk density in this soil, is related to greater density of mineral grains of sand particles as suggested by Zobeck et al., (2013). Therefore, results indicate that the greater soil bulk density in poorly aggregated sandy soils could be considered as one of the effective parameters for enhancing the transport capacity of particles and consequently, increase soil loss. Higher soil bulk density in fine sandy soils needs to be taken into account more accurately in the model structure to reduce likely underestimation of erosion values.

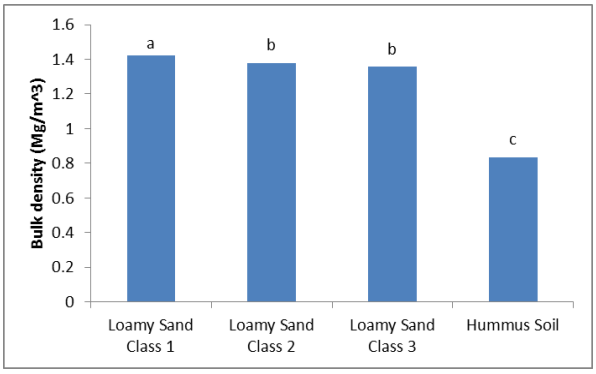

Figure 4.1. Mean comparison between soil bulk densities in different soil types (Different letters indicate statistically different values at $P < 0.05$ level, based on Duncan's multiple range test)

b) Soil size distributions

It seems that, the presence of 46 percent of fine sand and 4 percent of coarse sand content in loamy sand class 1 versus 27 and 29 percent fine sand and 9 and 10 percent coarse sand in loamy sands class 2 and 3 respectively, could be another main reason for underestimating results in the model. Liu et al., (2014) argued that the soil-estimating equations in SWEEP are not likely to be applicable to a pure sand surface. Therefore, in comparison to the bulk density, soil size distributions including fine sand, coarse sand and total sand fraction indicate more affective input parameters for the model which represent the higher intrinsic susceptibility of loamy sand class 1 (Figure 4.2).

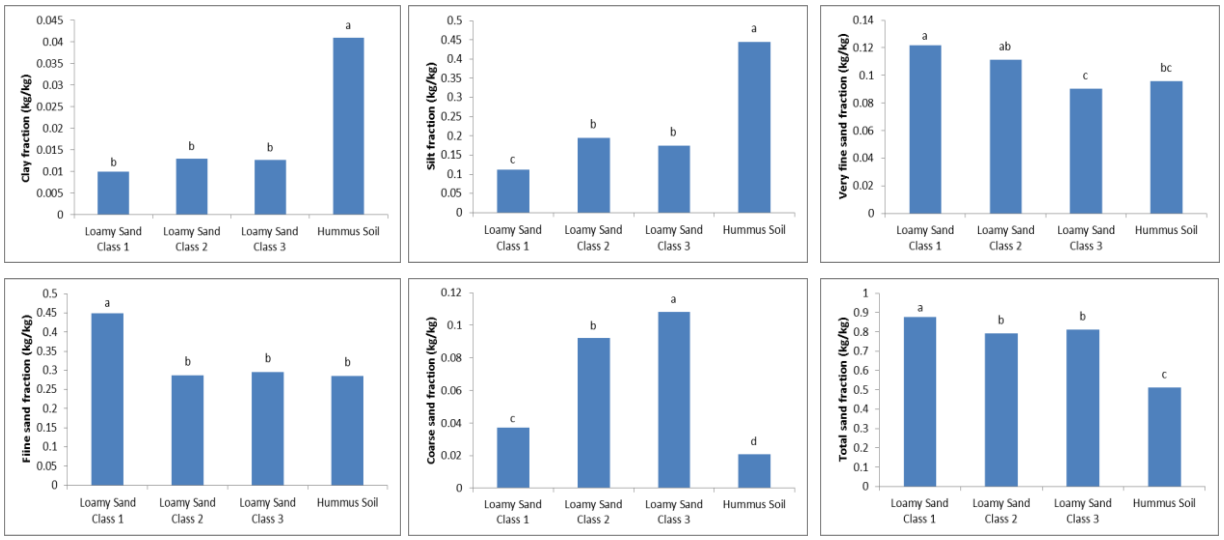

Figure 4.2. Mean comparison between soil fractions in different soil types

(Different letters indicate significant differences at P < 0.05 level)

c) Rock volume fractions

The presence of rock fractions on soil surfaces has a very important role in not only creating roughness and surface resistant to wind erosion, but also in causing the breakage of bombarding saltation/creep size aggregates (Feng and Sharratt, 2005). In this study, as shown in Figure 4.3 there is no significant difference between rock volume fractions in various soil types, because of a very low rock fraction in parent soils. Therefore, this factor cannot be the reason for the observed underestimation of erosion.

Figure 4.3. Mean comparison between rock volume fractions in different soil types

(Different letters indicate significant differences at P < 0.05 level)

d) Aggregate characteristics

The variables attributed to aggregate characteristics, such as average dry aggregate stability, geometric standard diameter (GSD) of aggregate size, and maximum aggregate size showed a

significant difference for loamy sand class 1 in comparison to loamy sands class 2 and 3 (Figure 4.4). The significant decrease of these soil aggregate indices in the finer sandy soil proved that this soil can be considered as the most susceptible soil with a lesser threshold wind velocity. However, since friction velocity is also affected by the aggregate characteristics, it seems that the model also needs to be re-validated against aggregate properties in poorly-aggregated soils, to reduce the underestimation of soil loss results. It seems that the decrease of aggregate characteristic values in comparison with grain size distribution accounted for more sensitivity of aggregate characteristics in agricultural land. This is in agreement with the spatial and temporal patterns of surface aggregates to control dust entrainment described by Zobeck et al., (2013) and Pi et al., (2014).

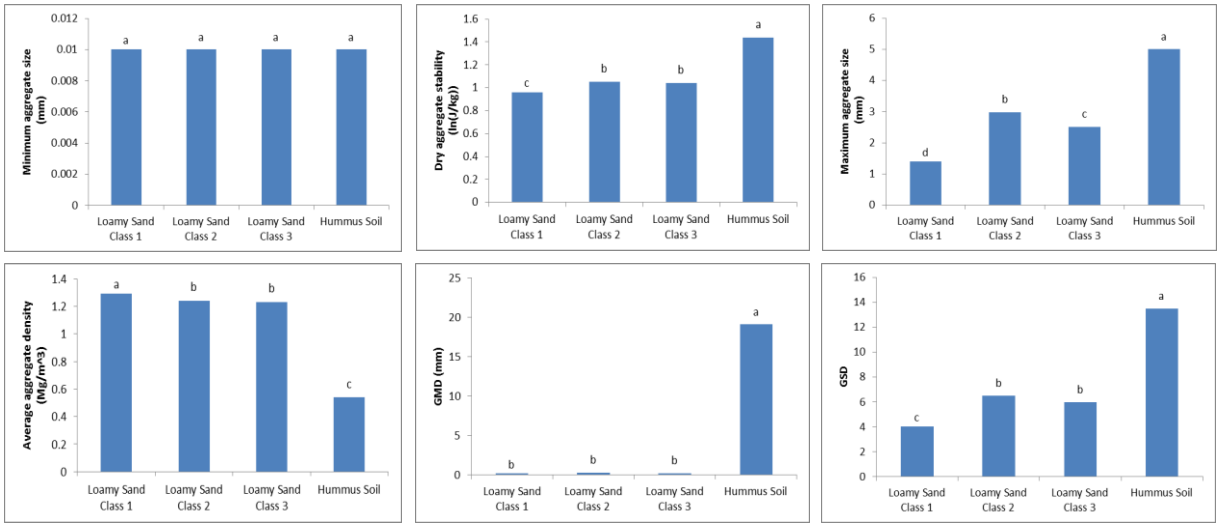

Figure 4.4. Mean comparison of the relation between various aggregate characteristics in different soils types

(Different letters indicate significant differences at $P < 0.05$ level)

e) Soil wilting point

As shown in Figure 4.5, there are significant differences in soil wilting point for loamy sand class 1 and the other soils. However a reduced soil wilting point water can sharply increase the threshold friction velocity, and consequently, decrease the rate of soil loss (Weinan et al., 1996). Hence, this parameter is not able to cause the underestimation of the model.

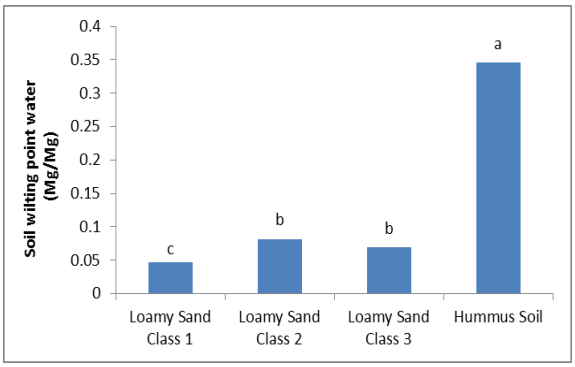

Figure 4.5. Mean comparison between soil wilting point in different soil types

(Different letters indicate significant differences at $P < 0.05$ level)

f) Impact of scale differences (plot dimension)

Regardless of errors related to data and parameter estimation, which exist in every model, it seems that the SWEEP model has a structural error to predict total soil loss in the finer sandy soil. Pi et al., 2014 highlighted the insensitivity of SWEEP for simulating wind erosion events because of overestimation of the threshold friction velocity. Therefore, as suggested by Feng and Sharratt (2007), the improvement of model results can be made by better specifying the static threshold friction velocity or coefficients that govern different soil loss equations.

Another likely cause for this difference can be associated with simulation components that control transport capacity and sediment transport modes (Saltation + Creep, and Suspension) in the model. Especially the difference between the dimensions of a wind tunnel plot in comparison to a field plot is important. Since downwind distance in a real field compared to a small scale wind tunnel is significantly longer, hence, most of the transported particles could be trapped by existing sink or obstacles created by aggregate and rock or other rough elements on the soil surface, whereas in a wind tunnel plot due to short downwind distance, the sediment particles could easily leave the plot or fall into the sediment trap. Of course, it should be mentioned that in reality, a larger part of the measured sediment transport originates from outside the plot and changes the transport coefficient (Visser et al., 2005). Therefore, considering wind tunnel scale and simulation processes, it would certainly help to improve the agreement between the observed and predicted values

As shown above, there are many different possibilities that could have been the reason for the underestimation of the observed erosion values, but much more research still is needed to actually be able to correctly weight the different parameters for the model. Further, as Feng and Sharratt, (2009) pointed out, the SWEEP model appears to be sensitive to various input parameters on the Columbian Plateau, consequently modifying this model is not straightforward and automatic calibration methods could be required to amend the internal

coefficients and empirical equations. However the intrinsic soil properties and soil surface characteristics have a separate impact upon the soil loss rates by wind erosion.

In conclusion to the actual research question of this section, it can be said that the testing of the model performance indicates that applied parametrization of the SWEEP model is able to provide satisfactory predictions of total soil loss. In comparison to results by Funk et al. (2002), who simulated wind erosion using the WEPS model during strong wind events on sandy soils near East Berlin, Germany, quite similar ranges of wind erosion were modeled. In this study erosion values between 2.18 -10.19 kg m^{-2} were predicted and Funk et al. (2002) reported a range between 0.11 - 10.46kg m^{-2}.

4) What are the main factors leading to an acceleration of wind erosion, based on a sensitivity analysis of the model?

Basically, sensitivities of different soil parameters are dynamic in both temporal and spatial dimensions, especially in agricultural lands due to changing weather conditions, strong impact of machinery on the soil surface, and the structure of aggregates. The linear sensitivity analysis showed that the most important parameter in the SWEEP model is the orientation of the tillage ridges in relations to the dominant wind direction, which confirms the results of simulations in wind tunnels by Hagen et al., 1999, and the results from field studies in cropland and fallow land in the Columbian Plateau by Feng and Sharratt, (2005). The actual ranking of the different parameters is given in table 3.8.

The second rank with frequency of 12% was related to random roughness. The random roughness affects the wind erosion rate by enhancing surface friction and consequently reducing the near surface wind velocity (Fryrear et al., 2000). However, oriented roughness can perform a more important role to control total soil loss (Hagen et al., 1999), which is described by the high sensitivity value of 25.5%.

The third rank was attributed to wind speed (10%). Wind erosion rate varies roughly with the cube of average wind velocity above the erosion threshold. As results demonstrated, an increase of 4 m/s in daily average wind speeds, for example from 7.5 to 11.5 m/s, would contribute about 10 % of the increased sensitivity of total soil loss.

5) What are the effects of erosive winds, soil moisture and tillage direction on the hazard and risk assessment of total soil, dust and nutrient losses?

A scenario analysis for different tillage orientations, soil moisture content, ridge height and daily average wind speed changes was accomplished to assess the hazard and risk of total soil,

PM_{10}, and nutrient losses, based on wind tunnel simulations and modelling using the SWEEP. Through the use of the SWEEP model it was also possible to evaluate the impact of wind breaks as a control mechanism around the four hypothesized fields with different soil types.

The number of 49 days with erosive wind events in dry periods was divided by the duration of the total time-series, which was used to calculate the wind velocity distribution (14 years). The resulting 3.5 days of erosive wind per year for the period from March to July correspond to the reported 0.03 up to 10 days per year for Denmark (EU report, 2010). The analysis of temporal variability for the 49 erosive winds indicated that they have a higher frequency during late winter and early spring. This result was in agreement with Funk et al., (2004) and Borrelli et al, (2014a) in Germany and European countries, respectively. Erosive wind data analysis showed that the critical hours for the occurrence of the highest wind speed fall between 12:00 p.m. and 15:00 p.m., similar to Hoffmann and Funk, 2015 results in NE-Germany which demonstrated that the maximum dust emissions happened between 10 a.m. and 15:00 p.m. under minimal moisture conditions of agricultural lands.

For all simulated scenarios with assumed average soil moisture content (> 0.15 Mg/Mg), no erosion was predicted for all test fields. The reason being, that the soil moisture increased the threshold wind velocity (u_t^*) consequently, the simulated u_t^* exceeded wind velocity (u*) for all erosive events as found by Van Donk and Skidmore, (2003) and Visser et al., (2005). Nickling, (1994) and Weinan et al., (1996) reported that, as soon as the moisture content is above 0.5% (gravimetric), the threshold wind velocity increases by a logarithmic function of soil moisture content. Therefore the SWEEP model is very sensitive to soil surface wetness (see also table 3.8). Ishizuka et al., (2005) observed that the wind velocity threshold is 1.27 times higher in wet (soil moisture content of 0.009 $m^3\ m^{-3}$) than in dry conditions. They therefore proposed that soil moisture content is one of the most sensitive parameters in erosion modelling.

The time period between late winter and early spring is the time with highest mechanical stress, because of tillage operations, and highest probability of erosive winds, as Hoffmann and Funk, 2015 suggested that the increase of wind erosion and dust emission risk in spring time is partly connected to times of agricultural operations by machinery which releases the dust particles into the atmosphere by tilling practices. Therefore, Warren, (2003) has recommended for European agricultural lands that farmers should keep fields as rough as possible during that period, by tilling the lands perpendicularly to the prevailing erosive wind direction. However, Hevia et al., 2007 have shown that with increased intensity of surface tillage operations, soil aggregate properties slightly decrease.

The comparison between different ridge orientations indicated that a perpendicular tillage to the erosive wind direction was able to reduce hazard and risk values of soil, dust and nutrient losses by 80% more than the parallel tillage. This reduction was in satisfying agreement with the wind tunnel simulation results obtained by Kardous et al., (2005) who mentioned that a ridged surface could reduce the risk values of wind erosion flux in a range between 65 to 85%. Fister and Ries, (2009) explained that increasing soil roughness led to a reduction of wind velocity near the surface and an increase of friction shear velocity, with the consequence, that the hazard of sediment transport rates in the central Ebro Basin decreased depending on the orientation and size of tillage ridges.

6) What is the effect of a wind break network on controlling hazard and risk of total soil, dust and nutrient losses?

The results of hazard and risk by wind erosion modelling were compared for sheltered and unsheltered fields. The wind barriers were assumed to be single row wind breaks with a 3.5 m height, 3m width and 35 percent porosity. The results revealed that establishing a wind break network in current conditions for field A and B, could decrease the hazard and risk values of soil, dust, and nutrient losses by more than 99 %. For field C, due to the field orientation and subsequent implementation of parallel tillage, 6 scenarios (two times more than for fields A and B) produced wind erosion. The reduction coefficient through the effect of the wind break varied between 70 to 100 percent. In total, results were in agreement with the wind tunnel simulations carried out by Zhang et al., (2010) who revealed that the sand transport rate in leeward side of shelterbelts have more than 80% reduction coefficient.

Also, it is generally accepted that the longest sheltering zone of a single row wind break with an optimum porosity is equal to the 10 H (height of trees) in the leeward side (Bilbro and Fryrear, 1997; Cornelis, and Gabriels, 2005; Bitog et al., 2011). Therefore if the (H) is considered 3.5 m, the length of sheltering zone in the leeward side is 350 m. Accordingly, the results for the study sites are applicable only for agricultural land with a fetch of 350 m length.

Shelterbelt porosity is the most important structural parameter of a wind break and effects the distribution and turbulence intensity of wind. Several simulation studies have shown that the optimal of wind break porosity to control wind erosion is between 20% and 40% (Cornelis and Gabriels 2005; Bitog et al. 2011). It seems that 35% porosity of hypothesized wind breaks in this study area combined with perpendicular ridge to the erosive wind direction in dry periods would be significantly sufficient to control the hazard and risk of wind erosion in the

study sites. In addition, results confirmed and illustrated that the sheltering effect of wind break networks in controlling the total soil loss, dust emission and consequently, different nutrients losses. Therefore, if a perpendicular tillage with a 10 cm ridge height in combination with shelterbelts can be performed there is no observed wind erosion when the daily average of wind speed is greater than 10 m/s.

University of Basel

Hazard and Risk Assessment of Wind Erosion and Dust Emissions in Denmark - A Simulation and Modelling Approach

Conclusions

"Science is organized knowledge. Wisdom is organized life. "

Immanuel Kant (1724-1804)

CHAPTER 5

5. Conclusions

Wind erosion and dust emission control are essential tasks in land management planning for susceptible areas. Lack of training in the local communities about effective mechanisms and key variables of the wind erosion and dust emission processes could increase the hazard and risk potential, especially when mixed soil types such as loamy sand are dominant in the study area. Understanding the present wind regimes in the study area is the first step for the assessment of wind erosion rates, hazards, and risk. Reducing soil erodibility by using preventive techniques and performing suitable farm management are two main drivers that should be considered as the most accessible measures in preventing and combating negative effects of wind erosion. However, farm lands are often covered with different kinds of crops, which require different management measures at different times of the year depending on their life cycle. The potential soil vulnerability to wind erosion is highest during the time between crop cultivation, seed germination and plant growth, until the soil surface is covered and protected again by the plants. The potential threat to the soil is particularly high, when erosive winds and low soil surface moisture contents coincide with cultivation of the fields.

The primary motivation for this study was the occurrence of wind erosion in one of the four study sites (field C) in central Jutland, North of Viborg in Denmark. While this field was managed in a similar way than the other farms, finding the main reason for this event propelled us to investigate the effect of tillage orientation on soil, dust, and nutrient losses by wind erosion. Since field C was oriented from North-West to South-East, unlike fields A and B, which were oriented from North to South, it was considered that the tillage ridge orientation was the most likely reason why the wind erosion event could have occurred on the study site. On poorly aggregated soils, tillage ridges are more or less the only roughness element that can be used to protect soils against wind erosion, until crop plants have grown enough and can provide enough protective cover.

The main aim of this study was to use the probability distribution of erosive wind velocities in dry periods for calculating hazard and risk assessment of soil, dust, and nutrient losses for single events of wind erosion, based on three soil surface scenarios (flat, parallel and perpendicular tillage). Because there are no quantitative data about wind erosion and dust

emission rates available for this region, the objectives of this investigation were to calculate the effect of ridge height and ridge orientation on wind erosion. Furthermore, the establishment of wind breaks around farm lands to control wind erosion intensity was another objective of the present study. Hence, this research was mainly conducted to:

1) Determine the temporal variations of erosive wind in dry periods between March to July, when the lands are ploughed and exposed to the erosive winds. The outputs of this section were used in order to get the probability distribution of erosive winds and risk assessment.

2) Determine the soil and nutrient losses based on the different surface scenarios using the wind tunnel simulation. The outputs of this section were used to investigate the enrichment ratios of different nutrients and dust particles under different tillage scenarios. Also the observed results gained from wind tunnel simulations utilized in the model calibration and hazard and risk assessment of nutrient loss under different scenario numbers resulted from modelling outputs.

3) Testing the feasibility of a single event wind erosion evaluation program (SWEEP) to determine the hazard and risk of soil, PM_{10}, and nutrient losses for sheltered and unsheltered fields by wind breaks, in combination with results of wind tunnel simulations.

This research is important for identifying and developing agricultural management practices that are less vulnerable to wind erosion and dust emission. Accordingly, the main findings of this thesis can be summarized below.

Based on the modelling results in different scenarios, the threshold wind velocity for loamy sand soils under tillage operation was calculated to be 11 m/s. Therefore, in this study, erosive winds were included if the hourly wind speeds were greater than 11 m/s.

Temporal analysis of erosive wind data in dry periods (March-July) reflected that more than 80 % of these winds occurred during March and April (61% in March and 20 % in April), when the crops were not high enough to protect the soil surface. The hourly erosive wind analysis suggested that the most likely time for the dust and wind erosion events fall between 12:00 p.m. and 15:00 p.m. In addition, results showed that there are on average 3.5 days of erosive winds in dry periods from March to July.

The dominant erosive wind direction during that period is North-West, whilst the prevailing wind direction for all-times is West. This result highlighted that the direction of prevailing winds not necessarily coincide with dominant direction of erosive winds. Therefore, the

fields, which are elongated and ploughed parallel to the erosive wind direction, can be classified into the high risk category.
Like other erosivity factors, the erosive winds with the highest speed did not indicate more probability of occurrence. Therefore, calculation of the probability distribution for each wind speed class leads to higher accuracy of hazard and risk estimations. This approach was considered as a stepping stone to more accurate estimation and calculation of the severity of wind erosion events.

The results of the wind tunnel simulations demonstrated that wind erosion could affect soil and nutrient properties significantly. In this research, results showed that changes in physical properties of soil, especially for finer particles had direct effects on the soil nutrient balance. Due to inherent susceptibility of fine sandy soils (loamy sand class 1) to wind erosion, there was no significant difference between flat surface (seedbed) and parallel tillage scenarios, whereas flat surface compared to parallel tillage in poorly aggregated soils shows less soil loss. The scenarios with parallel tillage operation experienced the highest erosion rates, due to the lack of obstacles. In contrast, the perpendicular tillage method leads to an enrichment of the eroded sediment and dust emissions, because the coarse particles were trapped between tillage rows. The dust ($PM_{2.5}$ and PM_{10}) enrichment ratio for perpendicular ridges was about 20%. Since finer particles tend to be more enriched by nutrients in comparison to coarser particles, the nutrient enrichment ratio was also higher. Most important nutrients included: TOC, $CaCO_3$ and N. In total, results confirmed that ridge tillages can decrease/increase the quantity and quality of soil and nutrient losses by wind erosion, depending on their orientation in relation to the dominant erosive wind direction.

Particle size distributions of sediments showed a bimodal grain-size distribution for parallel tillage. The main maximum was in the sand fraction and the secondary maximum was silt. The organic soil had the lowest soil bulk density and aggregate density in the tested soils. Nevertheless, it had the highest aggregate stability and soil moisture retention capacity, which control the threshold friction velocity. Accordingly, the organic soil proved to be less erodible than the sandy soils during the experiments.

For the evaluation of protection measures on these soil types in Denmark it is important to differentiate between their effectivity to reduce total soil erosion amount, dust emission, and nutrient loss. Finally, TOC and $CaCO_3$ as the most erodible nutrients in this study not only

can reduce physical protection to the soil, but are also important in wind erosion by diminishing soil and aggregate stability and soil fertility, if they operate for long time periods.

Overall, the performance testing of the model confirmed that SWEEP was capable to predict wind erosion on Danish agricultural soils. However, optimization of the SWEEP model for fine sandy soils under ploughing would be an important goal for future model development. Testing the model performance by three common criteria coefficients indicated that a similar relationship between observed and predicted outputs existed for loamy sands class 2, 3, and organic soil. However, results suggested that the SWEEP model tended to underestimate the observed wind erosion rates for loamy sand class1, due to an overestimation of the threshold friction velocity. This disparity between modelled and observed values for finer sandy soil was related to the differences in some input data and could be partly attributed to differences in transport capacity of between a wind tunnel simulation and a field scale model. It seems to be obvious that all of these factors contributed to the uncertainties in the model results for the fine sandy soil. Therefore, it would be required to amend the internal coefficients, which have an impact upon threshold friction velocity and to improve the empirical equations, which drive the transport capacity for the application of the SWEEP model in the sandy soils.

A sensitivity analysis can be used as an integral part of model development and it can represent the nature of interrelations between important variables for reliable models. A relative sensitivity index was used to identify the portions of the variance related to different input quantities, which are responsible for wind erosion rates in the study sites. The sensitivity analysis for ploughed fields indicated that the model results were most sensitive on the field and ridge orientation (50% of the total sensitivity values).

Wind barriers are an essential part of the agricultural systems in Denmark to reduce the hazard and risk of soil erosion, dust emission and nutrient loss. Results indicated that the performance of a single row wind break to control total soil, dust, and nutrient hazard and risk values was between 99 to 100 percent for perpendicular tilled fields, which means that the shelterbelts were able to fully protect the agricultural lands in currents conditions. However, in the study sites with parallel tillage operation, the wind break reduction coefficient was between 70 to 100 percent. Results also demonstrated that a 5 cm increase of ridge height under parallel tillage in unsheltered fields led to a minimal reduction of total soil loss hazard and risk values by 7 times.

Combining model predictions with additional information from wind tunnel simulations can provide a better understanding of wind erosion and nutrient loss, hazard, and risk. It can be further improved, if erosive wind velocities are selected for dry periods to differentiate between impacts of high and low wind speed probabilities in controlling wind erosion and dust emission risk values. If the average soil moisture content was used, there was no scenario in which wind erosion occurred. Thus, it can be suggested that a more precise knowledge about soil moisture thresholds could improve future wind erosion studies.

References

Aimar, S., Mendez, M., Funk R., Buschiazzo D.E., 2012. Soil properties related to potential particulate matter emissions (PM_{10}) of sandy soils. Aeolian Research 3, 437-443.

Armbrust, D. V., Chepil, W. S., Siddoway, F. H., 1964. Effects of ridges on erosion of soil by wind. Soil Science Society of America Journal 28, 557–560.

Bagnold, R. A., 1943. The physics of blown sand and desert dunes. London: Methue. 265 pp. ISBN: 978-94-009-5684-1.

Beinhauer, R., Kruse, B., 1994. Soil erosivity by wind in moderate climates. Ecological Modelling (75-76),279–287.

Bielders, Ch.L., Rajot, J.L., Amadou, M., 2002. Transport of soil and nutrients by wind in bush fallow land and traditionally managed cultivated fields in the Sahel. Geoderma 109, 19–39.

Bilbro, J.D., Fryrear, D.W., 1997. Comparative performance of forage sorghum, grain sorghum, kenaf, switchgrass, and slat fence windbarriers in reducing wind velocity. Journal of Soil and Water Conservation 52, 447–452.

Bitog, J. P., Lee, I. B., Hwang, H. S., Shin, M. H., Hong, S. W., Seo, I. H., Mostafa, E., Pang, Z., 2011. A wind tunnel study on aerodynamic porosity and windbreak drag. Forest Science and Technology 7(1), 8-16.

Böhner, J., Schäfer, W., Conrad, O., Gross, J., Ringeler, A., 2003. The WEELS model: methods, results and limitations. Catena 52, 289–308.

Borrelli, P., Ballabio, C., Panagos, P., Montanarella L., 2014a. Wind erosion susceptibility of European soils. Geoderma 232, 471-478.

Borrelli, P., Panagos, P., Ballabio, C., Lugato, E., Weynants, M., Montanarella, L., 2014b. Towards a pan-European assessment of land susceptibility to wind erosion. Land Degradation & Development. DOI:10.1002/ldr.2318.

Buschiazzo, D. E., Zobeck, T. M., 2008. Validation of WEQ, RWEQ and WEPS wind erosion for different arable land management systems in the Argentinean Pampas. Earth Surface Processes and Landforms 33, 1839–1850.

Buschiazzo, D.E., Funk, R., 2015. Wind erosion of agricultural soils and the carbon cycle; Soil Carbon: Science, Management and Policy for Multiple Benefits (eds S.A. Banwart, E. Noellemeyer and E. Milne).

Buschiazzo, D.E., Zobeck, T.M., Abascal, S.A., 2007. Wind erosion quantity and quality of an Entic Haplustoll of the semi-arid pampas of Argentina. Journal of Arid Environments 69, 29–39.

Callot, Y., Marticorena, B., Bergametti, G., 2000. Geomorphologic approach for modelling the surface features of arid environments in a model of dust emissions: application to the Sahara desert. Geodinamica Acta 13 (5), 245–270.

Chappell, A., Thomas, A.D., 2002. Modelling to reconstruct recent wind erosion history of fields in eastern England. In: Proceedings of ICAR5/GCTE-SEN Joint Conference, Lee, J.A. and Zobeck, T.M. (Eds),

International Center for Arid and Semiarid Lands Studies, Texas Tech University, Lubbock, Texas, USA Publication 02-2 p. 309.

Chepil, W. S., 1950. Properties of soil which influence wind erosion: I. The governing principle of surface roughness. Soil science 69(2), 149-162.

Cihacek, L. J, Sweeney, M. D., Deibert, E. J., 1992. Distribution of nitrate-N and soluble phosphorus in displaced wind erosion sediments in the Red River valley. Farm Research 49, 36–39.

Clemmensen, L. B., Andreasen, F., Nielsen, S.T., Sten, E., 1996. The late Holocene coastal dune field at Vejers, Denmark: characteristics, sand budget and depositional dynamics. Geomorphology 17, 79-98.

Coen, G. M., Tatarko, J., Martin, T. C., Cannon, K. R., Goddard, T.W., Sweetland. N.J., 2004. A method for using WEPS to map wind erosion risk of Alberta soils. Environmental Modelling and Software 19(2), 185-189.

Colazo, J.C., Buschiazzo, D.E., 2010. Soil dry aggregate stability and wind erodible fraction in a semiarid environment of Argentina. Geoderma 159, 228–236.

Conrad, O., Krüger, J.P., Bock, M., Gerold, G., 2006. Soil degradation risk assessment integrating terrain analysis and soil spatial prediction methods. In: Proceedings of the International Conference Soil and Desertification – Integrated Research for the Sustainable Management of Soils in Drylands 5-6 May 2006, Hamburg, Germany, pp. 1-9.

CORINE, 1992. CORINE: soil erosion risk and important land resources in the Southeastern regions of the European community. Publication EUR 13233, European Commission Luxembourg, Belgium, 32-48.

Cornelis, W.M., Gabriels, D,. 2005. Optimal windbreak design for winderosion control. Journal of Arid Environments 61, 315 -332.

Deumlich, D., Funk, R., Frielinghaus, M., Schmidt, W. A., Nitzsche, O., 2006. Basics of effective erosion control in German agriculture. Journal of Plant Nutrition and Soil Science 169, 370-381.

Deumlich, D., Thiere, J., Reuter, H. I., Völker, L., Funk, R., Kiesel , J., 2004. Site comparison method (SICOM) - a tool to generate maps and tables with administrative use as a basis for the evaluation of spatial equivalence of agri-environmental measures (AEM). 87th EAAE-Seminar of assessing rural development of the CAP. 21-23 April, 2004. Vienna (Austria).

Dodge, Y., 2008. The concise encyclopedia of statistics. Springer. 626 p.

EEA, 2003. Assessment and reporting on soil erosion. European Environment Agency, Technical Report 94, p. 103.

European Commission, 2006. Thematic strategy for soil protection. COM 2006, 231 pp.

European Union, 2010. EUReport on the project 'Sustainable Agriculture and Soil Conservation (SoCo)' Chapter 2: Soil degradation processes across Europe, Pages 29-66.

FAO, 1980. A provisional methodology for soil degradation assessment. Food and Agriculture Organization of the United Nations, Rome, Italy, 86 pp.

Feng, G. and Sharratt, B.S., 2009. Evaluation of the SWEEP model during high winds on the Columbia Plateau. Earth Surface Processes and Landforms 34, 1461-1468.

Feng, G., and Sharratt, B.S., 2005. Sensitivity analysis of soil and PM_{10} loss in WEPS using the LHS-OAT method. Transactions of the American Society of Agricultural Engineers 48(4), 1409–1420.

Feng, G., and Sharratt, B.S., 2007. Validation of WEPS for soil and PM_{10} loss from agricultural fields on the Columbia Plateau of the United States. Earth Surface Processes and Landforms 32, 743-753.

Fister, W., Iserloh, T., Ries, J.B., Schmidt, R. -G., 2012. A portable combined wind and rainfall simulator for in situ soil erosion measurements. Catena 91, 72–84.

Fister, W., Ries, J. B., 2009. Wind erosion in the central Ebro Basin under changing land use management: Field experiments with a portable wind tunnel. Arid Environments 73(11), 996-1004.

Fister, W., Schmidt, R. -G., 2008. Concept of a single device for simultaneous simulation of wind and water erosion in the field. In: Gabriels, D., Cornelis, W.M., Eyletters, M. & Hollenbosch, P. [Hrsg.]: Combating desertification. Assessment, adaptation and mitigation strategies. Proceedings of the Conference on Desertification, 23.01.2008, UNESCO Chair of Eremology, and Belgian Development Cooperation, Gent, Belgien, p. 106-113.

Fryrear, D. W., Bilbro, J. D., Saleh, A., Schomberg, H., Stout, J. E., Zobeck, T. M., 2000. RWEQ: Improved wind erosion technology. Soil and Water Conservation 55, 183–189.

Fryrear, D. W., 1984. Soil ridges-clods and wind erosion. Transactions of the ASAE 27(2), 445-448.

Fryrear, D. W., Krammes, C. A., Williamson, D. L. and Zobeck, T. M., 1994. Computing the wind erodible fraction of soils. Soil Water Conservation 49, 183-188.

Funk, R., Reuter, H. I., 2006. Wind erosion in Europe. Soil erosion in Europe. Boardman, J., Poesen, J., (eds). Wiley: Chichester; 563-582.

Funk, R., Skidmore, E. L., Hagen, L. J., 2004. Comparison of wind erosion measurements in Germany with simulated soil loss by WEPS, Environmental Modelling & Software 19, 177-183.

Funk, R., Skidmore, E.L., Hagen, L.J., 2002. Comparison of wind erosion measurements in Germany with simulated soil losses by WEPS. In: Lee, J.A., Zobeck, T.M. (Eds.), Proceedings of ICAR5/GCTE-SEN Joint Conference, Publication 02-2, International Center for Arid and Semiarid Lands Studies: Lubbock, TX. , pp. 235.

Gao, F., Feng, G., Sharratt, B., Zhang M., 2014. Tillage and straw management affect PM_{10} emission potential in subarctic Alaska. Soil & Tillage Research 144, 1–7.

Gomes, L., Arru´, J.L., Lo´pez, M.V., Sterk, G., Richard, D., Gracia, R., Sabre. M., Gaudichet, A., Frangi, J.P., 2003. Wind erosion in a semiarid agricultural area of Spain: the WELSONS project, Catena 52, 235–256.

Goossens, D., and Riksen, M., 2004. Wind erosion and dust dynamics at the commencement of the 21st century. In: D. Goossens and M. Riksen (Editors), Wind erosion and dust dynamics: observations, simulation, modelling. ESW publications, Wageningen, pp. 7-13.

Goossens, D., Gross, J., Spaan, W., 2001. Aeolian dust dynamics in agricultural land areas in Lower Saxony, Germany. Earth Surface Processes and Landforms 26, 701–720.

Goossens, D., Offer, Z., London, G., 2000. Wind tunnel and field calibration of five aeolian sand traps. Geomorphology 35(3), 233–252.

Grini, A., Myhre, G., Zender, C., Sundet, J., Isakssen, I., 2003. Model simulations of dust source and transport in the global troposphere: Effects of soil erodibility and wind speed variability. Institute Report Series No. 124. Norway, University of Oslo, Department of Geosciences.

Hagen, L. J., Armbrust, D. V., 1992. Aerodynamic roughness and saltation trapping efficiency of tillage ridges. Transactions of the American Society of Agricultural Engineers 35(4), 1179–1184.

Hagen, L. J., 1996. Erosion Sub-model. In: Hagen, L. J., Wagner, L.E., Tatarko J., (Eds.). Wind Erosion Prediction System: WEPS Technical Documentation. USDA-ARS Wind Erosion Research Unit, Manhattan, KS, pp. E1–E50.

Hagen, L. J., 2001. Validation of the wind erosion prediction system (WEPS) erosion submodel on small cropland fields. In: Ascough, J.C. II, Flanagan, D.C. (Eds.), Soil Erosion Research for the 21st Century. ASAE (American Society of Agricultural Engineers) Publication 701P0007, pp. 479–482.

Hagen, L. J., 2004. Evaluation of the Wind Erosion Prediction System (WEPS) erosion submodel on cropland fields. Environmental Modelling and Software. 19(2), 171-176.

Hagen, L. J., Van Pelt, S., Sharratt, B., 2010. Estimating the saltation and suspension components from field wind erosion. Aeolian Research 1, 147-153.

Hagen, L. J., Wagner, L.E., Skidmore, E.L., 1999. Analytical solutions and sensitivity analysis for sediment transport in WEPS. Transactions of the ASAE 42(6), 1715–1721.

Han, Q., Qu, J., Zhang, K., Zu, R., Niu, Q., Liao, K., 2009. Wind tunnel investigation of the influence of surface moisture content on the entrainment and erosion of beach sand by wind using sands from tropical humid coastal southern China. Geomorphology 104, 230-237.

Hassenpflug, W., 1998. Bodenerosion durch Wind, in Richter, G. (ed.): Bodenerosion – Analyse und Bilanz eines Umweltproblems. Wissenschaftliche Buchgesellschaft, Darmstadt, pp. 69–82.

Hevia, G. G., Mendez, M., Buschiazzo, D. E., 2007. Tillage affects soil aggregation parameters linked with wind erosion. Geoderma 140, 90–96.

Hevia, G.G., Buschiazzo, D.E., Hepper, E.N., Urioste, A.M., Antón, E.L., 2003. Organic matter in size fractions of soils of the semiarid Argentina: Effects of climate, soil texture and management. Geoderma 116, 265–277.

Hoffmann, C., Funk, R., 2015. Diurnal changes of PM_{10}-emission from arable soils in NE-Germany. Aeolian Research 17, 117–127.

IPCC (2001), Climate Change 2001, edited by J. T. Houghton et al., Cambridge University Press, New York.

IPCC, 2005. Report of the IPCC Expert Meeting on Emission Estimation of Aerosols Relevant to Climate Change. 2-4 May 2005, Geneva, Switzerland.

Ishizuka, M., Mikami, M., Yamada, Y., Zeng, F., Gao, W., 2005. An observational study of soil moisture effects on wind erosion at a gobi site in the Taklamakan Desert. Journal of Geophysical Research 110(D18), 1-10.

Jakeman, A.J., Letcher, R.A., Norton, J.P., 2006. Ten iterative steps in development and evaluation of environmental models. Environmental Modelling & Software 21 (5), 602–614.

Jia, Q., Al-Ansari, N., Knutsson, S., 2014. Modeling of Wind Erosion of the Aitik Tailings Dam Using SWEEP Model. Engineering 6, 355-364.

Jönsson, P., 1994. Influence of shelter on soil sorting by wind erosion - a case study. Journal of Catena V. 22, Issue 1, pp 35–47.

Kardous, M., Bergametti, G., Marticorena, B., 2005. Wind tunnel experiments on the effects of tillage ridge features on wind erosion horizontal fluxes. Annales Geophysicae, 23, 3195–3206.

Krause, P., Boyle, D. P., Base, F. 2005. Comparison of different efficiency criteria for hydrological model assessment, Advances in Geosciences 5, 89–97.

Kristensen, S. P., 2001. Hedgerow planting activities by Danish farmers: a case study from central Jutland. Geografisk Tidsskrift, Danish Journal of Geography 101, 101-114.

Kuhlman, H., 1986. Vinden og landbruget. Wind and agriculture. In: Jensen, K.M. and Reenberg, A., 1986.

Lal, R. 2001. Soil degradation by erosion. Land Degradation & Development 12, 519 –539.

Larney, F. J., Bullock, M. S., Janzen, H. H., Ellert, B.H., Olson, E.C.S., 1998. Wind erosion effects on nutrient redistribution and soil productivity. Journal of Soil and Water Conservation, 53(2), 133–140.

Legates, D. R., and G. J. McCabe, 1999. Evaluating the use of “goodness-of-fit” measures in hydrologic and hydroclimatic model validation. Water Resources Research 35(1), 233-241.

Leys, J. F., 1999. Wind erosion on agricultural lands. In: A.S. Goudie, Livingstone, I., Stokes, S. (Editor), Aeolian Environments, Sediments and Landforms. John Wiley & Sons Ltd, Chichester. pp. 143-166.

Leys, J., McTainsh, G., Strong, C., Heidenreich, S., Biesaga, K., 2008. DustWatch: Using community networks to improve wind erosion monitoring in Australia. Earth Surface Processes and Landforms 33(12), 1912-1926.

Leys, J.F., McTainsh, G.H., 1999. Dust and nutrient deposition to riverine environments of south-eastern Australia. Zeitschrift für Geomorphologie Supplementbände 116, 59–76.

Li, J., Okin, G.S., Alvarez, L., Epstein, H., 2007. Quantitative effects of vegetation cover on wind erosion and soil nutrient loss in a desert grassland of southern New Mexico, USA. Biogeochemistry 85, 317–332.

Li, Sh., Lobb, D. A., McConkey, B.G., 2010. The impacts of land use on the risk of soil erosion on agricultural land in Canada. 19th World Congress of Soil Science, Soil Solutions for a Changing World 1-6 August 2010, Brisbane, Australia.

Liu, B., Qu, J., Niu, Q., Han, Q., 2014. Comparison of measured wind tunnel and SWEEP simulated soil losses. Geomorphology 207, 23–29.

Liu, M.X., Wang, J. A., Yan, P., Liu, L. Y., Ge, Y. Q., Li, X. Y., Hu, X., Song, Y., Wang, L., 2006. Wind tunnel simulation of ridge-tillage effects on soil erosion from cropland. Soil & Tillage Research 90, 242-249.

Loague, K., and Green R. E., 1991. Statistical and graphical methods for evaluating solute transport models: overview and application. Contaminant Hydrology 7, 51–73.

Lopez, M.V., Gracia, R., Arrue, J.L., 2000. Effects of reduced tillage on soil surface properties affecting wind erosion in semiarid fallow lands of Central Aragon. European Journal of Agronomy 12, 191–199.

Lu, H., and Shao, Y., 2001. Toward quantitative prediction of dust storms: an integrated wind erosion modelling system and its applications. Environmental Modelling & Software 16, 233-249.

Mastersizer 2000E, 2004. Integrated system for particle sizing, Mastersizer 2000E operator's guide. Malvern Instruments Ltd., Worcestershire, UK.

Maurer, T., Hermann, L., Gaiser, T., Mounkaila, M., Stahr, K., 2006. A mobile wind tunnel for wind erosion field measurements Arid Environments 66(2), 257-271.

McCoy, M.D., Hartshorn, A.S., 2007. Wind Erosion and Intensive Prehistoric Agriculture: A Case Study from the Kalaupapa Field System, Moloka'i Island, Hawai'i. International Journal of Geoarchaeology 22, No. 5, 511–532.

McKenna Neuman, C., Boulton, J. W., Sanderson, S., 2009. Wind tunnel simulation of environmental controls on fugitive dust emissions from mine tailings, Atmospheric Environment 43, 520-529.

McTainsh, G.H., Leys, J.F., Nickling, W.G., 1999. Wind erodibility of arid lands in the channel country of Western Queensland, Australia. Zeitschrift für Geomorphologie NF 116, 113–130.

Mendez, M.J., Buschiazzo, D.E., 2010. Wind erosion risk in agricultural soil under different tillage systems in the semiarid Pampas of Argentina, Soil and Tillage Research 106, 311–316.

Mezösi, G., Szatmári, J., 1998. Assessment of wind erosion risk on the agricultural area of the southern part of Hungary. Hazardous Materials 61, 139-153.

Moriasi, D.N., Arnold, J.G., Van Liew, M.W., Bingner, R.L., Harmel, R.D., Veith, T.L., 2007. Model evaluation guidelines for systematic quantification of accuracy in watershed simulations. Transactions of the ASABE, 50 (3), 885–900.

Munodawafa, A., 2011. The significance of soil erosion on soil fertility under different tillage systems and granitic sandy soils in semi-arid Zimbabwe: A comparison of nutrient losses due to sheet erosion, leaching and plant uptake. Soil Erosion Issues in Agriculture, Dr. Danilo Godone (Ed.), ISBN: 978-953-307-435-1.

Naeini, M. S., Fister, W., Heckrath, G., Kuhn, N. J., 2015. Separation of dry and wet periods from regular weather station data for the analysis of wind erosion risk. Poster presentation at the General Assembly der EGU 2015, Session SSS 2.1 "Soil science and environmental issues today", April 12-17 2015, Vienna, Austria. (Geophysical Research Abstracts Vol. 17, EGU2015-11335, 2015).

Nash, J. E., and Sutcliffe, J. V., 1970. River flow forecasting through conceptual models: Part 1. A discussion of principles. Hydrology 10(3), 282-290.

Nickling, W. G., 1983. Grain-size characteristics of sediment transported during dust storms, Journal of Sedimentary Petrology 53, 1011 – 1024.

Nickling, W. G., and McKenna Neuman, C., 1997. Wind tunnel evaluation of a wedge-shaped aeolian sediment trap, Geomorphology 18, 333-345.

NOAA-NCDC. (2013). Daily, hourly/sub-hourly weather element time series (n-2013). NOAA/National Climatic Data Center. Asheville, North Carolina: NOAA/National Climatic Data Center.

Nordstrom, K. F., and Hotta, S., 2004. Wind erosion from cropland in the USA: a review of problems, solutions and prospects. Geoderma 121, 157–167.

Odgaard, B., Rømer, J. R., 2009. Danske landbrugslandskaber gennem 2000 år. Fra digevoldninger til støtteordninger. Aarhus Universitetsforlag, 301 pp.

Okin, G.S., 2005. Dependence of wind erosion on surface heterogeneity: stochastic modeling. Journal of Geophysical Research 110 (D11208), 1-10.

Oldeman, L. R., 1994. The global extent of soil degradation. In: Greenland, D.J., Szabolcs, I. (Eds.), Soil Resiliance and Sustainable Land Use. CAB International, pp. 99–118. Chapter 7.

Pi, H., Feng, G., Sharratt, B. S., Li, X., Zheng, Z., 2014. Validation of SWEEP for Contrasting Agricultural Land Use Types in the Tarim Basin. Soil Science 179, 433-445.

Podhrazska, J., and Novotny, I., 2007. Evaluation of the wind erosion risks in GIS. Soil & Water Resources 2 (1), 10–13.

Potter, K. N., Zobeck, T. M., Hagen, L. J., 1990. A microrelief index to estimate soil erodibility by wind. Transactions of the American Society of Agricultural Engineers 33(1), 151–155.

Prospero, J. M., Ginoux, P., Torres, O., Nicholson, S., Gill, T., 2002. Environmental characterization of global sources of atmospheric soil dust identified with the NIMBUS-7 TOMS Absorbing Aerosol Product. Reviews of Geophysics 40, 1-31.

Raupach, M., McTainsh G., Leys, J., 1994. Estimates of dust mass in recent major dust storms. Australian Journal of Soil and Water Conservation7, 20-24.

Ravi, S., Zobeck, T., Over, T., 2006. On the effect of moisture bonding forces in air-dry soils on threshold friction velocity of wind erosion. Sedimentology, 53, 597–609.

RC612, 2006. Instruction Manual RC612, Multiphase Carbon/Hydrogen/Moisture Determinator. Version 1.0. Leco Corporation.

Refsgaard, J.C., Jeroen, P., Anker, L.H., Peter, A.V., 2007. Uncertainty in the environmental modelling process - A framework and guidance. Environmental Modelling & Software 22, 1543–1556.

Reiche, M., Funk, R., Zhang, Z., Hoffmann, C., Reiche, J., Wehrhan, M., Li, Y., Sommer, M., 2012. Application of satellite remote sensing for mapping wind erosion risk and dust emission-deposition in Inner Mongolia grassland, China. Grassland Science 58, 8–19.

Riksen, M. and de Graaff, J., 2001. On-site and off-site effects of wind erosion on European light soils, Land Degradation and Development 12 (1), 1-11.

Riksen, M., Brouwer, F., de Graaaf, J., 2003. Soil conservation policy measures to control wind erosion in North-Western Europe. Catena 52, 309-326.

Roney, J. A., White, B. R., 2010. Comparison of a two-dimensional numerical dust transport model with experimental dust emissions from soil surfaces in a wind tunnel. Atmospheric Environment 44, 512-522.

Sankey, J.B., Germino, M.J., Benner, Sh.G., Glenn, N.F., Hoover, A.N., 2012. Transport of biologically important nutrients by wind in an eroding cold desert. Aeolian Research 7, 17–27.

Saxton, K., Chandler, D., Schillinger, W., 1999. Wind erosion and air quality research in the Northwest U.S. Columbia Plateau: Organization and progress, 10th International Soil Conservation Organization Meeting held May 24-29, 1999 at Purdue University and the USDA-ARS National Soil Erosion Research Lab oratory.

Saxton, K.E., Rawls, W.J., Romberger, J.S., Papendick, R.I., 1986. Estimating generalized soil water characteristics from texture. Transactions of the ASAE 50, 1031–1035.

Schjønning, P., Heckrath, G., and Christensen, B.T., 2009. Threats to soil quality in Denmark - A review of existing knowledge in the context of the EU Soil Thematic Strategy. DJF Report Plant Science, no. 143. Aarhus University, Faculty of Agricultural Sciences, Research Centre Foulum, Tjele, Denmark.

Shang, K. Z., Wang, S. G., Ma, Y. X., Zhou, Z. J., Wang, J. Y., Liu, H. L., Wang, Y. Q., 2007. A scheme for calculating soil moisture content by using routine weather data. Atmospheric Chemistry and Physics 7(19), 5197–5206.

Shao Y., 2008. Physics and modelling of wind erosion. Springer Science & Business Media, Cologne.

Sharratt, B., 2011. Size distribution of windblown sediment emitted from agricultural fields in the Columbia Plateau. Soil & Water Management & Conservation 75 (3), 1-7.

Shi, H. D., J. Y. Liu, D. F. Zhuang, Hu, Y.F., 2007. Using the RBFN model and GIS technique to assess wind erosion hazard of Inner Mongolia, China. Land Degradation & Development 18, 413-422.

Skidmore, E.L., 1986. Wind erosion climatic erosivity. Climate Change 9, 195-208.

Sterk, G., Hermann, L., Bationo, A., 1996. Wind-blown nutrient transport and soil productivity change in southwest Niger. Land Degradation and Rehabilitation 7(4), 325–335.

Sterk, G., Stein, A., 1997. Mapping windblown mass transport by modelling variability in space and time. Soil Science Society of America Journal 61, 232–239.

Stout, J. E., Zobeck, T. M., 1996. Establishing the threshold condition for soil movement in wind-eroding fields. In: International Conference on Air Pollution from Agricultural Operations, Kansas City, Missouri, USA, Midwest Plan Service (MWPS C-3), Iowa State University, Ames, Iowa, USA, 65-71.

Tegen, I., and Fung, I., 1995. Contribution to the atmospheric mineral aerosol load from land surface modification. Geophysical Research 100(D9), 18707-18726.

Tye, A., 2007. Mapping soil erosion risks. British Geological Survey, Earthwise 25, 22-23.

United Nations (UN), 1997. Dry land degradation keeping hundreds of millions in poverty; Press Release: Secretariat of the United Nations Convention to Combat Desertification, Geneva, Switzerland.

United Nations (UN), 2002. Living with Risk: A global review of disaster reduction initiatives. Preliminary version 2002. Geneva, July 2002.

USDA, ARS wind Erosion Research Unit (WERU), 2008. SWEEP User Manual, Manhattan, Kansas, USA.

Van Donk, S.J., Skidmore, E.L., 2003. Measurement and simulation of wind erosion, roughness degradation and residue decomposition on an agricultural field. Earth Surface Processes and Landforms 28(11),1243-1258.

Van Pelt, R. S., and Zobeck ,T. M., 2013. Portable Wind Tunnels for Field Testing of Soils and Natural Surfaces: Wind tunnel designs and their diverse engineering applications, Dr. Noor Ahmed (Ed.), ISBN: 978-953-51-1047-7, InTech, DOI: 10.5772/54141.

Van Pelt, R., and Zobeck, T., 2007. Chemical constituents of fugitive dust. Environmental Monitoring and Assessment 130, 3-16.

Van Pelt, R., Zobeck, T., Baddock, M., Cox, J., 2010. Design, construction, and calibration of a portable boundary layer wind tunnel for field use. Transactions of the ASAE 53(3), 1413-1422.

Veihe, A., Hasholt, B., Schiøtz, I. G., 2003. Soil erosion in Denmark: processes and politics. Environmental Science & Policy 6, 37-50.

Visser S. M., Stroosnijder, L., Chardon, W. J., 2005. Nutrient losses by wind and water, measurements and modeling. Catena 63,1-22.

Vrieling, A., Sterk, G., Beaulieu, N., 2002. Erosion risk mapping: A methodological case study in the Colombian Eastern Plains. Journal of Soil and Water Conservation 57(3), 158-163.

Wainwright, J., Mulligan, M., 2013. Book Review, environmental modelling: Finding simplicity in complexity. Environmental Engineering and Management Vol.12, No. 4, 847-850.

Wang, X. B., Oenema, O., Hoogmoed, W. B., Perdok, U. D., Cai, D. X., 2006. Dust storm erosion and its impact on soil carbon and nitrogen losses in northern China.Catena 66, 221-227.

Wang, Y.Q., and Shao, M.A., 2013. Spatial variability of soil physical properties in a region of the Loess Plateau of PR China subject to wind and water erosion. Land Degradation & Development 24, 296-304.

Warren, A., 2002. Wind erosion on agricultural land in Europe. European commission, directorate-general for Research. Environment and Sustainable Development Programme. Report No. 20370.

Warren, A., 2003. Wind erosion on agricultural land in Europe. Publication EUR 20370, European Commission Environment and Sustainable Development Programme. Luxembourg, Belgium.

Warren, A., 2007. Sustainability: A view from the wind-eroded field. Journal of Environmental Sciences 19, 470–474.

Webb, N. P., 2008. Modelling land susceptibility to wind erosion in Western Queensland, Australia. PhD Thesis, School Geography, Planning and Architecture, The University of Queensland, Australia.

Webb, N. P., McGowan, H. A., 2009. Approaches to modelling land erodibility by wind. Progress in Physical Geography 33(5), 587–613.

Webb, N. P., McGowan, H. A., Phinn, S. R., McTainsh, G. H., 2006. AUSLEM (AUStralian Land Erodibility Model): A tool for identifying wind erosion hazard in Australia. Geomorphology 78(3-4), 179-200.

Webb, N. P., Strong, C. L., Chappell, A., Marx, S. K., McTainsh, G. H., 2013. Soil organic carbon enrichment of dust emissions: magnitude, mechanisms and its implications for the carbon cycle. Earth Surface Process & Landforms 38, 1662-1671.

Webb, N., and Strong, C., 2011. Soil erodibility dynamics and its representation for wind erosion and dust emission models. Aeolian Research 3(2), 165-179.

Weinan, C., Zhibao, D., Zhenshan, L., Zuotao, Y., 1996. Wind tunnel test of the influence of moisture on the erodibility of loessial sandy loam soils by wind. Arid Environments 34, 391-402.

White, K.L., Chaubey, I., 2005. Sensitivity analysis, calibration, and validations for a multisite and multivariable SWAT model. Journal of the American Water Resources Association (JAWRA) 41(5), 1077–1089.

Willmot, C. J., 1984. On the evaluation of model performance in physical geography: Spatial Statistics and Models. editors: Gaile, G. L., and Willmot, C. J., D. Reidel, Dordrecht, Netherlands. 443–460.

Willmott, C. J., 1981. On the validation of models. Physical Geography 2, 184-194.

Woodruff, N. P., Siddoway F. H., 1965. A wind erosion equation. Science Society of America Proceedings 29, 602–608.

Yan, H., Wang, SH., Wang, CH., Zhang, G., Patel, N., 2005. Losses of soil organic carbon under wind erosion in China. Global Change Biology 11, 828–840.

Yan, Y., Xu, X., Xin, X., Yang, G., Wang, X., Yan, R., Chen, B., 2011. Effect of vegetation coverage on aeolian dust accumulation in a semiarid steppe of northern China. Catena 87, 351–356.

Yang, S., Ping, Y., Lianyou, L., 2006. A review of the research on complex erosion by wind and water. Geographical Sciences 16 (2), 231-241.

Youssef, I. F., Visser, S. M., Karssenberg, D., Bruggeman, A., Erpul, G., 2012. Calibration of RWEQ in a patchy landscape: A first step towards a regional scale wind erosion model. Aeolian Research, 3(4), 467-476.

Zar, J.H., 2010. Biostatistical analysis. Pearson. 960 p.

Zhang, N., Kang J. H., Lee, S. J., 2010. Wind tunnel observation on the effect of a porous wind fence on shelter of saltating sand particles. Geomorphology 120, 224-232.

Zhao, H. L., Yi, X. Y., Zhou, R. L., Zhou, X. Y., Zhang, T. H., Drake, S., 2006. Wind erosion and sand accumulation effects on soil properties in Horqin Sandy Farmland, Inner Mongolia. Catena 65(1), 71–79.

Zobeck, T. M., Fryrear, D., 1986. Chemical and physical characteristics of windblown sediment: II: Chemical characteristics and total soil and nutrient discharge. Transactions of the ASAE 29(4), 1037-1041.

Zobeck, T. M., Van Pelt, R. S., 2014. Wind Erosion. Publications from USDA-ARS / UNL Faculty. Paper 1409.

Zobeck, T., Van Pelt, R., 2011. Wind Erosion, 2011. Soil management, Building a Stable Base for Agriculture, chapter14. Published by: Soil Science Society of America. doi: 10.2136/2011.

Zobeck, T.M., 1991. Soil properties affecting wind erosion. Soil and Water Conservation 46(2), 112-118.

Zobeck, T.M., Baddock, M., Van Pelt, R.S., Tatarko, J., Acosta-Martinez, V., 2013. Soil property effects on wind erosion of organic soils. Aeolian Research 10, 43-51.